Chapter 1: Introduction

1.1 Practical column base details in steel structures

1.1.1 Practical column base details

Every structure must transfer vertical and lateral loads to the supports. In some cases, beams or other members may be supported directly, though the most common system is for columns to be supported by a concrete foundation. The column will be connected to a baseplate, which will be attached to the concrete by some form of so-called „holding down" assembly.

Typical details are shown in Figure 1.1. The system of column, baseplate and holding down assembly is known as a column base. This publication proposes rules to determine the strength and stiffness of such details.

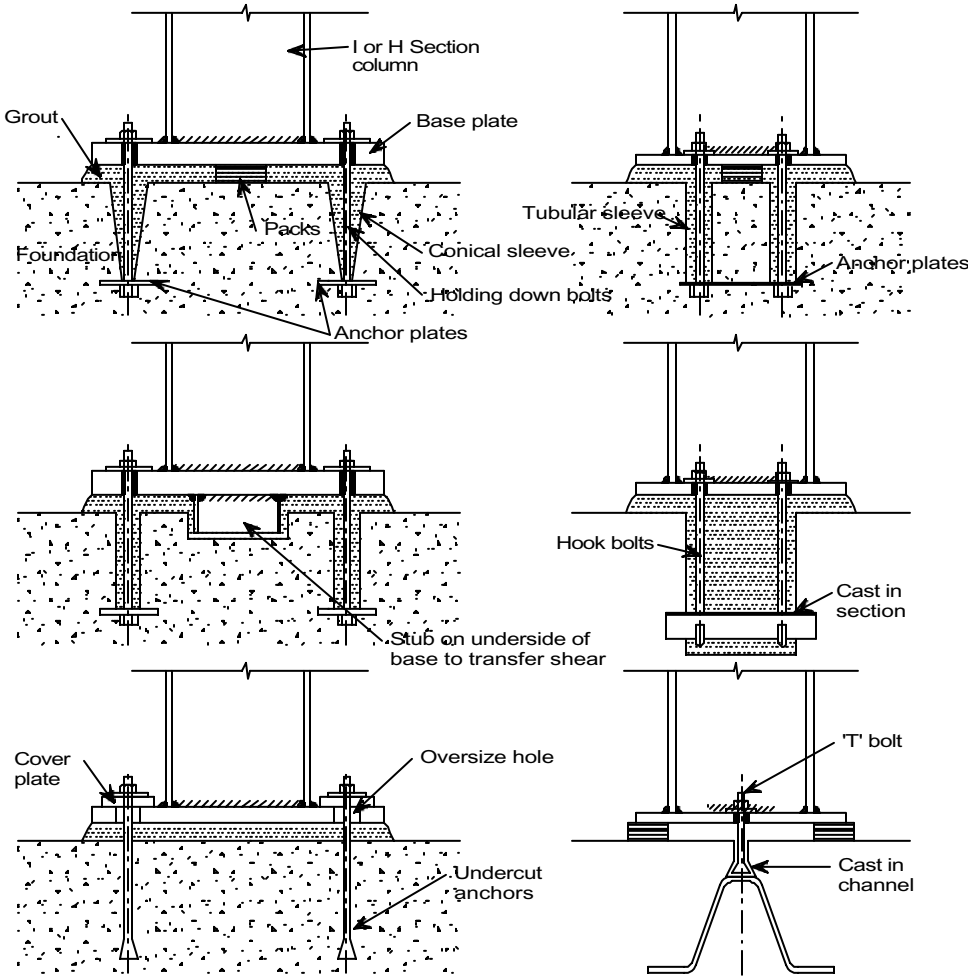

Figure 1.1 Typical column base details

Other column base details may be adopted, including embedding the lower portion of column into a pocket in the foundation, or the use of baseplates strengthened by additional horizontal steel members. These types of base are not covered in this publication, which is limited to unstiffened baseplates for I or H sections. Although no detailed guidance is given, the principles in this publication may be applied to the design of bases for RHS or CHS section columns.

Foundations themselves are supported by the sub-structure. The foundation may be supported directly on the existing ground, or may be supported by piles, or the foundation may be part of a slab. The influence of the support to the foundation, which may be considerable in certain ground conditions, is not covered in this document.

Concrete foundations are usually reinforced. The reinforcement may be nominal in the case of pinned bases, but will be significant in bases where bending moment is to be transferred. The holding down assembly comprises two, but more commonly four (or more) holding down bolts. These may be cast in situ, or post-fixed to the completed foundation. Cast in situ bolts usually have some form of tubular or conical sleeve, so that the top of the bolts are free to move laterally, to allow the baseplate to be accurately located. Other forms of anchor are commonly used, as shown in Figure 1.2. Baseplates for cast-in assemblies are usually provided with oversize holes and thick washer plates to permit translation of the column base. Post-fixed anchors may be used, being positioned accurately in the cured concrete. Other assemblies involve loose arrangements of bolts and anchor plates, subsequently fixed with cementicious grout or fine concrete. Whilst loose arrangements allow considerable translation of the baseplate, the lack of initial fixity can mean that the column must be propped or guyed whilst the holding down arrangements are completed. Anchor plates or similar embedded arrangements are attached to the embedded end of the anchor assembly to resist pull-out. The holding down assemblies protrude from the concrete a considerable distance, to allow for the grout, the baseplate, the washer, the nut and a further threaded length to allow some vertical tolerance. The projection from the concrete is typically around 100 mm, with a considerable threaded length.

Post-fixed assemblies include expanding mechanical anchors, chemical anchors, undercut anchors and grouted anchors. Various types of anchor are illustrated in Figure 1.2.

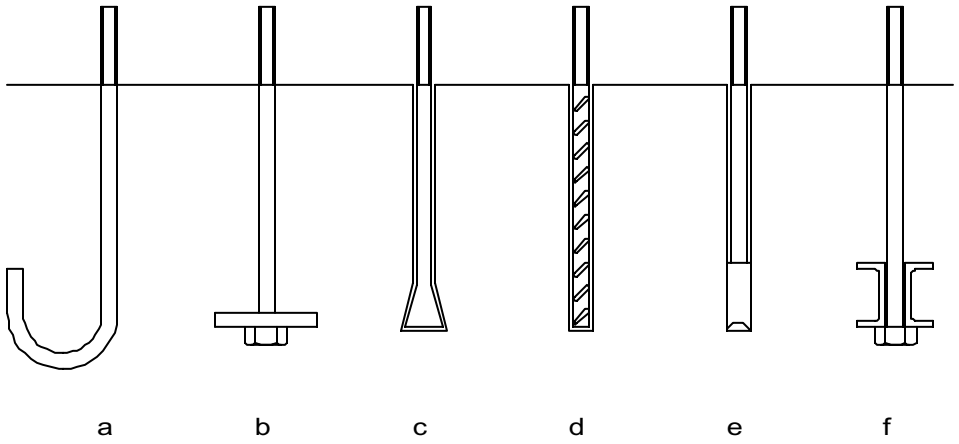

a, b	cast in place
c	post fixed, undercut
d	post fixed chemical or cementicius grout
e	post fixed expanding anchor
f	fixed to grillage and cast in-situ

Figure 1.2 Alternative holding-down anchors

The space between the foundation and the baseplate is used to ensure the baseplate is located at the correct absolute level. On smaller bases, this may be achieved by an additional set of nuts on the holding down assemblies, as shown in Figure 1.3. Commonly, the baseplate is located on a series of thin steel packs as shown in Figure 1.4, which are usually permanent. Wedges are commonly used to assist the plumbing of the column.

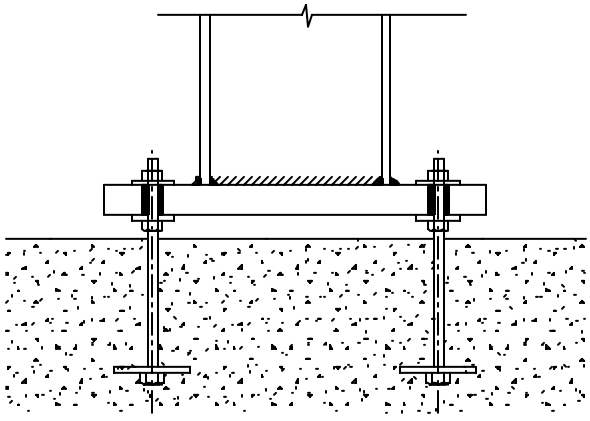

Figure 1.3 Baseplate with levelling nuts

The remaining void is filled with fine concrete, mortar, or more commonly, non-shrink cementicious grout, which is poured under and around the baseplate. Large baseplates

generally have holes to allow any trapped air to escape when the baseplate is grouted.

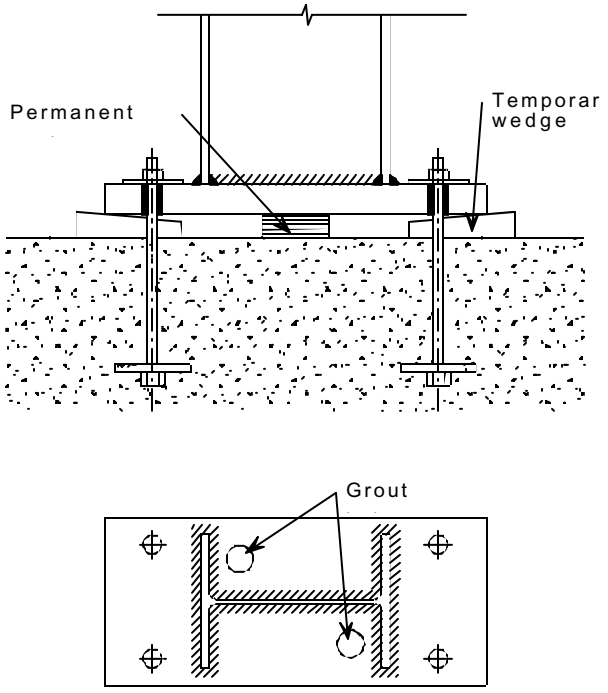

Figure 1.4 Baseplate located on steel packs

The plate attached to the column is generally rectangular. The dimensions of the plate are as required by design, though practical requirements may mean the base is larger than necessitated by design. Steel erectors favour at least four bolts, since this is a more stable detail when the column is initially erected. Four bolts also allow the baseplate to be adjusted to ensure verticality of the column. Bolts may be located within the profile of the I or H section, or outside the profile, or both, as shown in Figure 1.1. Closely grouped bolts with tubular or conical sleeves are to be avoided, as the remaining concrete may not be able to support the column and superstructure in the temporary condition.

Bases may have stubs or other projections on the underside which are designed to transfer horizontal loads to the foundations. However, such stubs are not appreciated by steelwork erectors and should be avoided if possible. Other solutions may involve locating the base in a shallow recess or anchoring the column directly to, for example, the floor slab of the structure.

Columns are generally connected to the baseplate by welding around part or all of the section profile. Where corrosion is possible a full profile weld is recommended.

1.1.2 Pinned base details

Pinned bases are assumed in analysis to be free to rotate. In practice pinned bases are often detailed with four holding down bolts for the reasons given above, and with a baseplate which is significantly larger than the overall dimensions of the column section. A base detailed in this way will have significant stiffness and may transfer moment, which assists erection. In theory, such a base should be detailed to provide considerable rotational capacity, though in practice, this is rarely considered.

1.1.3 Fixed base details

Fixed (or moment-resisting) bases are assumed in analysis to be entirely rigid. Compared to pinned bases, fixed bases are likely to have a thicker baseplate, and may have a larger number of higher strength holding down assemblies. Occasionally, fixed bases have stiffened baseplates, as those shown in Figure 1.5. The stiffeners may be fabricated from plate, or from steel members such as channels.

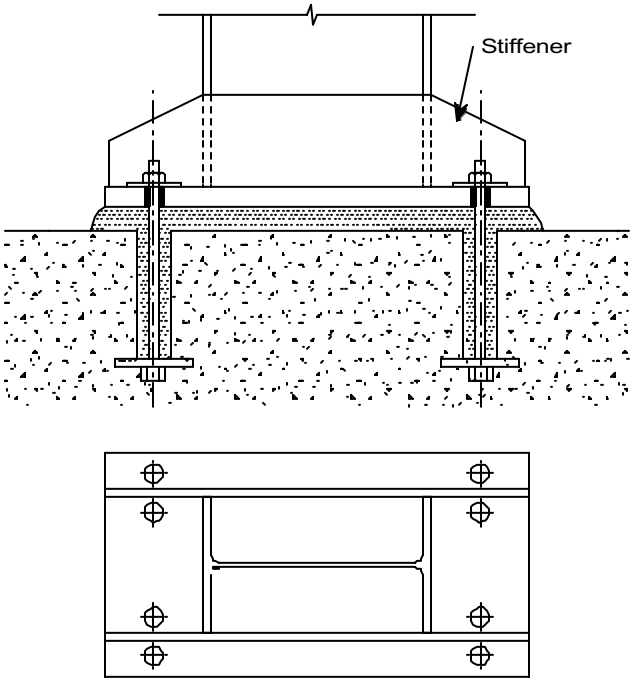

Figure 1.5 Typical stiffened column base detail

1.1.4 Resistance of column bases

Eurocode 3, Section 6 and Annex L contain guidance on the strength of column bases. Section 6 contains principles, and Annex L contains detailed application rules, though these are limited bases subject to axial loads only. The principles in Section 6 cover the moment resistance of bases, though there are no application rules for moment resistance and no principles or rules covering the stiffness of such bases.

Traditional approaches to the design of moment-resisting bases involve an elastic analysis, based on the assumption that plane sections remain plane. By solving equilibrium equations, the maximum stress in the concrete (based on a triangular distribution of stress), the extent of the stress block and the tension in the holding down assemblies may be determined. Whilst this procedure has proved satisfactory in service over many years, the approach ignores the flexibility of the baseplate in bending, the holding down assemblies and the concrete.

1.1.5 Modelling of column bases in analysis

Traditionally, column bases are modelled as either pinned or as fixed, whilst acknowledging that the reality lies somewhere within the two extremes. The opportunity to either calculate or to model the base stiffness in analysis was not available. Some national application standards recommend that the base fixity be allowed for in design.

The base fixity has an important effect on the calculated frame behaviour, particularly on frame deflections.

1.2 Calculation of column base strength and stiffness

1.2.1 Scope of the publication

In recent years, Wald, Jaspart and others have directed significant research effort to the determination of resistance and stiffness. Based on the results of this research, recommendations for the design and verification of moment-resisting column bases could be drafted. This permits the modelling in analysis of semi-continuous bases in addition to the traditional practice of pinned and fixed bases. Both resistance and stiffness can be determined.

This publication contains proposals for the calculation of the capacity and of the stiffness of moment-resisting bases, with the intention that these be included in Eurocode 3. This publication is focused on I or H columns with unstiffened baseplates, though the principles in this publication may be applied to baseplates for RHS or CHS columns. Embedded column base details are excluded from the recommendations in this publication

The effect of the concrete-substructure interaction on the resistance and stiffness of the column base is excluded.

1.2.2 'Component' method

The philosophy adopted in this publication is known as the 'component' method. This approach accords with the approach already followed in EC3 and, in particular, Annex J, where rules for the determination of beam to column strength and stiffness are presented.

The component approach involves identifying each of the important features in the base connection and determining the strength and stiffness of each of these 'components'.

The components are then 'assembled' to produce a model of the complete arrangement. Each individual component and the assembly model are validated against test results.

1.3 Document structure

Section 2 of this document contains details of the components in a column base connection, namely:

- The compression side - the concrete in compression and the flexure of the baseplate.
- The column member.
- The tension side - the holding-down assemblies in tension and the flexure of the baseplate.
- The transfer of horizontal shear.

Each sub-section covers a component and follows the following format:

- A description of the component.
- A review of existing relevant research.
- Details of the proposed model.
- Results of validation against test data.

Section 3 describes the proposed assembly model and demonstrates the validity of the proposals compared to test data. Section 4 makes recommendations for the practical use of this document in analysis of steel frames. Section 5 makes recommendations for the classification of bases as sway or non-sway, in braced and unbraced frames.

Chapter 2: Component characteristics

2.1 Concrete in compression and base plate in bending

2.1.1 Description of the component

The components concrete in compression and base plate in bending including the grout represent the behaviour of the compressed part of a column base with a base plate. The strength of these components depend primarily on the bearing resistance of the concrete block. The grout is influencing the column base bearing resistance by improving the resistance due to application of high quality grout, or by decreasing the resistance due to poor quality of the grout material or due to poor detailing.

The deformation of this component is relatively small. The description of the behaviour of this component is required for the prediction of column bases stiffness loaded by normal force primarily.

2.1.2 Overview of existing material

The technical literature concerned with the bearing strength of the concrete block loaded through a plate may be treated in two broad categories. Firstly, investigations focused on the bearing stress of rigid plates, most were concerned the prestressed tendons. Secondly, studies were concentrated on flexible plates loaded by the column cross section due to an only portion of the plate.

The experimental and analytical models for the components concrete in compression and plate in bending included the ratio of concrete strength to plate area, relative concrete depth, the location of the plate on the concrete foundation and the effects of reinforcement. The result of these studies on foundations with punch loading and fully loaded plates offer qualitative information on the behaviour of base plate foundations where the plate is only partially loaded by the column. Failure occurs when an inverted pyramid forms under the plate. The application of limit state analysis on concrete can include the three-dimensional behaviour of materials, plastification and cracking. Experimental studies (Shelson, 1957; Hawkins, 1968, DeWolf, 1978) led to the development of an appropriate model for column base bearing stress estimation that was adopted into the current codes.

The separate check of the concrete block itself is necessary to provide to check the shear resistance of the concrete block as well as the bending or punching shear resistance according to the concrete block geometry detailing.

The influence of a flexible plate was solved by replacing the equivalent rigid plate (Stockwell, 1975). This reasoning is based on recognition that uniform bearing pressure is unrealistic and

that maximum pressure would logically follow the profile shape. This simple practical method was modified and checked against the experimental results, (Bijlaard, 1982; Murray, 1983). Eurocode 3 (Annex L, 1990) adopted this method in conservative form suitable for standardisation using an estimate including the dimensions of the concrete block cross-section and its height. It was also found (DeWolf and Sarisley, 1980; Wald, 1993) that the bearing stress increases with larger eccentricity of normal force. In this case is the base plate in larger contact with the concrete block due to its bending. In case, when the distance between the plate edge and the block edge is fixed and the eccentricity is increased, the contact area is reduced and the value of bearing stress increases. In case of the crushing of the concrete surface under the rigid edge is necessary to apply the theory of damage. These cases are unacceptable from design point of view and are determining the boundaries of above described analysis.

2.1.3 Proposed model

2.1.3.1 Strength

The proposed design model resistance of the components concrete in compression and base plate in bending is given in Eurocode 3 Annex L, 1990. The resistance of these components is determined with help of an effective rigid plate concept.

The concrete block size has an effect on the bearing resistance of the concrete under the plate. This effect can be conservatively introduced for the strength design by the concentration factor

$$k_j = \sqrt{\frac{a_1 \; b_1}{a \; b}} \tag{2.1.1}$$

where the geometry conditions, see Figure 2.1.1, are introduced by

$$a_1 = min \begin{Bmatrix} a + 2\, a_r \\ 5\, a \\ a + h \\ 5\, b_1 \end{Bmatrix}, \; a_1 \geq a \tag{2.1.2}$$

$$b_1 = min \begin{Bmatrix} b + 2\, b_r \\ 5\, b \\ b + h \\ 5\, a_1 \end{Bmatrix}, b_1 \geq b \tag{2.1.3}$$

This concentration factor is used for evaluation of the design value of the bearing strength as

follows

$$f_j = \frac{\beta_j \, k_j \, f_{ck}}{\gamma_c} \tag{2.1.4}$$

where joint coefficient is taken under typical conditions with grout as $\beta_j = 2/3$. This factor β_j represents the fact that the resistance under the plate might be lower due to the quality of the grout layer after filling.

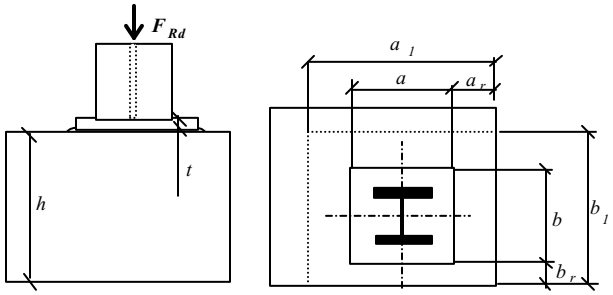

Figure 2.1.1 Evaluation of the concrete block bearing resistance

The flexible base plate, of the area A_p can be replaced by an equivalent rigid plate with area A_{eq}, see Fig 2.1.2. The formula for calculation of the effective bearing area under the flexible base plate around the column cross section can be based on estimation of the effective width c. The prediction of this width c can be based on the T-stub model. The calculation secures that the yield strength of base plate is not exceeded. Elastic bending moment resistance of the base plate per unit length should be taken as

$$M' = \frac{1}{6} \, t^2 \, f_y \tag{2.1.4}$$

and the bending moment per unit length on the base plate acting as a cantilever of span c is, see Figure 2.1.3.

$$M' = \frac{1}{2} \, f_j \, c^2 \tag{2.1.4}$$

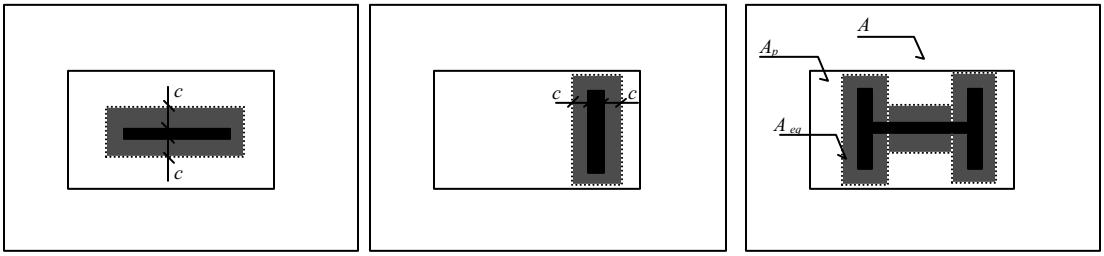

Figure 2.1.2 Flexible base plate modelled as a rigid plate of effective area with effective width *c*

When these moments are equal, the bending moment resistance is reached and the formula evaluating *c* can be obtained

$$\frac{1}{2} f_j \; c^2 = \frac{1}{6} t^2 \; f_y \tag{2.1.4}$$

as

$$c = t \sqrt{\frac{f_y}{3 f_j \; \gamma_{M0}}} \tag{2.1.5}$$

The component is loaded by normal force F_{Sd}. The strength, expecting the constant distribution of the bearing stresses under the effective area, see Figure2.1.3 is possible to evaluate for a component by

$$F_{sd} \leq F_{Rd} = A_{eq} \; f_j = (2 \; c + t_w) \; L \; f_j \tag{2.1.6}$$

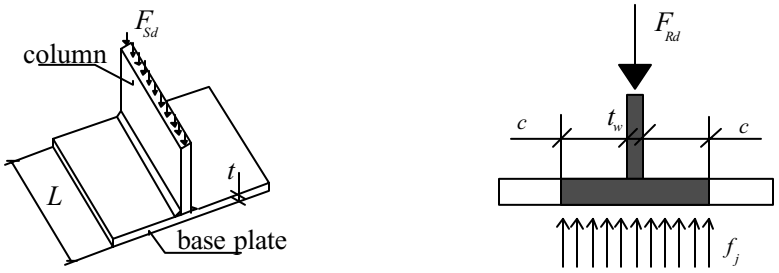

Figure 2.1.3 The T stub in compression, the effective width calculation

The improvement of effective area due to the plate behaviour for plates fixed on three or four edges can be based on elastic resistance of plates (Wald, 1995) or more conservatively can be limited by the deformations of plate as is reached for cantilever prediction. This improvement is not significant for open cross sections, till about 3%. For tubular columns the plate

behaviour increase the strength up to 10% according to the geometry.

The practical conservative estimation of the concentration factor, see Eq. (2.1.1), can be precised by introduction of the effective area into the calculation; into the procedure Eq. (2.1.1) - (2.1.3). This leads however to an iterative procedure and is not recommended for practical purposes.

The grout quality and thickness is introduced by the joint coefficient β_j, see SBR (1973). For $\beta_j = 2 / 3$, it is expected the grout characteristic strength is not less than $0,2$ times the characteristic strength of the concrete foundation $f_{c.g} \geq 0,2\, f_c$ and than the thickness of the grout is not greater than $0,2$ times the smaller dimension of the base plate $t_g \leq 0,2$ *min (a ; b)*.

In cases of different quality or high thickness of the grout $t_g \geq 0,2$ *min (a ; b)*, it is necessary to check the grout separately. The bearing distribution under 45° can be expected in these cases, see Figure 2.1.4., (Bijlaard, 1982).

The influence of packing under the steel plate can be neglected for the design (Wald at al, 1993). The influence of the washer under plate used for erection can be also neglected for design in case of good grout quality $f_{c.g} \geq 0,2\, f_c$. In case of poor grout quality $f_{c.g} \leq 0,2\, f_c$ it is necessary to take into account the anchor bolts and base plate resistance in compression separately.

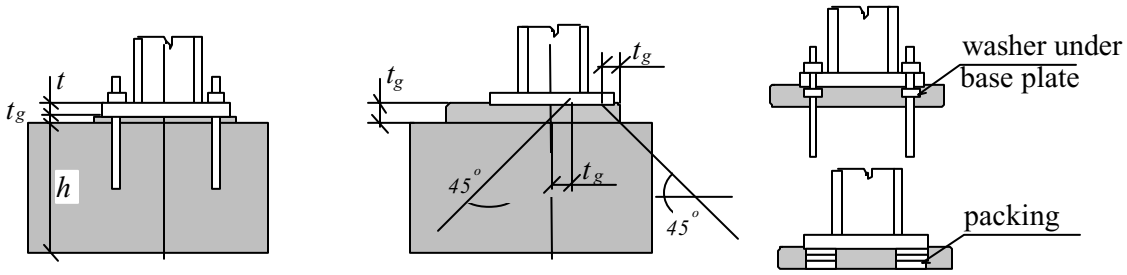

Figure 2.1.4 The stress distribution in the grout

2.1.3.2 Stiffness

The elastic stiffness behaviour of the T-stub components concrete in compression and plate in bending exhibit the interaction between the concrete and the base plate as demonstrated for the strength behaviour. The initial stiffness can be calculated from the vertical elastic deformation of the component. The complex problem of deformation is influenced by the flexibility of the base plate, and by the concrete block quality and size.

The simplified prediction of deformations of a rigid plate supported by an elastic half space is considered first including the shape of the rectangular plate. In a second step, an indication is given how to replace a flexible plate by an equivalent rigid plate. In the last step, assumptions are made about the effect of the size of the block to the deformations under the plate for practical base plates.

The deformation of a rectangular rigid plate in equivalent half space solved by different authors is given in simplified form by Lambe & Whitman, 1967 as

$$\delta_r = \frac{F \ \alpha \ a_r}{E_c \ A_r}, \tag{2.1.6}$$

where

δ_r is the deformation under a rigid plate,
F the applied compressed force,
a_r the width of the rigid plate,
E_c the Young's modulus of concrete,
A_r the area of the plate, $A_r = a_r L$,
L the length of the plate,
α a factor dependent on ratio between L and a_r .

The value of factor α depends on the Poison's ratio of the compressed material, see in Table 2.1.1, for concrete $(\nu \approx 0{,}15)$. The approximation of this values as $\alpha \approx 0{,}85\sqrt{L / a_r}$ can be read from the following Table 2.1.1.

Table 2.1.1 Factor α and its approximation

L / a_r	α according to (Lambe and Whitman, 1967)	Approximation as $\alpha \approx 0{,}85\sqrt{L / a_r}$
1	0,90	0,85
1,5	1,10	1,04
2	1,25	1,20
3	1,47	1,47
5	1,76	1,90
10	2,17	2,69

With the approximation for α, the formula for the displacement under the plate can be rewritten

$$\delta_r = \frac{0,85\ F}{E_c \sqrt{L\ \ a_r}} \qquad (2.1.7)$$

A flexible plate can be expressed in terms of equivalent rigid plate based on the same deformations. For this purpose, half of a T-stub flange in compression is modelled as shown in Figure 2.1.5.

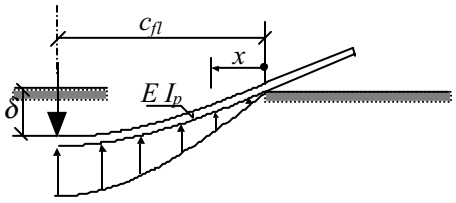

Figure 2.1.5 A flange of a flexible T-stub

The flange of a unit width is elastically supported by independent springs. The deformation of the plate is a sine function, which can be expressed as

$$\delta\,(x) = \delta \sin\,(\,½\pi\ x\ /\ c_{fl}) \qquad (2.1.8)$$

The uniform stress on the plate can then be replaced by the fourth differentiate of the deformation multiplied by $E\ I_p$, where E is the Young's modulus of steel and I_p is the moment of inertia per unit length of the steel plate with thickness t ($I_p = t^3 / 12$).

$$\sigma_{(x)} = E_s\ I_p\ (\,½\pi\ /\ c_{fl})^4\ \delta \sin\,(½\pi\ x\ /\ c_{fl}) = E_s\ \frac{t^3}{12}\ (½\pi\ /\ c_{fl})^4\ \delta \sin\,(\,½\pi\ x\ /\ c_{fl}) \qquad (2.1.9)$$

The concrete part should be compatible with this stress

$$\delta(x) = \sigma_{(x)}\ h_{ef}\ /\ E_c \qquad (2.1.10)$$

where h_{ef} is the equivalent concrete height of the portion under the steel plate. Assume that $h_{ef} = \xi\ c_{fl}$ hence

$$\delta(x) = \sigma_{(x)}\ \xi\ c_{fl}\ /\ E_c \qquad (2.1.11)$$

Substitution gives

$$\delta \sin\,(½\pi\ x\ /\ c_{fl}) = E\ t^3\ /\ 12\ (½\pi\ /\ c_{fl})^4\ \delta \sin\,(\,½\pi\ x\ /\ c_{fl})\ \xi\ c_{fl}\ /\ E_c \qquad (2.1.12)$$

This may be expressed as

$$c_{fl} = t \sqrt[3]{\frac{(\pi/2)^4}{12} \xi \frac{E}{E_c}} \tag{2.1.13}$$

The flexible length c_{fl} may be replaced by an equivalent rigid length c_r such that uniform deformations under an equivalent rigid plate give the same force as the non uniform deformation under the flexible plate:

$$c_r = c_{fl}\ 2 / \pi \tag{2.1.14}$$

The factor ξ represents the ratio between h_{ef} and c_{fl}. The value of h_{ef} can be expressed as $\alpha\, a_r$. From Tab. 2.1 can be read that factor α for practical T-stubs is about equal to *1,4*. The width a_r is equal to $t_w + 2\ c_r$, where t_w is equal to the web thickness of the T-stub. As a practical assumption it is now assumed that t_w equals to 0,5 c_r which leads to

$$h_{ef} = 1{,}4 \cdot (0{,}5 + 2)\ c_r = 1{,}4 \cdot 2{,}5\ c_{fl}\ 2 / \pi = 2{,}2\ c_{fl} \tag{2.1.15}$$

hence $\xi = 2{,}2$

For practical joints can be estimated by $E_c \cong 30\,000\ N/mm^2$ and $E \cong 210\,000\ N/mm^2$, which leads to

$$c_{fl} = t \sqrt[3]{\frac{(\pi/2)^4}{12} \xi \frac{E}{E_c}} \approx t \sqrt[3]{\frac{(\pi/2)^4}{12} 2{,}2 \frac{210\,000}{30\,000}} \cong 1{,}98\ . \tag{2.1.16}$$

or

$$c_r = 1{,}26\ t \approx 1{,}25\ t\ , \tag{2.1.17}$$

which gives for the effective width calculated based on elastic deformation

$$a_{eq.el} = t_w + 2{,}5\ t \tag{2.1.18}$$

The influence of the finite block size compared to the infinite half space can be neglected in practical cases. For example the equivalent width a_r of the equivalent rigid plate is about $t_w + 2\ c_r$. In case t_w is *0,5* c_r and $c_r = 1{,}25\ t$ the width is $a_r = 3{,}1\ t$. That means, peak stresses are even in the elastic stage spread over a very small area.

In general, a concrete block has dimensions at least equal to the column with and column depth. Furthermore it is not unusual that the block height is at least half of the column depth. It means, that stresses under the flange of a T-stub, which represents for instance a plate under a column flange, are spread over a relative big area compared to $a_r = 3{,}1\ t$. If stresses are spread, the strains will be low where stresses are low and therefore these strains will not contribute significantly to the deformations of the concrete just under the plate. Therefore, for

simplicity it is proposed to make no compensation for the fact that the concrete block is not infinite.

From the strength procedure the effective with of a T-stub is calculated as

$$a_{eq.str} = t_w + 2\,c = t_w + 2\,t\sqrt{\frac{f_y}{3\,f_j\,\gamma_{M0}}} \tag{2.1.19}$$

Based on test, see Figure 2.1.7 - 2.1.8, and FE simulation, see Figure 2.1.9, it may occur that the value of $a_{\text{eq.str}}$ is also a sufficient good approximation for the width of the equivalent rigid plate as the expression based on elastic deformation only. If this is the case, it has a practical advantage for the application by designers. However, in the model $a_{\text{eq.str}}$ will become dependent on strength properties of steel in concrete, which is not the case in the elastic stage, On Figure 2.1.6 is shown the influence of the base plate steel quality for particular example on the concrete quality - deformation diagram for flexible *plate* $t = t_w = 20\,mm$, $L_{eff} = 300\,mm, F = 1000\,kN$. From the diagram it can be seen that the difference between $a_{eq.el} = t_w + 2{,}5\,t$ and $a_{eq.str} = t_w + 2\,c$ is limited.

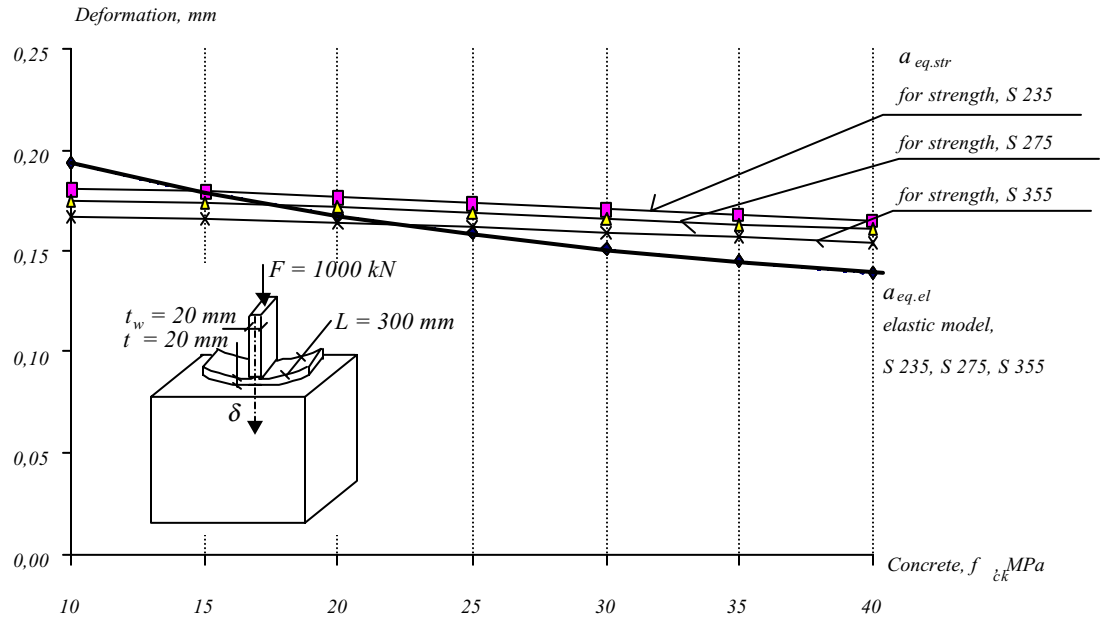

Figure 2.1.6 Comparison of the prediction of the effective width on concrete - deformation diagram for particular example for unlimited concrete block $k_j = 5$, base plate and web thickness $20\,mm$, $L = 300\,mm$, force $F = 1000\,kN$

The concrete surface quality is affecting the stiffness of this component. Based on the tests Alma and Bijlaard, (1980), Sokol and Wald, (1997). The reduction of modulus of elasticity

of the upper layer of concrete of thickness of *30 mm* was proposed (Sokol and Wald, 1997) according to the observation of experiments with concrete surface only, with poor grout quality and with high grout quality. For analytical prediction the reduction factor of the surface quality was observed from *1,0* till *1,55*. For the proposed model the value *1,50* had been proposed, see Figure 2.1.12 and 2.1.13, see Eq. (2.1.20).

The simplified procedure to calculate the stiffness of the component concrete in compression and base plate in bending can be summarised in Eurocode 3 Annex J form as

$$k_c = \frac{F}{\delta E} = \frac{E_c \sqrt{a_{eq.el} L}}{1{,}5 * 0{,}85 E} = \frac{E_c \sqrt{a_{eq.el} L}}{1{,}275\, E}, \tag{2.1.20}$$

where

$a_{eq.el}$	the equivalent width of the T-stub, $a_{e.el} = t_w + 2{,}5\ t$,
L	the length of the T-stub,
t	the flange thickness of the T-stub, the base plate thickness,
t_w	the web thickness of the T-stub, the column web or flange thickness.

2.1.4 Validation

The proposed model is validated against the tests for strength and for stiffness separately. 50 tests in total were examined in this part of study to check the concrete bearing resistance (DEWOLF, 1978, HAWKINS, 1968). The test specimens consist of a concrete cube of size from 150 to 330 mm with centric load acting through a steel plate. The size of the concrete block, the size and thickness of the steel plate and the concrete strength are the main variables.

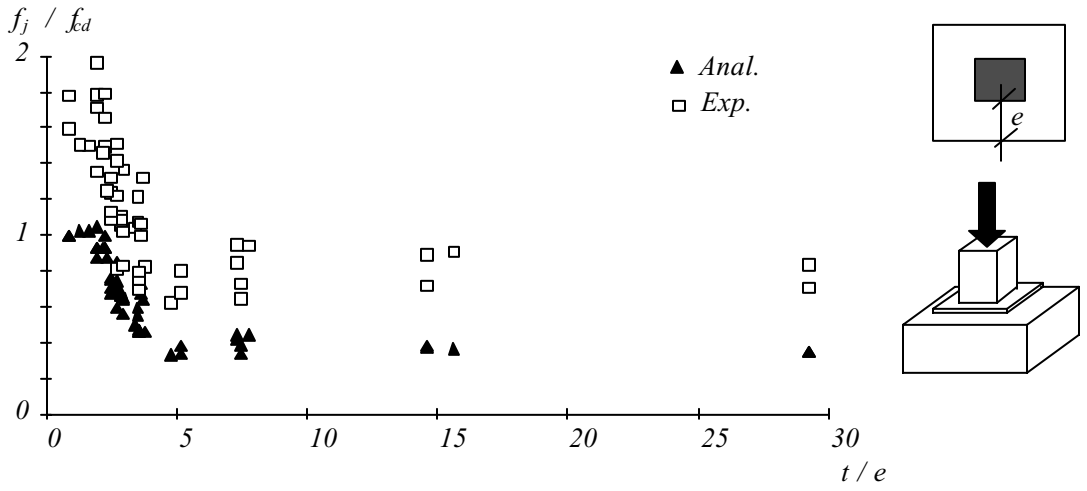

Figure 2.1.7 Relative bearing resistance-base plate slenderness relationship (experiments DeWolf, 1978, and Hawkins, 1968)

Figure 2.1.7 shows the relationship between the slenderness of the base plate, expressed as a ratio of the base plate thickness to the edge distance and the relative bearing resistance. The design approach given in Eurocode 3 is in agreement with the test results, but conservative. The bearing capacity of test specimens at concrete failure is in the range from 1,4 to 2,5 times the capacity calculated according to Eurocode 3 with an average value of 1,75.

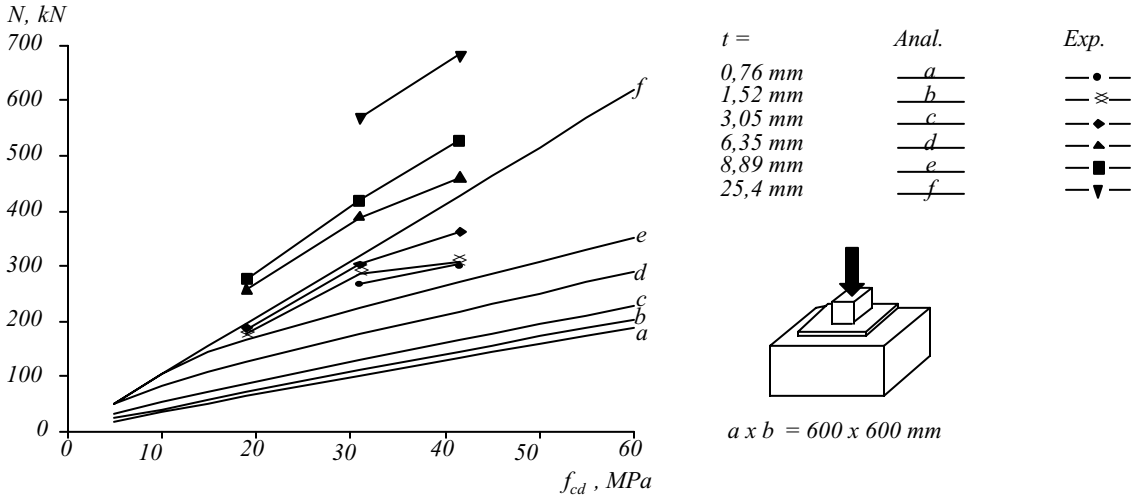

Figure 2.1.8 Concrete strength - ultimate load capacity relationship (Hawkins, 1968)

The influence of the concrete strength is shown on Figure 2.1.8, where is shown the validation of the proposal based on proposal $t_w + 2\,c$. A set of 16 tests with similar geometry and material properties was used in this diagram from the set of tests (Hawkins, 1968). The only variable was the concrete strength of *19, 31* and *42 MPa*.

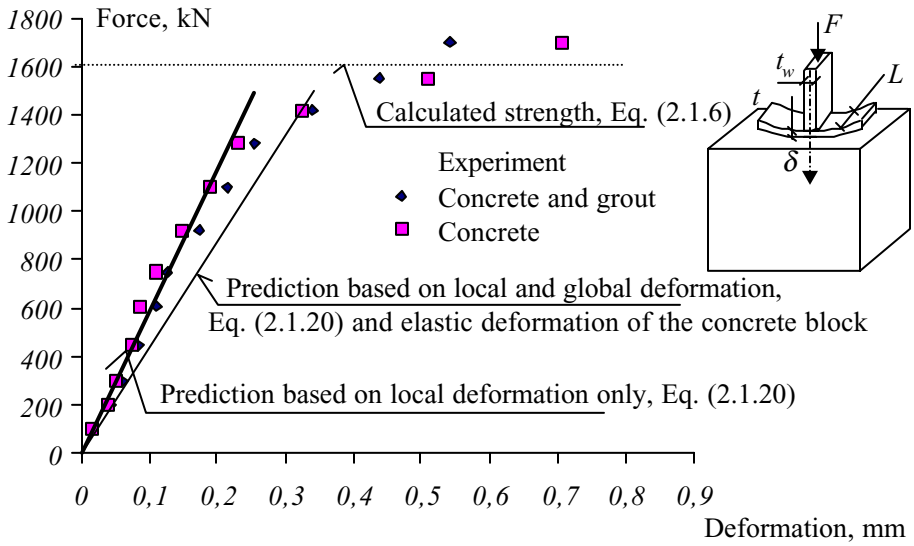

Figure 2.1.9 Comparison of the stiffness prediction to Test 2.1, (Alma and Bijlaard, 1980), concrete block *800x400x320 mm,* plate thickness $t = 32{,}2$ *mm*, T stub length $L = 300$ *mm*

The stiffness prediction is compared to tests Alma and Bijlaard, (1980) in Figure 2.1.9. and 2.1.10. The tests of flexible plates on concrete foundation are very sensitive to boundary conditions (rigid tests frame) and measurements accuracy (very high forces and very small deformations). The predicted value based on eq. (2.1.7) is the local deformation only. The elastic global and local deformation of the whole concrete block is shown separately. Considering the spread in test results and the accuracy achievable in practice, the comparison shows a sufficiently good accuracy of prediction.

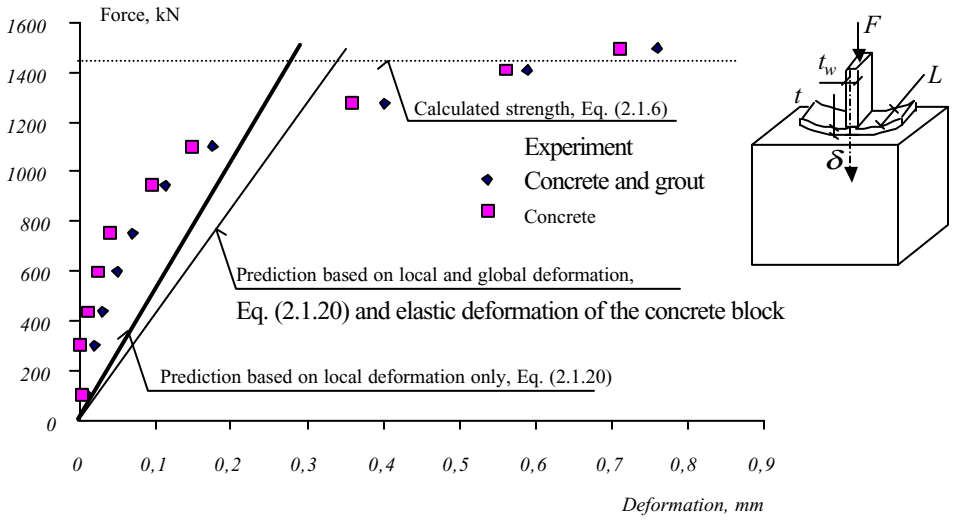

Figure 2.1.10 Comparison of the stiffness prediction to Test 2.2, (Alma and Bijlaard, 1980), concrete block *800x400x320 mm*, plate thickness $t = 19$ *mm*, T stub length $L = 300$ *mm*

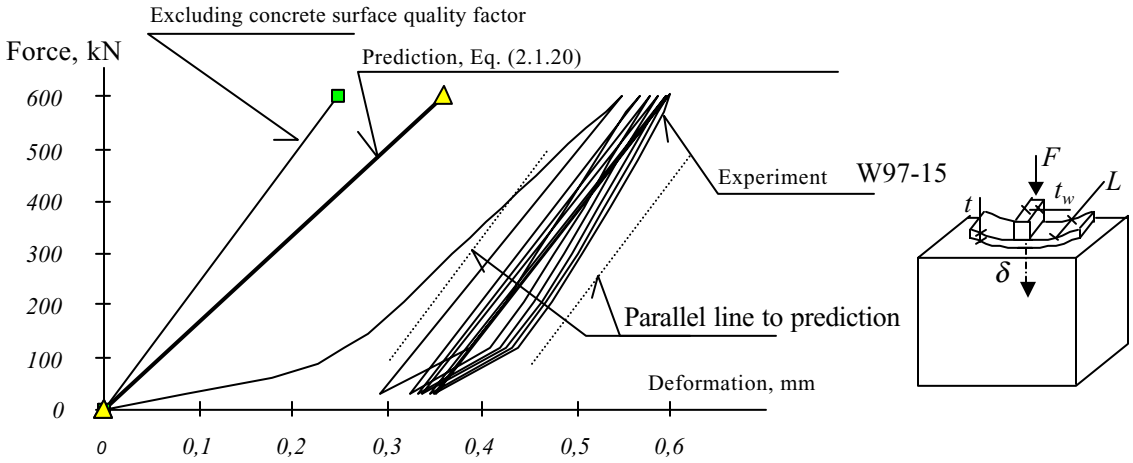

Figure 2.1.11 Comparison of the stiffness prediction to Test W97-15, repeated loading, cleaned concrete surface without grout only (Sokol and Wald, 1997), concrete block *550 x 550 x 500 mm*, plate thickness $t = 12$ *mm*, T stub length $L = 335$ *mm*

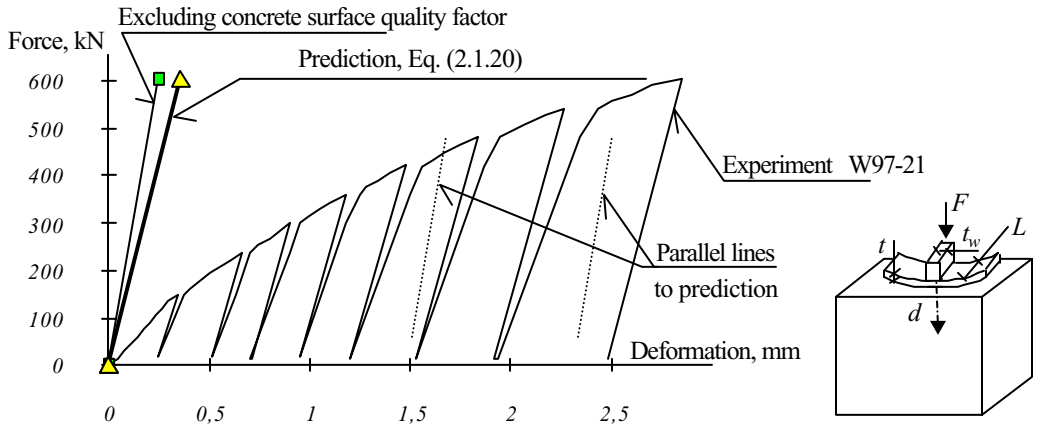

Figure 2.1.12 Comparison of the stiffness prediction to Test W97-15 repeated and increasing loading, cleaned concrete surface low quality grout (Sokol and Wald, 1997), concrete block *550 x 550 x 500 mm*, plate thickness $t = 12$ *mm*, T stub length $L = 335$ *mm*

The comparison of local and global deformations can be shown on Finite Element (FE) simulation. In Figure 2.1.11 the prediction of elastic deformation of rigid plate 100 x 100 mm on concrete block 500 x 500 x 500 mm is compared to calculation using the FE model.

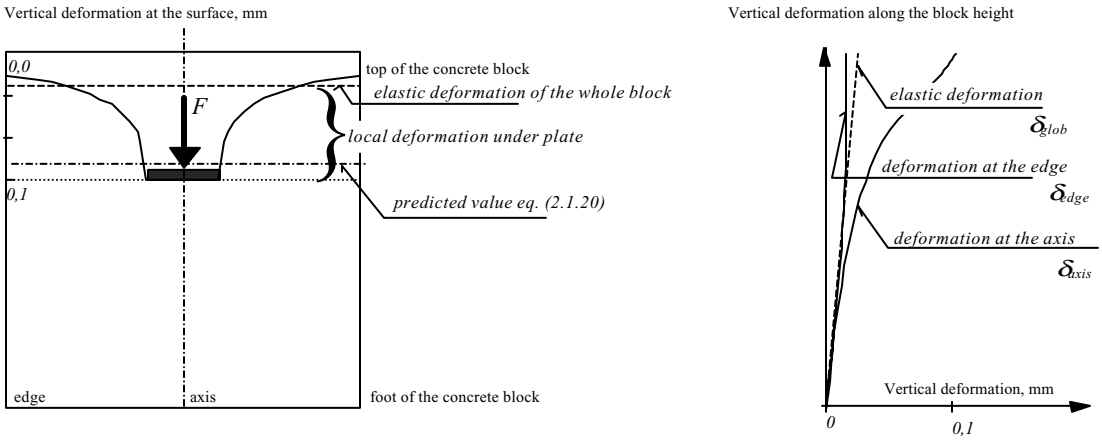

Figure 2.1.13 Calculated vertical deformations of a concrete block *0,5 x 0,5 x 0,5 m* loaded to a deflection of *0,01 mm* under a rigid plate *0,1 x 0,1 m*; in the figure on the right, the deformations along the vertical axis of symmetry δ_{axis} are given and the calculated deformations at the edge δ_{edge}, included are the global elastic deformations according to $\delta_{glob} = F\,h\,/(E_c\,A_c)$, where A_c is full the area of the concrete block

Based on these comparisons, the recommendation is given that for practical design, besides the local effect of deformation under a flexible plate, the global deformation of the supporting concrete structure must be taken into consideration.

2.2 Column flange and web in compression

2.2.1 Description of the component

In this section, the mechanical characteristics of the "column flange and web in compression" component are presented and discussed. This component, as its name clearly indicates, is subjected to tension forces resulting from the applies bending moment and axial force in the column (Figure 2.2.1).

The proposed rules for resistance and stiffness evaluation given hereunder are similar to those included in revised Annex J of Eurocode 3 for the "beam flange and web in compression" component in beam-to-column joints and beam splices.

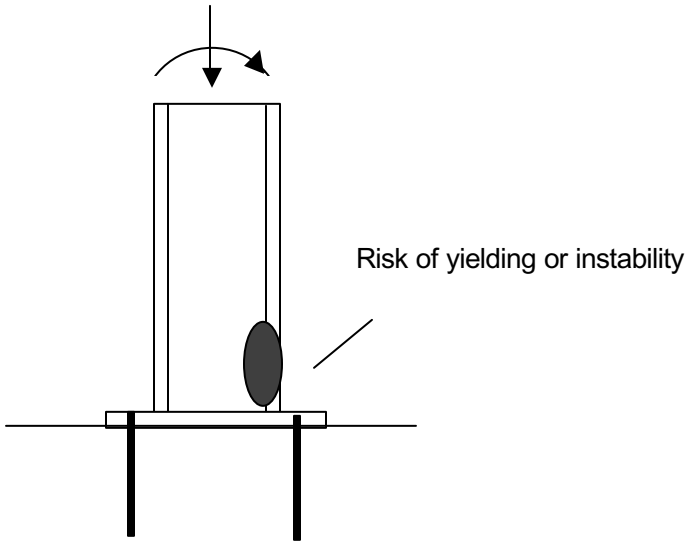

Figure 2.2.1 Component "column flange and web in compression"

2.2.2 Resistance

When a bending moment M and a axial force N are carried over from the column to the concrete block, a compression zone develops in the column, close to the column base; it includes the column flange and a part of the column web in compression. The compressive force F_c carried over by the joint may, as indicated in Figure 2.2.2, is quite higher than the compressive force F in the column flange resulting from the resolution, at some distance of the joint, of the same bending moment M and axial force N. In Figure 2.2.2, the forces F and F_c are applied to the centroï d of the column flange in compression.

This assumption is usually made for sake of simplicity but does not correspond to the reality as the compression zone is not only limited to the column flange.

The force F_c, quite localized, may lead to the instability of the compressive zone of the column cross-section and has therefore to be limited to a design value which is here defined in a similar way than in Annex J for beam flange and web in compression :

$$F_{c.fb.Rd} = M_{c.Rd} /(h_c - t_{fc}) \qquad (2.2.1)$$

where :

$M_{c.Rd}$ is the design moment resistance of the column cross-section reduced, when necessary, by the shear forces; $M_{c.Rd}$ takes into consideration by itself the potential risk of instability in the column flange or web in compression;

h_b is the whole depth of the column cross-section;

t_{fb} is the thickness of the column flange.

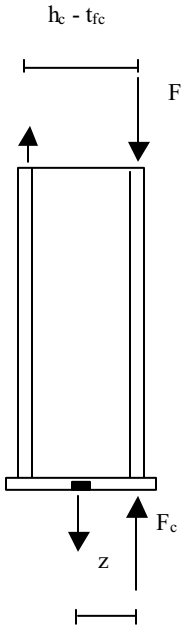

- M and N applied as in Figure 2.2.1
- $F = N/2 + M/(h_b-t_{fb})$
- $F_c = N/2 + M/z$

  $\Rightarrow F < F_c$

Figure 2.2.2 Localized compressive force in the column cross-section located close to the column base

It has to be pointed out that Formula (2.2.1) limits the maximum force which can be carried over in the compressive zone of the joint because of the risk of loss of resistance or instability in the possibly overloaded compressive zone of the column located close to the joint. It therefore does not replace at all the classical verification of the resistance of the column cross-

section.

It has also to be noted that formula (2.2.1) applies whatever is the type of connection and the type of loading acting on the column base. It is also referred to in the preliminary draft of Eurocode 4 Annex J in the case of composite construction and applies also to beam-to-column joints and beam splices where the beams are subjected to combined moments and shear and axial compressive or tensile forces. It is therefore naturally extended here to column bases.

The design resistance given by Formula (2.2.1) has to be compared to the compressive force F_c (see Figure 2.2.2) which results from the distribution of internal forces in the joint and which is also assumed to be applied at the centroïd of the column flange in compression. It integrates the resistance of the column flange and of a part of the column web; it also covers the potential risk of local plate instability in both flange and web.

2.2.3 Stiffness

The deformation of the column flange and web in compression is assumed not to contribute to the joint flexibility. No stiffness coefficient is therefore needed.

2.3 Base plate in bending and anchor bolt in tension

When the anchor bolts are activated in tension, the base plate is subjected to tensile forces and deforms in bending while the anchor bolts elongate. The failure of the tensile zone may result from the yielding of the plate, from the failure of the anchor bolts, or from a combination of both phenomena.

Two main approaches respectively termed "plate model" and "T-stub model" are referred to in the literature for the evaluation of the resistance of such plated components subjected to transverse bolt forces.

The first one, the "plate model", considers the component as it is - i.e. as a plate - and formulae for resistance evaluation are derived accordingly. The actual geometry of the component, which varies from one component to another, has to be taken into consideration in an appropriate way; this leads to the following conclusions :

- the formulae for resistance varies from one plate component to another;
- the complexity of the plate theories are such that the formulae are rather complicated and therefore not suitable for practical applications.

The T-stub idealisation, on the other hand, consists of substituting to the tensile part of the joint T-stub sections of appropriate effective length ℓ_{eff}, connected by their flange onto a presumably infinitely rigid foundation and subject to a uniformly distributed force acting in the web plate, see Figure 2.3.1.

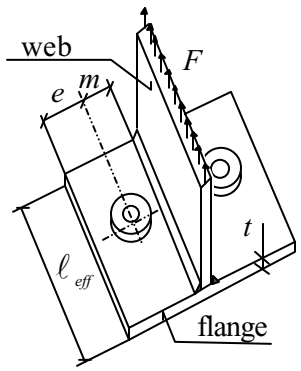

Figure 2.3.1 T-stub on rigid foundation

In comparison with the plate approach, the T-stub one is easy to use and allows to cover all the plated components with the same set of formulae. Furthermore, the T-stub concept may also be referred to for stiffness calculations as shown in (Jaspart, 1991) and Yee, Melchers, 1986).

This explains why the T-stub concept appears now as the standard approach for plated components and is followed in all the modern characterisation procedures for components, and in particular in Eurocode 3 revised Annex J (1998) for beam-to-column joints and column bases.

In the next pages, the evaluation of the resistance and stiffness properties of the T-stub are discussed in the particular context of column bases and proposals for inclusion in forthcoming European regulations are made.

2.3.1 Design resistance of plated components

2.3.1.1 Basic formulae of Eurocode 3

The T-stub approach for resistance, as it is described in Eurocode 3, has been first introduced by Zoetemeijer (1974) for unstiffened column flanges. It has been then improved (Zoetemeijer, 1985) so as to cover other plate configurations such as stiffened column flanges and end-plates. In Jaspart (1991), it is also shown how to apply the concept to flange cleats in bending.

In plated components, three different failure modes may be identified :

a) Bolt fracture without prying forces, as a result of a very large stiffness of the plate (Mode 3)

b) Onset of a yield lines mechanism in the plate before the strength of the bolts is exhausted (Mode 1)

c) Mixed failure involving yield lines - but not a full plastic mechanism - in the plate and exhaustion of the bolt strength (Mode 2).

Similar failure modes may be observed in the actual plated components (column flange, end plates, …) and in the flange of the corresponding idealised T-stub. As soon as the effective length ℓ_{eff} of the idealised T-stubs is chosen such that the failure modes and loads of the actual plate and the Tstub flange are similar, the T-stub calculation can therefore be substituted to that of the actual plate.

In Eurocode 3, the design resistance of a T-stub flange of effective length ℓ_{eff} is derived as follows for each failure mode :

Mode 3: bolt fracture (Figure 2.3.2.a)

$$F_{Rd,3} = \Sigma B_{t.Rd} \tag{2.3.1}$$

Mode 1: plastic mechanism (Figure 2.3.2.b)

$$F_{Rd,1} = \frac{4\ell_{eff} m_{pl,Rd}}{m} \tag{2.3.2}$$

Mode 2: mixed failure (Figure 2.3.2.c)

$$F_{Rd,2} = \frac{2\ell_{eff} m_{pl,Rd} + \Sigma B_{t.Rd} n}{m+n} \tag{2.3.3}$$

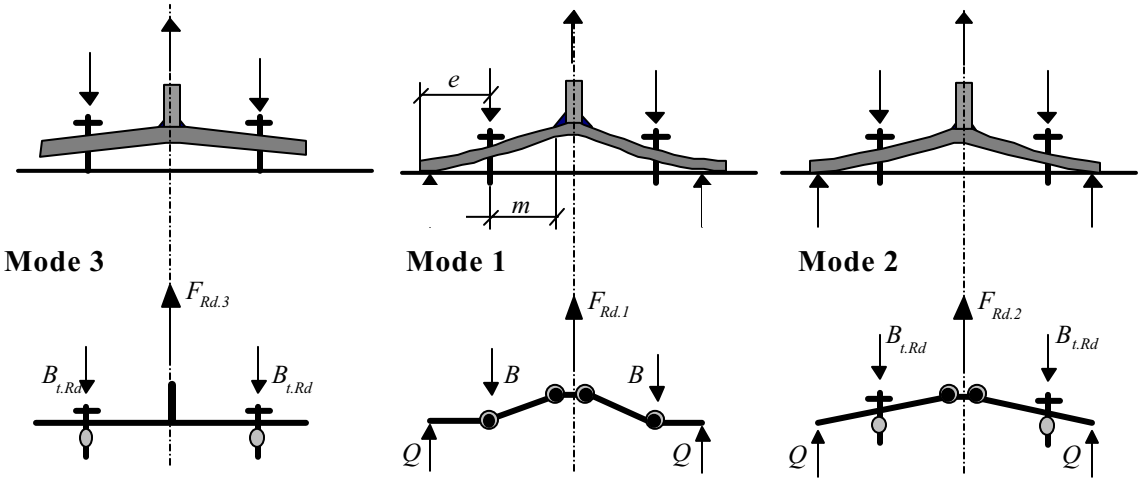

Figure 2.3.2 Failure modes in a T-stub

In these expressions :

$m_{pl,Rd}$	is the plastic moment of the T-stub flange per unit length ($\frac{1}{4} t^2 f_y / \gamma_{M0}$) with t = flange thickness, f_y = yield stress of the flange, γ_{M0} = partial safety factor)
m and e	are geometrical characteristics defined in Figure 2.3.2.
$\Sigma B_{t.Rd}$	is the sum of the design resistances $B_{t.Rd}$ of the bolts connecting the T-stub to the foundation ($B_{t.Rd} = 0,9\ A_s f_{ub} / \gamma_{Mb}$ where A_s is the tensile stress area of the bolts, f_{ub} the ultimate stress of the bolts and γ_{Mb} a partial safety factor)
n	designates the place where the prying force Q is assumed to be applied, as shown in Figure 2.3.2 ($n = e$, but its value is limited to 1,25 m).
ℓ_{eff}	is derived at the smallest value of the effective lengths corresponding to all the possible yield lines mechanisms in the specific T-stub flange being considered.

The design strength F_{Rd} of the T-stub is derived as the smallest value got from expressions (2.3.1) to (2.3.3) :

$$F_{Rd} = min(F_{Rd,1}, F_{Rd,2}, F_{Rd,3}) \qquad (2.3.4)$$

In Jaspart (1991), the non-significative influence of the possible shear-axial-bending stress interactions in the yield lines on the design capacity of T-stub flanges has been shown.

In Annex J, the influence on Mode 1 failure of backing plates aimed at strengthening the column flanges in beam-to-column bolted joints is also considered. A similar influence may result, in

column bases, from the use of washer plates. The effect of the latter on the base plate resistance will be taken into consideration in a similar way than it is done in Annex J for backing plates.

This calculation procedure recommended first by Zoetemeijer has been refined when revising the Annex J of Eurocode 3.

Eurocode 3 distinguishes now between so-called circular and non-circular yield lines mechanisms in T-stub flanges (see Figure 2.3.3.a). These differ by their shape and lead to specific values of T-stub effective lengths noted respectively $\ell_{eff,cp}$ and $\ell_{eff,np.}$ But the main difference between circular and non-circular patterns is linked to the development or not of prying forces between the T-stub flange and the rigid foundation : circular patterns form without any development of prying forces Q, and the reverse happens for non-circular ones.

The direct impact on the different possible failure modes is as follows :

Mode 1 : the presence or not of prying forces do not alter the failure mode which is linked in both cases to the development of a complete yield mechanism in the plate. Formula (2.3.2) applies therefore to circular and non-circular yield patterns.

Mode 2 : the bolt fracture clearly results here from the over-loading of the bolts in tension because of prying effects; therefore Mode 2 only occurs in the case of non-circular yield lines patterns.

Mode 3 : this mode does not involve any yielding in the flange and applies therefore to any T-stub.

As a conclusion, the calculation procedure differs according to the yield line mechanisms developing in the T-stub flange (Figure 2.3.3.b) :

$$F_{Rd} = min(F_{Rd,1} ; F_{Rd,3}) \qquad \text{for circular patterns} \qquad (2.3.5.a)$$

$$F_{Rd} = min(F_{Rd,1} ; F_{Rd,2} ; F_{Rd,3}) \qquad \text{for non-circular patterns} \qquad (2.3.5.b)$$

In Annex J, the procedure is expressed in a more general way. All the possible yield line patterns are considered through recommended values of effective lengths grouped into two categories : circular and non-circular ones. The minimum values of the effective lengths - respectively termed $\ell_{eff,cp}$ and $\ell_{eff,np}$ - are therefore selected for category. The failure load is then derived, by means of Formula (2.3.4), by considering successively all the three possible failure modes, but with specific values of the effective length :

Mode 1 : $\ell_{eff,1} = \min(\ell_{eff,cp}; \ell_{eff,nc})$ (2.3.6.a)

Mode 2 : $\ell_{eff,2} = \ell_{eff,nc}$ (2.3.6.b)

Mode 3 : - (2.3.6.c)

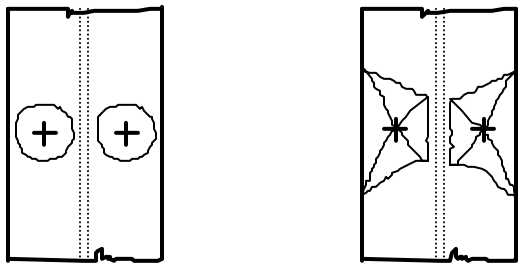

Circular pattern ($\ell_{eff,cp}$) Non-circular patterns ($\ell_{eff,nc}$)

(a) Different yield line patterns

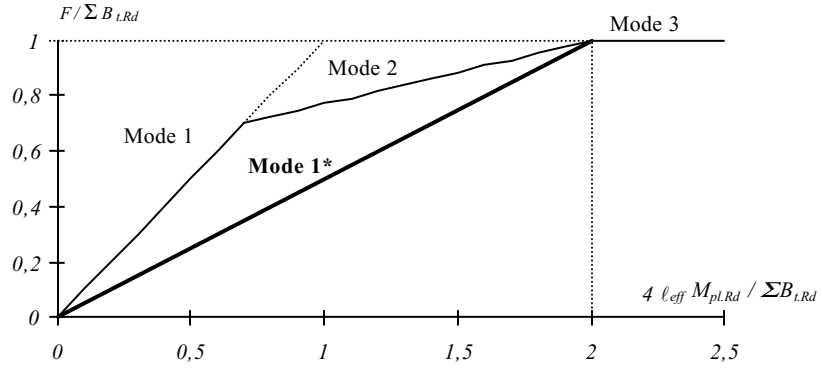

(b) Design resistance

Figure 2.3.3 T-stub resistance according revised Annex J

2.3.1.2 Alternative approach for Mode 1 failure

The accuracy of the T-stub approach is quite good when the resistance is governed by failure modes 2 and 3. The formulae for failure mode 1, on the other hand, has been seen quite conservative, and sometimes too conservative, when a plastic mechanism forms in the T-stub flange (Jaspart, 1991).

Therefore the question raised whether refinements could be brought to the T-stub model of Eurocode 3 with the result that the amended model would provide a higher resistance for failure mode 1 without altering significantly the accuracy regarding both failure modes 2 and 3.

In (Jaspart, 1991), an attempt has been made in this respect. In the Zoetemeijer's approach, the forces in the bolts are idealised as point loads. Thus, it is never explicitly accounted for the actual sizes of the bolts and washers. If this is done, the following resistance may be expressed for Mode 1 (Jaspart, 1991):

$$F_{Rd,1} = \frac{(8n - 2e_w)\ell_{eff,1} m_{pl,Rd}}{\left[2mn - e_w(m+n)\right]} \qquad (2.3.7)$$

with $e_w = 0.25\, d_w$ (d_w designates the diameter of the bolt/screw or of the washer if any.

Of course, Equation (2.3.7) confines itself to Zoetemeijer's formulae (2.3.2) when distance e_w is vanishing.

During the recent revision of Annex J of Eurocode 3, formula (2.3.7) which describes the Mode 1 failure as dependent on the actual bolt dimensions has been agreed for inclusion as an alternative to formula (2.3.2).

2.3.2 Initial stiffness of plated components

2.3.2.1 Application of the T-stub approach

For plated components, it is also referred to the T-stub concept, see Figure 2.3.4.

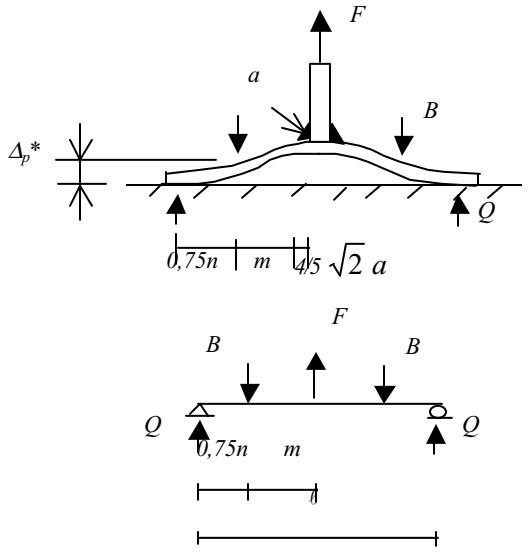

Figure 2.3.4 T-stub elastic deformability

In a T-stub, the tensile stiffness results from the elastic deformation of the T-stub flange in bending and of the bolts in tension (the role of the latter is plaid by the anchor bolts in section 2.3.3 dealing explicitly with column bases). When evaluating the stiffness of the T-stub, the compatibility between the respective deformabilities of the T-stub flange and of the bolts has to be ensured :

$$\Delta^*_p = \Delta_b \tag{2.3.8}$$

where Δ_p* is the deformation of the end-plate at the level of the bolts;

Δ_b is the elongation of the bolts.

In Jaspart (1991), expressions providing the elastic initial stiffness of the T-stub are proposed; they allow the coupling effect between the T-stubs to be taken into consideration. These expressions slightly differ from those given in the original publication of Yee and Melchers (1986).

The elongation Δ_b of the bolts simply results from the elongation of the bolt shank subjected to tension:

$$\Delta_b = \frac{B}{E\ A_S} L_b \qquad (2.3.9)$$

where L_b is approximately defined as the length of the bolt shank in Eurocode 3.

From these considerations, the elastic deformation of the two T-stub may be derived :

$$\Delta_p = \frac{F}{E\ k_{i,p}} \qquad (2.3.10)$$

where the stiffness coefficient $k_{i,p}$ is expressed as :

$$k_{i,p} = \left[Z\ (\frac{1}{8} - \frac{1}{4} q\ \alpha\ ) \right]^{-1} \qquad (2.3.11)$$

$$q = \frac{Z_p a_1}{Z\ \alpha_2 + \frac{\ell_b}{2A_S}} \qquad (2.3.12)$$

In these formulae :

$Z = 2\ \ell^3 / b\ t^3$ $\qquad$ $\ell = 2\ (m + 0{,}75\ n\ )$

$\alpha_1 = 1{,}5\ \alpha - 2\ \alpha^3$ $\qquad$ b is the T-stub length

$\alpha_2 = 6\ \alpha^2 - 8\ \alpha^3$ $\qquad$ $\alpha = 0{,}75\ n / \ell$

All the geometrical properties are defined in Figure 3.2.4.

The validity of these formulae has been demonstrated in Jaspart (1991) on the basis of a quite large number of comparisons with test results on joints with end-plate and flange cleated connections got from the international literature.

2.3.2.2 Simplified stiffness coefficients for inclusion in Eurocode 3

The application of the T-stub concept to a simplified stiffness calculation - as that to be included in a code such Eurocode 3 - requires to express the equivalence between the actual component and the equivalent T-stub in the elastic range of behaviour and that, in a different way than at collapse; this is achieved through the definition of a new effective length called $\ell_{eff,ini}$ which differs from the ℓ_{eff} value to which it has been referred to in section 2.3.1. In

view of the determination of the stiffness coefficient k_{ip}, two problems have to be investigated:

- the response of a T-stub in the elastic range of behaviour;
- the determination of $\ell_{eff,ini}$.

These two points are successively addressed hereunder.

T-stub response

The T-stub response in the elastic range of behaviour is covered in section 2.3.1.1. The corresponding expressions are rather long to apply, but some simplifications may be introduced:

- to simplify the formulae: n is considered as equal to $1{,}25\,m$;
- to dissociate the bolt deformability (Figure 2.3.5.c) from that of the T-sub (Figure 2.3.5.b).

The value of q given by expressions (2.3.12) may then be simplified to :

$$q = \frac{\alpha_1}{\alpha_2} = \frac{1{,}5\,\alpha - 2\,\alpha^3}{6\,\alpha^2 - 8\,\alpha^3} \tag{2.3.13}$$

as soon as it is assumed, as in Figure 2.3.5.b, that the bolts are no more deforming in tension $(A_s = \infty)$. q further simplifies to:

$$q = 1{,}282 \tag{2.3.14}$$

by substituting $1{,}25\,m$ to $0{,}75\,n$ as assumed previously.

The stiffness coefficient given by formula (2.3.11) therefore becomes :

$$k_{i,p} = \frac{193{,}64}{Z} = \frac{193{,}64\;\; t^3 \ell_{eff,ini}}{2(4{,}5m)^3} \tag{2.3.15}$$

The effective length $\ell_{eff,ini}$ has been substituted to b.

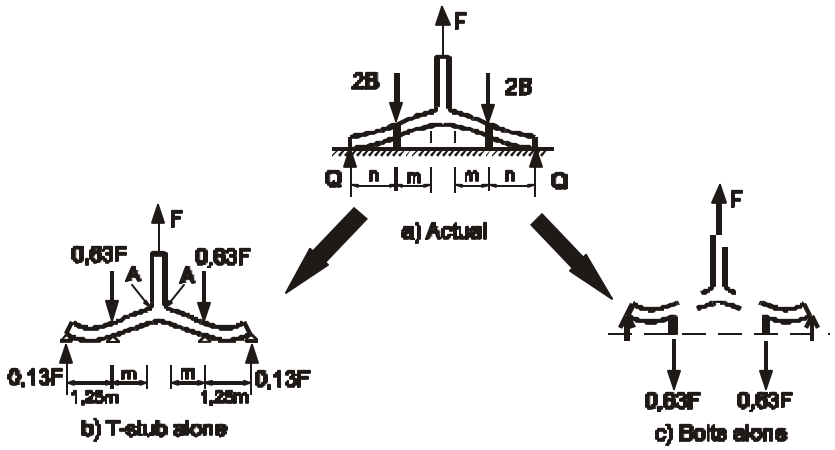

Figure 2.3.5 Elastic deformation of the T-stub

Finally :

$$k_{i,p} = 1{,}063\frac{\ell_{eff,ini}t^3}{m^3} \approx \frac{\ell_{eff,ini}t^3}{m^3} \tag{2.3.16}$$

In the frame of the assumptions made, it may be shown that the prying effect increases the bolt force from 0,5 F to 0,63 F (Figure 2.3.5.c). In Eurocode 3, the deformation of a bolt in tension is taken as equal to :

$$\Delta_b = \frac{B\,L_b}{E\,A_s} \tag{2.3.17}$$

By substituting B by $0{,}63\,F$ in (2.3.17), the stiffness coefficient of a bolt row with two bolts may be derived :

$$k_{i,b} = 1{,}6\frac{A_s}{L_b} \tag{2.3.18}$$

Definition of effective length $\ell_{eff,ini}$

In Figure 2.3.5.c, the maximum bending moment in the T-stub flange (points A) is expressed as $M_{max} = 0{,}322\,F\,m$. Based on this expression, the maximum elastic load (first plastic hinges in the T-stub at points A) to be applied to the T-stub may be derived :

$$F_{e\ell} = \frac{4\ell_{eff,ini}}{1{,}288\,m}\frac{t^2 f_y}{4\gamma_{M0}} = \frac{\ell_{eff,ini}\,t^2}{1{,}288\,m}\frac{f_y}{\gamma_{M0}} \tag{2.3.19}$$

In Annex J, the ratio between the design resistance and the maximum elastic resistance of each of the components is taken as equal to 3/2 so :

$$F_{Rd} = \frac{3}{2} F_{e\ell} = \frac{\ell_{eff,ini}\, t^2}{0{,}859\, m} \frac{f_y}{\gamma_{MO}} \tag{2.3.20}$$

As, in Figure 2.3.5.b, the T-stub flange is supported at the bolt level, the only possible failure mode of the T-stub is the development of a plastic mechanism in the flange. The associated failure load is given by Annex J as:

$$F_{Rd} = F_{Rd} = \frac{\ell_{eff}\, t^2 f_y}{m\, \gamma_{Mo}} \tag{2.3.21}$$

where ℓ_{eff} is the effective length of the T-stub for strength calculation.

By identification of expressions (2.3.20) and (2.3.21), $\ell_{eff,ini}$ may be derived :

$$\ell_{eff,ini} = 0{,}859 \quad \ell_{eff} = 0{,}85 \quad \ell_{eff} \tag{2.3.22}$$

Finally, by introducing equation (2.3.22) in the expression (2.3.18) giving the value of $k_{i,p}$ for any plated component :

$$k_{i,p} = \frac{0{,}85 \quad \ell_{eff,1}\, t^3}{m^3} \tag{2.3.23}$$

2.3.3 Extension to base plates

To evaluate the resistance and stiffness properties of a base plate in bending and anchor bolts in tension, reference is also made to the T-stub idealisation.

2.3.3.1 Resistance properties

Three failure modes are identified in Section 2.3.1.1 for equivalent T-stubs of beam end-plates and column flanges: Mode 1, Mode 2 and Mode 3. Related formulae may be applied to column base plates as well.

But in the particular case of base plates, it may happen that the elongation of the anchor bolts

in tension is such, in comparison to the flexural deformability of the base plate, that no prying forces develop at the extremities of the T-stub flange. In this case, the failure results either from that of the anchor bolts in tension (Mode 3) or from the yielding of the plate in bending (see Figure 2.3.6) where a "two hinges" mechanism develops in the T-stub flange. This failure is not likely to appear in beam-to-column joints and splices because of the limited elongation of the bolts in tension. This particular failure mode is named "Mode 1*".

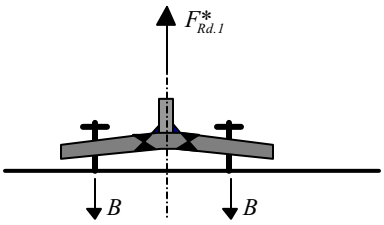

Figure 2.3.6 Mode 1** failure

The corresponding resistance writes :

$$F^{**}_{Rd.1} = \frac{2\,\ell_{eff}\,m_{pl.Rd}}{m} \qquad (2.3.24)$$

When the Mode 1* mechanism forms, large base plate deformations develop; they may result in contacts between the concrete block and the extremities of the Tstub flange, i.e. in prying forces. Further loads may therefore be applied to the T-stub until failure is obtained through Mode 1 or Mode 2. But to reach this level of resistance, large deformations of the T-stub are necessary, what is not acceptable in design conditions. The extra-strength which separates Mode 1* from Mode 1 or Mode 2 in this case is therefore disregarded and Formula (2.3.24) is applied despite the discrepancy which could result from comparisons with some experimental tests.

As a result, in cases where no prying forces develop, the design resistance of the T-stub is taken as equal to :

$$F_{Rd} = min\left(F^{**}_{Rd,1}, F_{Rd,3}\right) \qquad (2.3.25)$$

when $F_{Rd,3}$ is given by formula (2.3.1).

In other cases, the common procedure explained in section 2.3.1 is followed.

The criterion to distinguish between situations with and without prying forces is discussed in section 2.3.3.3.

As explained in Section 2.3.1.1, circular and non-circular yield line patterns have to be

differentiated when deriving the effective length ℓ_{eff} of the T-stub :

- The non-circular patterns referred to in revised Annex J of Eurocode 3 cover cases where prying forces develop at the extremities of the plated component.
- The circular patterns develop without any prying.

Concerning Mode 1* failure, only circular patterns have therefore to be taken into consideration and the non-circular patterns proposed by Eurocode3 have to be disregarded. Mode 1* identifies then exactly to Mode 1 and, in order to ensure that the design resistances provided by formulae (2.3.2) and (2.3.24) are equal, the effective lengths for circular patterns defined in revised Annex J have to be multiplied by a factor 2 before being implemented in Formula (2.3.24).

Besides that, non-circular patterns not involving prying forces in the bolts may occur. These ones may be considered through Formula (2.3.24), but by introducing appropriate effective length characteristics. The lowest of the effective lengths between those derived for circular and non-circular patterns respectively is that which will determines the design resistance of the T-stub.

Table 2.3.1 indicates how to select the values of ℓ_{eff} for two classical base plate configurations, in cases where prying forces develop and do not develop.

PLATE CONFIGURATIONS	PRYING FORCES DEVELOP	PRYING FORCES DO NOT DEVELOP
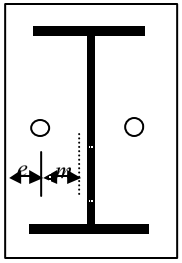 **Figure 2.3.7** Anchor bolts located between the flanges	$\ell_1 = 2\alpha m - (4m + 1{,}25e)$ $\ell_2 = 2\pi m$ $\ell_{eff,1} = min(\ell_1; \ell_2)$ $\ell_{eff,2} = \ell_1$ where m and n are represented in Figure 2.3.7. and α is defined in EC3 Annex J.	$\ell_1 = 2\alpha m - (4m + 1{,}25e)$ $\ell_2 = 4\pi m$ $\ell_{eff,1} = min(\ell_1; \ell_2)$ $\ell_{eff,2} = \ell_1$ where m and n are represented in Figure 2.3.7. and α is defined in EC3 Annex J.
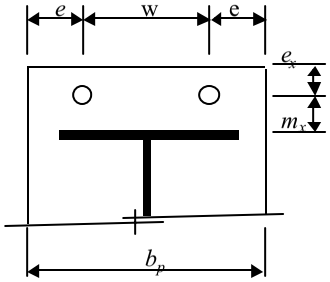 **Figure 2.3.8** Anchor bolts located in the extended part of the base plate	$\ell_1 = 4.m_x + 1{,}25\ e_x$ $\ell_2 = 2\pi\ m_x$ $\ell_3 = 0{,}5.b_p$ $\ell_4 = 0{,}5.w + 2.m_x + 0{,}625.e_x$ $\ell_5 = e + 2.m_x + 0{,}625.e_x$ $\ell_6 = \pi\ m_x + 2e$ $\ell_{eff,1} = min(\ell_1; \ell_2; \ell_3; \ell_4; \ell_5; \ell_6)$ $\ell_{eff,2} = min(\ell_1; \ell_3; \ell_4; \ell_5)$ where b_p, m, e, m_x, e_x and w are given in Figure 2.3.8.	$\ell_1 = 4.m_x + 1{,}25\ e_x$ $\ell_2 = 4\pi\ m_x$ $\ell_3 = 0{,}5.b_p$ $\ell_4 = 0{,}5.w + 2.m_x + 0{,}625.e_x$ $\ell_5 = e + 2.m_x + 0{,}625.e_x$ $\ell_6 = 2\pi\ m_x + 4e$ $\ell_{eff,1} = min(\ell_1; \ell_2; \ell_3; \ell_4; \ell_5; \ell_6)$ $\ell_{eff,2} = min(\ell_1; \ell_3; \ell_4; \ell_5)$ where b_p, m, e, m_x, e_x and w are given in Figure 2.3.8.

Table 2.3.1 Values of the T-stub effective length

It has to be noted that these formulae only apply to base plates where the anchor bolts are not located outside the beam flanges, as indicated in Figure 2.3.9.

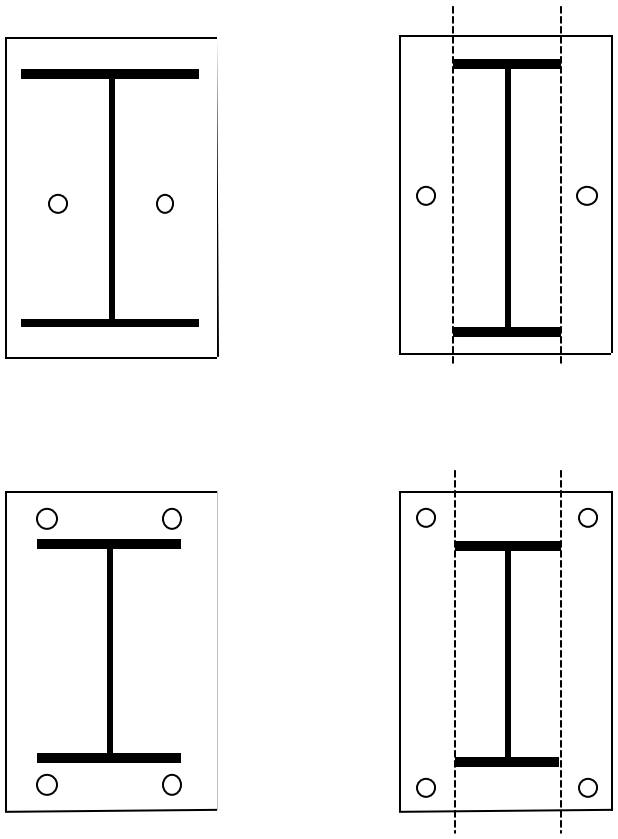

(a) Cases covered *(b) Cases not covered*

Figure 2.3.9 Limits of validity of the formulae given in Figures 2.3.7 and 2.3.8.

2.3.3.2 Stiffness properties

The elastic deformation of a T-stub in tension is discussed in section 2.3.2.1 and accurate formulae for stiffness evaluation are suggested. They have been used in section 2.3.2.2 to derive simplified expressions for inclusion in Revised Annex J of Eurocode 3.

- the stiffness coefficient for the T-stub flange in bending :

$$k_p = \frac{0{,}85\, \ell_{eff}\, t^3}{m^3} \qquad (2.3.26)$$

- the stiffness coefficient for the anchor bolts in tension:

$$k_b = 1{,}6\,\frac{A_s}{L_b} \qquad (2.3.27)$$

where L_b is the anchor bolt length described hereunder. These two expressions relate to situations where prying forces develop at the extremities of the T-stub flange as a result of a limited bolt-axial deformation in comparison with the bending deformation of the flange.

In "no prying cases", the deformation Δ_p of the base plate is easily derived as :

$$\Delta_p = \frac{F}{E\ k_{i,p}} \qquad (2.3.28.a)$$

where the stiffness coefficient $k_{i,p}$ is expressed as :

$$k_{i,p} = \frac{l_{eff,ini}\ t^3}{2\ m^3} \qquad (2.3.29.b)$$

and that of the bolts (without preloading) :

$$\Delta_b = \frac{F}{E\ k_{i,b}} \qquad (2.3.30.a)$$

with :

$$k_{i,b} = \frac{2A_s}{L_b} \qquad (2.3.31.b)$$

L_b is the effective free length of the anchor bolts (Figure 3.2.10). It is defined as the sum of two contributions L_{fl} and L_{el}. L_{fl} is the free length of the anchor bolts, i.e. the part of the bolt which is not embedded. L_{el} is the equivalent free length of the embedded part of the anchor bolt; it may be approximated to $8d$ (Wald, 1993), where d is the nominal diameter of the anchor bolt. Should the embedded length of the bolt be shorter than $8d$, then the actual length of the bolt would be considered. A justification of this definition of L_{el} is given in section 2.3.5.

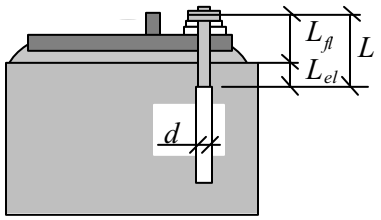

Figure 2.3.10 Effective length of the anchor bolts

If the approximation of the $\ell_{eff,ini}$ value suggested in section 2.3.3.2 is again considered - formula (2.3.26) -, the stiffness coefficient for the base plate in the case of "no prying" conditions may be finally expressed as :

$$k_{i,p} = 0{,}425 \frac{l_{eff}\, t^3}{m^3} \tag{2.3.32}$$

2.3.3.3 Boundary for prying effects

The elastic deformed shape of a T-stub in tension depends on the relative deformability of the flange in bending and the anchor bolts in tension (see section 2.3.2). In Figure 3.2.11, the bolt and flange deformations compensate such that the contact force Q just vanishes. For a higher bolt deformability, no contact will develop, while contact forces will appear for a lower bolt deformability. The situation illustrated in Figure 2.3.11 therefore constitutes a limit case to which a prying boundary may be associated. This is expressed as follows :

$$L_{b.boundary} = \frac{7 m^2 n\, A_s}{\ell_{eff} t^3}. \tag{2.3.33}$$

If, as a further assumption, n is defined as equal to $1{,}25\, m$ (section 2.3.2.2), then :

$$L_{b.boundary} = \frac{8{,}82\, m^3\, A_s}{\ell_{eff} t^3}. \tag{2.3.34}$$

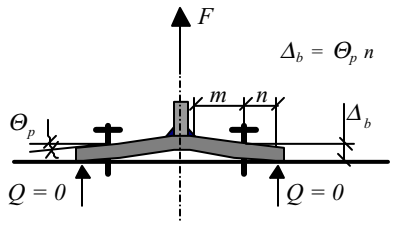

Figure 2.3.11 The T-stub deformation when prying force Q vanishes

If L_b is higher than $L_{b,boundary}$, then the following formulae apply :

- formulae (2.3.32) and (2.3.31.b) for stiffness;
- formulae (2.3.24) and (2.3.1) for resistance.

In the opposite case, other formulae have to be referred to :

- formulae (2.3.26) and (2.3.27) for stiffness;
- formulae (2.3.1), (2.3.2) – or (2.3.7) – and (2.3.3) for resistance.

2.3.3.4 Agreement between the simplified and sophisticated stiffness models

In the following figures, the validity of the simplifications brought to the theoretical stiffness model presented in section 2.3.2.1 to derive the so-called simplified model described in sections 2.3.2.2 and 2.3.3.2 is shown on three examples :

- T-stub with : $\ell_{eff} = 458,333\ mm$, $L_b = 150\ mm$, $A_s = 480\ mm^2$, $m = 50\ mm$ (Figure 2.3.12.a), where the n/m ratio takes the following values: *0,5; 1,0; 1,5* and *2.0* .
- T-stub with : $\ell_{eff} = 458,333\ mm$, $L_b = 300\ mm$, $A_s = 480\ mm^2$, $m = 50\ mm$, (Figure 2.3.12.b), where the n/m ratio takes the following values : *0,5; 1,0; 1,5* and *2.0* .
- T-stub with : $\ell_{eff} = 458,333\ mm$, $L_b = 600\ mm$, $A_s = 480\ mm^2$, $m = 50\ mm$, (Figure 2.3.12.c), where the n / m ratio takes the following values : *0,5; 1,0; 1,5* and *2.0* .

The boundary between "prying" and "no prying" fields is computed by means of formulae (2.3.33) and (2.3.34) for the theoretical and simplified models respectively.

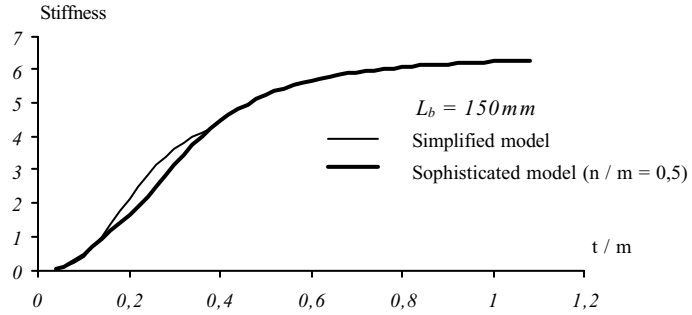
Stiffness
7
6
5
4
3
2
1
0
L_b = 150mm
Simplified model
Sophisticated model (n / m = 0,5)
t / m
0
0,2
0,4
0,6
0,8
1
1,2

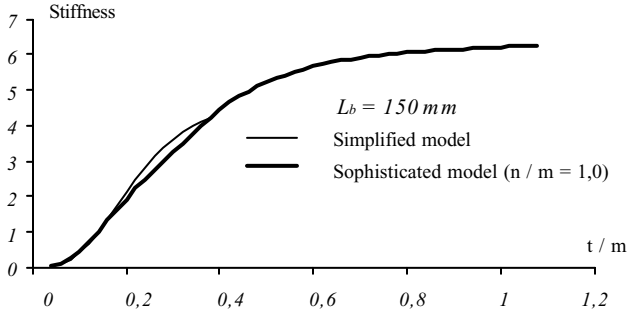
Stiffness
7
6
5
4
3
2
1
0
L_b = 150 mm
Simplified model
Sophisticated model (n / m = 1,0)
t / m
0
0,2
0,4
0,6
0,8
1
1,2

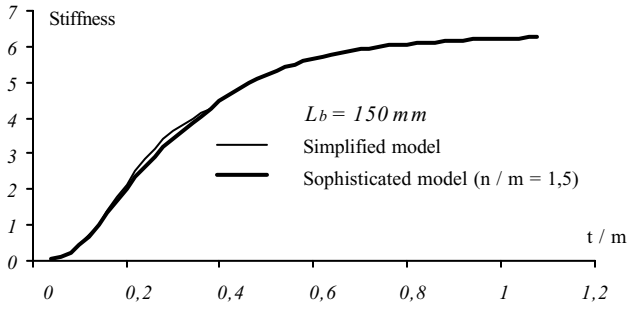
Stiffness
7
6
5
4
3
2
1
0
L_b = 150 mm
Simplified model
Sophisticated model (n / m = 1,5)
t / m
0
0,2
0,4
0,6
0,8
1
1,2

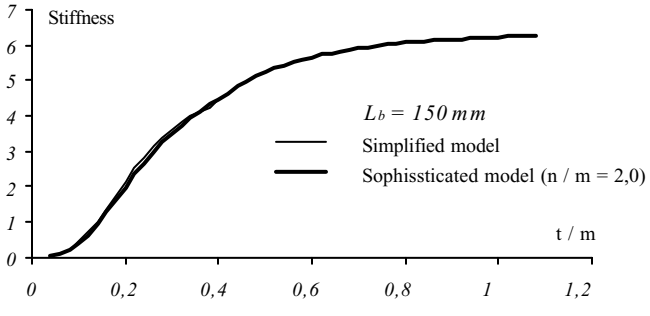
Stiffness
7
6
5
4
3
2
1
0
L_b = 150 mm
Simplified model
Sophisticated model (n / m = 2,0)
t / m
0
0,2
0,4
0,6
0,8
1
1,2

(a) L_b = 150 mm

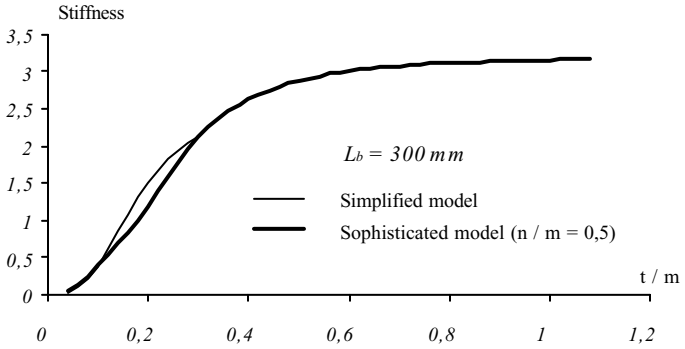
Stiffness
3,5
3
2,5
2
1,5
1
0,5
0
Lb = 300 mm
Simplified model
Sophisticated model (n / m = 0,5)
t / m
0
0,2
0,4
0,6
0,8
1
1,2

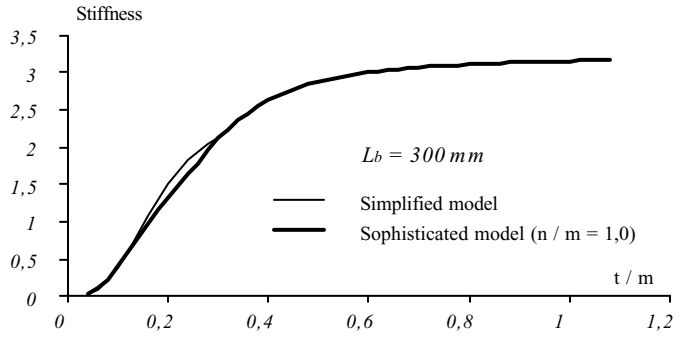
Stiffness
3,5
3
2,5
2
1,5
1
0,5
0
Lb = 300 mm
Simplified model
Sophisticated model (n / m = 1,0)
t / m
0
0,2
0,4
0,6
0,8
1
1,2

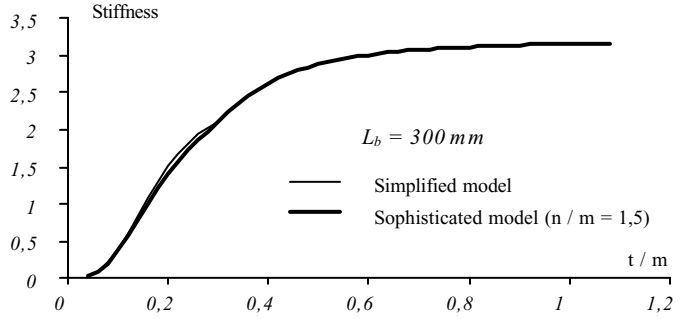
Stiffness
3,5
3
2,5
2
1,5
1
0,5
0
Lb = 300 mm
Simplified model
Sophisticated model (n / m = 1,5)
t / m
0
0,2
0,4
0,6
0,8
1
1,2

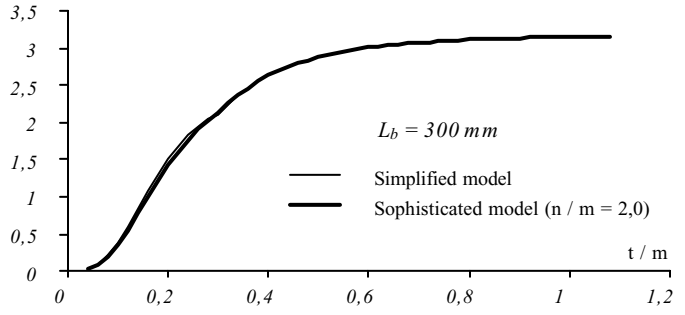
3,5
3
2,5
2
1,5
1
0,5
0
Lb = 300 mm
Simplified model
Sophisticated model (n / m = 2,0)
t / m
0
0,2
0,4
0,6
0,8
1
1,2

(b) L_b = 300 mm

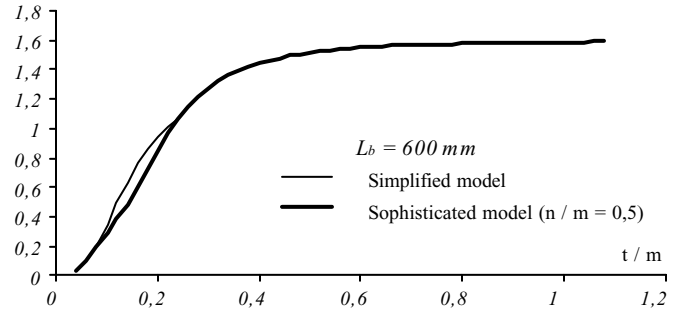

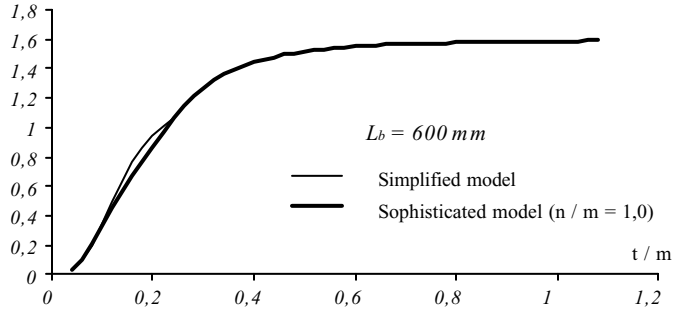

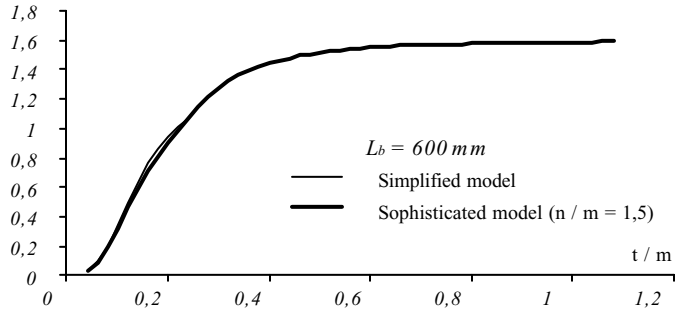

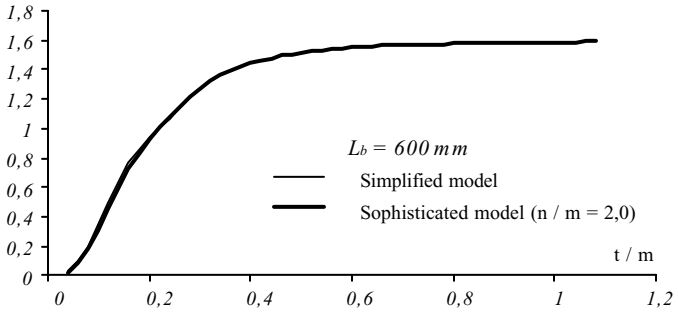

(c) $L_b = 600$ mm

Figure 2.3.12 Comparisons between theoretical and simplified models

2.3.4 Anchorage of the bolts in the concrete block

Different types of anchor bolts are used as shown in Figure 2.3.13.

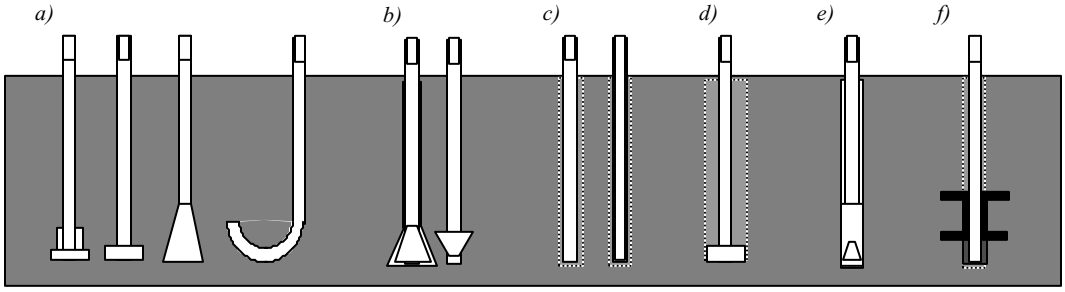

cast-in-place (a), undercut (b), adhesive (c), grouted (d), expansion (e), anchoring to grillage beams (f)

Figure 2.3.13 Basic types of anchoring

The anchoring resistance is provided by CEB rules based on the ultimate limit state concept. As already said, this resistance has to be such that the anchor bolts fail in tension before the anchorage (pull-out of the anchor, failure of the concrete, …) reach its own resistance.

For a single anchor, the following failure modes have to be considered (CEB, 1994):

- Pull-out failure ($N_{Rd.p}$)
- Concrete cone failure ($N_{Rd.c}$)
- Splitting failure of the concrete ($N_{Rd.sp}$)

Similar verifications are required for anchor groups.

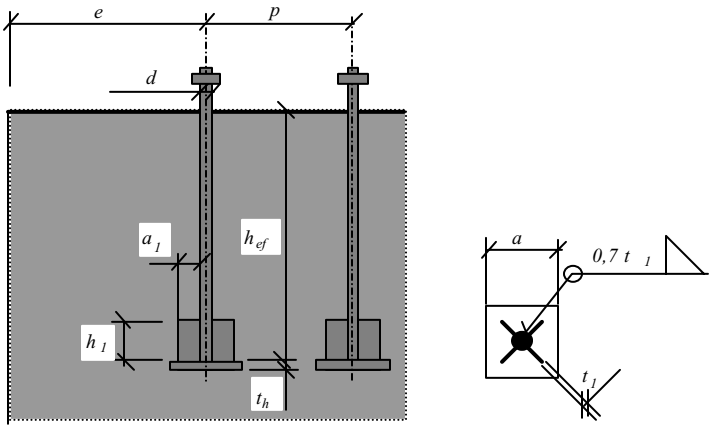

Figure 2.3.14 The geometry of the in-situ-cast headed anchor bolts

The most economical solutions for anchoring are, for instance, hooked bars for light anchoring, cast-in-place headed anchors and bounded anchors to drilled holes. The more expensive anchoring systems such as "grillage beams embedded in concrete" are designed for large frames. Models for the anchoring design resistance compatible with Eurocodes have been published in CEB Guide (CEB, 1997) and by Eligehausen in (Eligehausen, 1990) and (Eligehausen, 1991).

The calculation of the anchoring design resistance of cast-in-situ headed anchor bolts loaded in tension is presented here below.

The pullout failure design resistance may be obtained as:

$$N_{Rd.p} = p_k A_h / \gamma_{Mp} \tag{2.3.35}$$

where p_k is taken in non-cracked concrete as:

$$p_k = 11{,}0\ f_{ck} \tag{2.3.36}$$

and A_h is the bearing area of the head; for circular head of diameter d_h, it writes:

$$A_h = \pi\ (d_h^2 - d^2) / 4 \tag{2.3.37}$$

The concrete cone failure design resistance is given as

$$N_{Rd.c} = N^0_{Rd.c} \frac{A_{c.N}}{A^0_{c.N}} \Psi_{s.N} \Psi_{ec.N} \Psi_{re.N} \Psi_{ucr.N}, \tag{2.3.38}$$

where

$$N^0_{Rk.c} = k_1 f_{ck}^{0,5} h_{ef}^{1,5} / \gamma_{Mc} \tag{2.3.39}$$

is the characteristic resistance of a single fastener. The coefficient k_1 could be taken for non cracked concrete as:

$$k_1 = 11{,}0\ \ [\sqrt{N / mm}\,] \tag{2.3.40}$$

The geometric effect of spacing p and edge distance e is included in calculation of the area of the cone, see Figure 2.3.15, as:

$$A^0_{c.N} = p_{cr.N}{}^2 \tag{2.3.41}$$

$$A_{c.N} = (p_{cr.N} + p_1)(p_{cr.N} + p_2) \tag{2.3.42}$$

for examples in Figure 2.3.15.a and 2.3.15.b or as:

$$A_{c.N} = \left(e + 0{,}5\ p_{cr.N}\right) p_{cr.N} \tag{2.3.43}$$

for Figure 2.3.15c.

It is possible to consider approximately:

$$p_{cr.N} \cong 2{,}0\ e_{cr.N} \cong 3{,}0\ h_{ef} \tag{2.3.44}$$

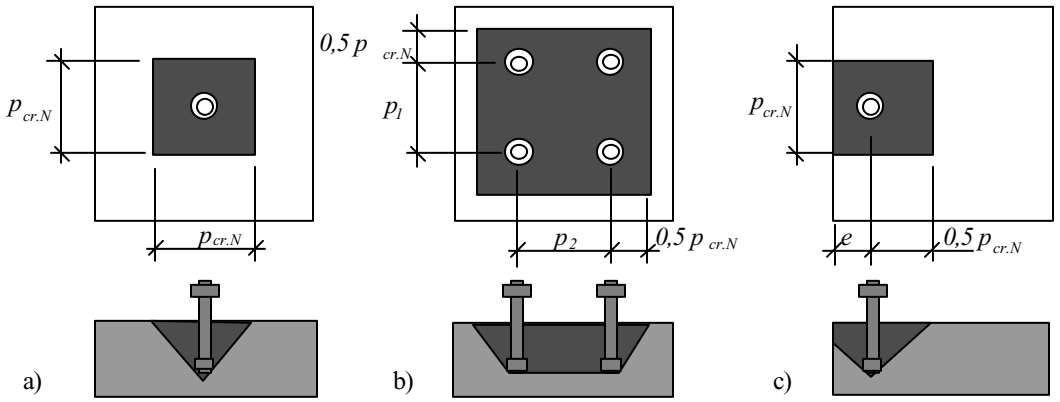

Figure 2.3.15 An idealised concrete cone, individual anchor (a), anchor group (b), single anchor at edge (c)

The disturbance of the stress distribution in the concrete may be introduced through the following parameter:

$$\Psi_{s.N} = 0{,}7 + 0{,}3\frac{e}{e_{cr.N}} \le 1 \tag{2.3.45}$$

The parameter $\Psi_{ec.N}$ takes into account the group effect. Parameter $\Psi_{re.N}$ is used for small embedded depths ($h_{ef} \le 100\ mm$). The resistance is increased in non-cracked concrete by parameter $\Psi_{ure.N} = 1{,}4$.

The splitting failure for the in-situ-cast anchors is prevented if the concrete is reinforced or by limiting:

The spacing:

$$p_{min} = 5\ d_h \ge 50\ mm \tag{2.3.46}$$

The edge distances:

$$e_{min} = 3\ d_h \geq 50\ mm \qquad (2.3.47)$$

And the height of the concrete block:

$$h_{min} = h_{ef} + t_h + c_{\varnothing}, \qquad (2.3.48)$$

where:

t_h is thickness of the anchor bolt head and

$c_{\varnothing}$ the required concrete cover for reinforcement.

For fastenings with an edge distance $e > 0,5\ h_{ef}$ in all directions, a check of the characteristic pull-out resistance may be omitted.

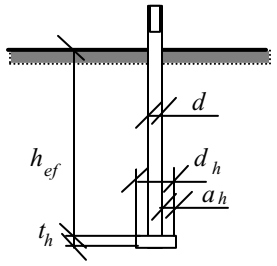

Figure 2.3.16 Headed embedded anchor bolt

The detailed complex description of the evaluation formulae for the design resistance of different types of fastenings in tension is included in the CEB Guide (CEB, 1997). When calculating the anchoring resistance, the tolerances for the position of the bolts should be taken into account according to Eurocode 3, clause 7.7.5 (ENV 1992-1-1, Part 1.1).

2.3.5 Definition of the equivalent free length of the anchor bolts

The relative displacement Δ between the surface of a concrete foundation and an embedded bar subjected to tension forces has been observed experimentally by Salmon (1957), Wald (Wald et al, 1993; Wald, 1995). From these experimental observations, the length L_t on which the tensile stress in the embedded part of the bar decreases from a σ value (at the concrete surface) to a zero value is seen to be approximately equal to $24\ d$. This length may obviously vary during the loading and dramatically change because of local looses of bound resistance between steel and concrete. In the calculations of the stiffness properties of the anchor bolts in tension, a constant stress in the bar σ is assumed to act on a so-called equivalent free length L_{el} (see Figure 2.3.10); Δ is therefore expressed as:

$$\Delta = \frac{B\ L_{el}}{E\ A_s} \tag{2.3.49}$$

If σ_{bx} designates the bond stress between the concrete and the embedded bar (see Figure 2.3.17), the axial stress σ_x along the bar writes:

$$\sigma_x = \sigma - \int_0^x \frac{4\sigma_{bx}}{d} dx \tag{2.3.50}$$

where $\sigma = B/A_s$ is the axial stress in the non-embedded part of the bar at the concrete surface.

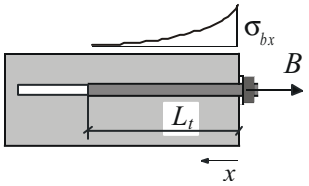

Figure 2.3.17 Example of bond stress distribution along the embedded bar

In $x = L_t$ (Figure 2.3.17), σ_x equals zero and therefore:

$$\sigma = \int_0^{L_t} \frac{4\sigma_{bx}}{d} dx\,. \tag{2.3.51}$$

The strain along the bar writes $\varepsilon_x = \sigma_x / E$; by considering this relation and Equations (2.3.50) and (2.3.51), the elongation of the bar Δ may be expressed as:

$$\Delta = \int_0^{L_t} \varepsilon_x dx = \frac{4}{dE} \int_0^{L_t} \int_x^{L_t} \sigma_{bx} dx^2. \tag{2.3.52}$$

From Equation (2.3.52), Δ is seen to depend on the distribution of σ_{bx} stresses along the bar. Hereunder three different assumptions are made for what regards the distribution: constant, linear and parabolic.

- If σ_{bx} is constant and independent of x ($\sigma_{bx} = \sigma_b$), see Figure 2.3.18:

$$s = \frac{2\ \sigma_b\ L_t^2}{d\ E} \tag{2.3.53}$$

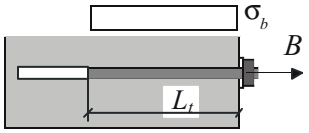

Figure 2.3.18 Constant distribution of bond stresses along the embedded bar

$$\sigma_b = \frac{\sigma\, d}{4\ L_t} \tag{2.3.54}$$

and:

$$\Delta = \frac{2\sigma_b L_t^2}{d\,E} = \frac{2\sigma\ \ d L_t}{4 d L_t E} = \frac{\sigma\ \ L_t}{2E} \tag{2.3.55.a}$$

$$\Delta = \frac{F_b L_{eqt}}{E\,A} \tag{2.3.55.b}$$

Finally by comparing Equations (2.3.55.b) and (2.3.49):

$$L_{el} = \frac{L_t}{2} = 12d \tag{2.3.56}$$

- If the bond stress varies linearly, as shown in Figure 2.3.19:

$$\Delta = \frac{2\sigma_{b0} L_t^2}{3d\,E} \tag{2.3.57}$$

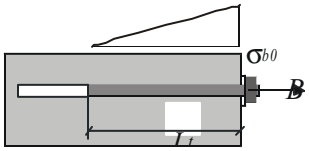

Figure 2.3.19 Linear distribution of bond stresses along the embedded bar

$$\sigma_{b0} = \frac{\sigma\, d}{2\ L_t} \tag{2.3.58}$$

and:

$$L_{el} = \frac{L_t}{3} = \frac{24d}{3} = 8d \tag{2.3.59}$$

- If the bond stress varies non-linearly, as shown in Figure 2.3.20 (cubic parabola):

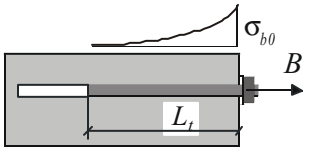

Figure 2.3.20 Non-linear distribution of bond stresses along the embedded bar

$$\Delta \cong \frac{2\sigma_{b0} L_t^2}{5dE} \tag{2.3.60}$$

and:

$$L_{el} = \frac{L_t}{5} = \frac{24d}{5} = 4{,}8d\ . \tag{2.3.61}$$

In order to select the distribution of bound stresses in an appropriate way, FEM simulations corroborated by experiments (Wald et al, 1995; Sokol, Wald, 1997) have been carried out in Prague. An example of such simulations is shown in Figure 2.3.21. From these numerical work, the linear distribution of bound stresses has been selected and, as a result, the equivalent free length of the embedded part of the anchor bolt is considered as equal to:

$$L_{el} = 8d \tag{2.3.62}$$

as indicated in section 2.3.3.2.

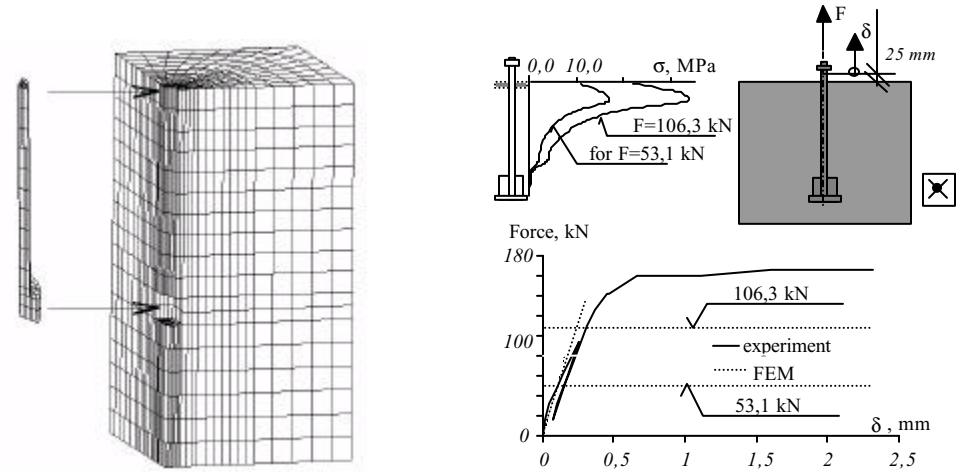

Figure 2.3.21 FEM simulation of bolt elongation

Results of comparisons between experimental tests and Equation (2.3.62) are shown in Figures 2.3.22 and 2.3.23. The agreement is seen to be quite good.

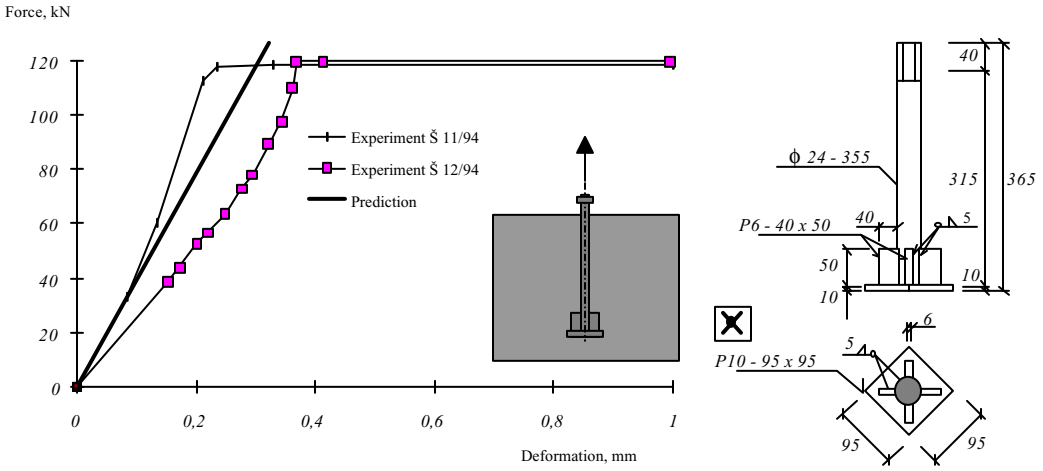

Figure 2.3.22 Comparison to experiments with long bolts (Wald et al, 1995) $d = 24$ *mm*, $f_{ck} = 40{,}1$ *MPa*

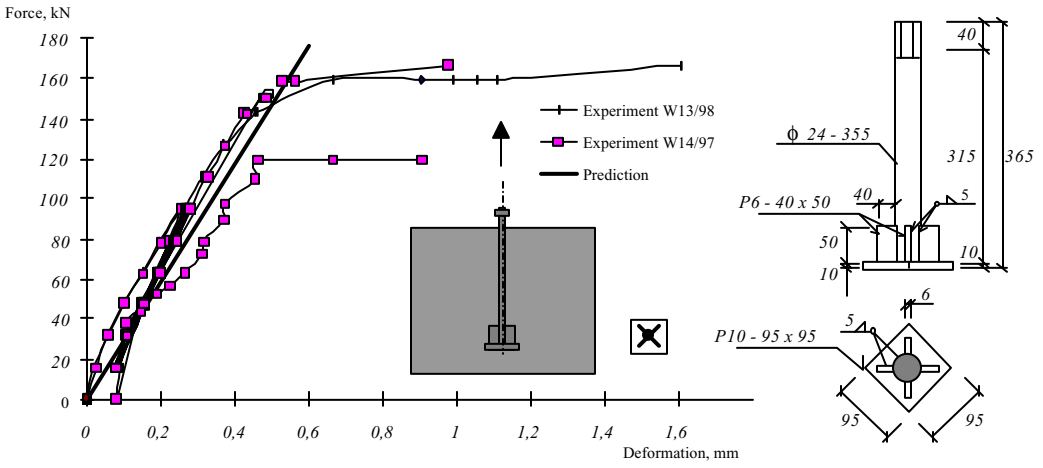

Figure 2.3.23 Comparison to experiments with long bolts (Sokol and Wald, 1997), $d = 24$ *mm*, $f_{ck} = 33{,}3$ *MPa*,

In the case of short anchor bolts with an embedded length smaller than $24d$, Formula (2.3.62) no more applies.

2.3.6 Experimental validation of the proposed formulae

In the following figures, comparisons between experimental tests on isolated T-stubs in tension and the models for characterisation described in this section are presented.

Three curves are reproduced on each diagram:

- The experimental curve *B-Δ;*
- The theoretical curve based on the more sophisticated available models for stiffness and strength prediction (the model is said "complex");
- The theoretical curve based on the more simple available rules for stiffness and strength prediction (the model is said "simplified");

The comparisons of these simplified and complex calculation models give very similar results (except for experiments W97-01 and W97-02). On the other hand, a quite good agreement with the experimental tests is observed.

In tests W97-01 and 97-02, the resistances given by the complex and simplified models are significantly different. The explanation is the following: according to the simplified model, prying forces develop between the T-stub and the concrete foundation while no such prying forces develop according to the complex model. The formulae used for the strength prediction are therefore different. Anyway, the level of safety and accuracy of the simplified curve remains quite good in both tests by comparison with the experimental results.

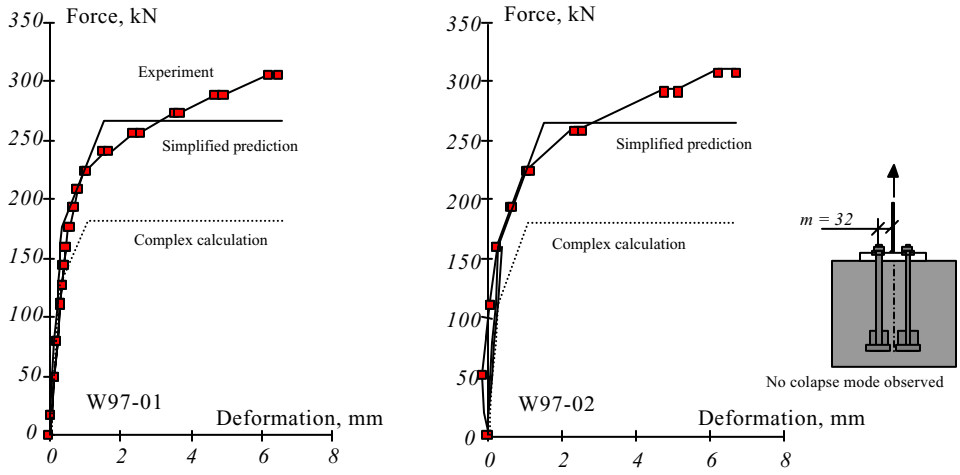

Figure 2.3.24 Load- deflection diagrams for experiments W 97-01 and W 97-02 (Sokol and Wald, 1997). Bolts M24, plate 20 mm, m = 32 mm, n = 40 mm, concrete block 550 x 550 x 500 mm. No collapse was reached due to loading cell limitation

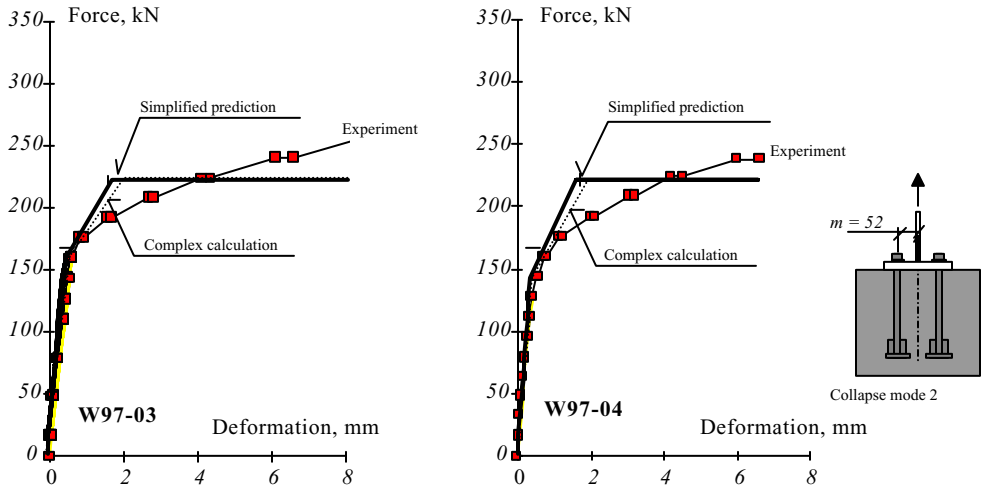

Figure 2.3.25 Load-deflection diagrams for experiments W 97-03 and W 97–04 (Sokol and Wald, 1997). Bolts M24, plate 20 mm, m = 52 mm, n = 40 mm, concrete block 550 x 550 x 500 mm. Mode 2 collapse (breaking of bolts and plate mechanism).

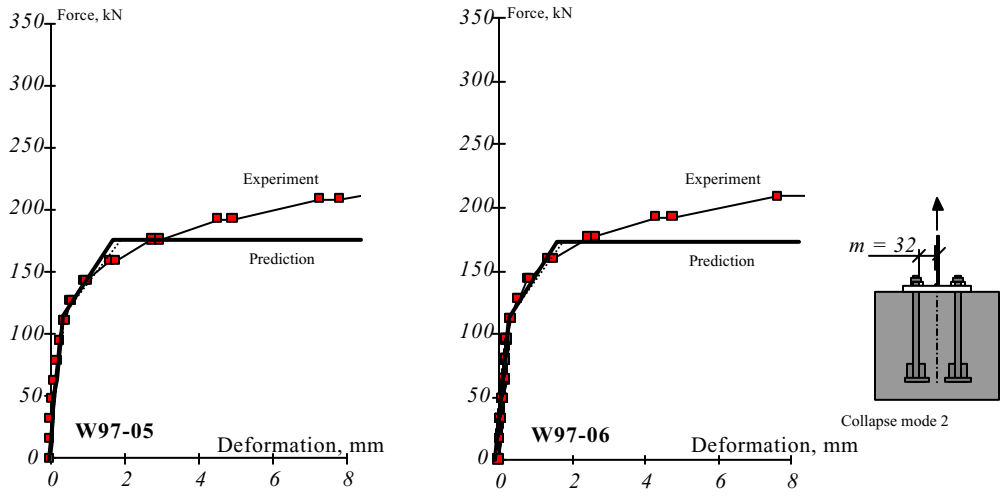

Figure 2.3.26 Load-deflection diagrams for experiments W 97-05 and W 97-06. (Sokol and Wald, 1997). Bolts M24, plate 12 mm, m = 32 mm, n = 40 mm, concrete block 550 x 550 x 500 mm. Mode 2 collapse (breaking of bolts and plate mechanism).

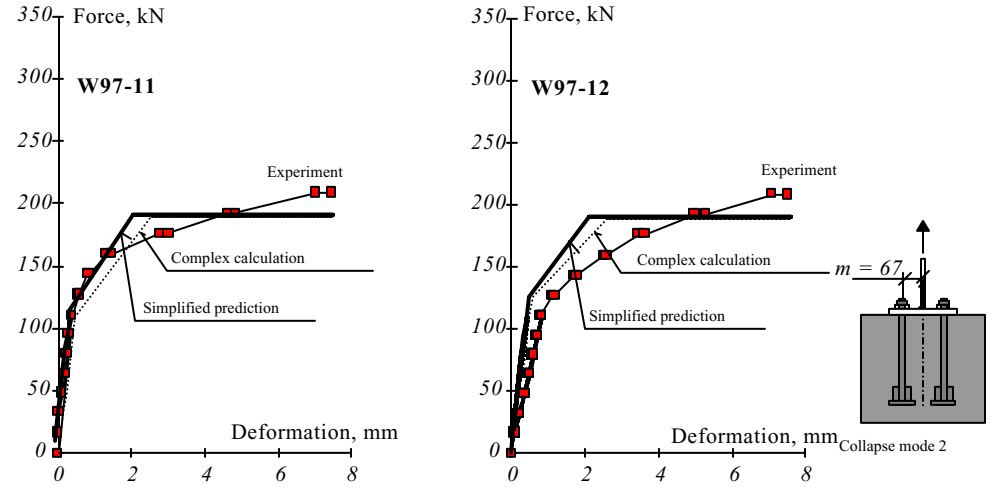

Figure 2.3.27 Load-deflection diagrams for experiments W 97-11 and W 97-12. (Sokol and Wald, 1997). Bolt M24, plate 20 mm, m = 67 mm, n = 40 mm, concrete block 550 x 550 x 500 mm. Mode 2 collapse (breaking of bolts and plate mechanisms).

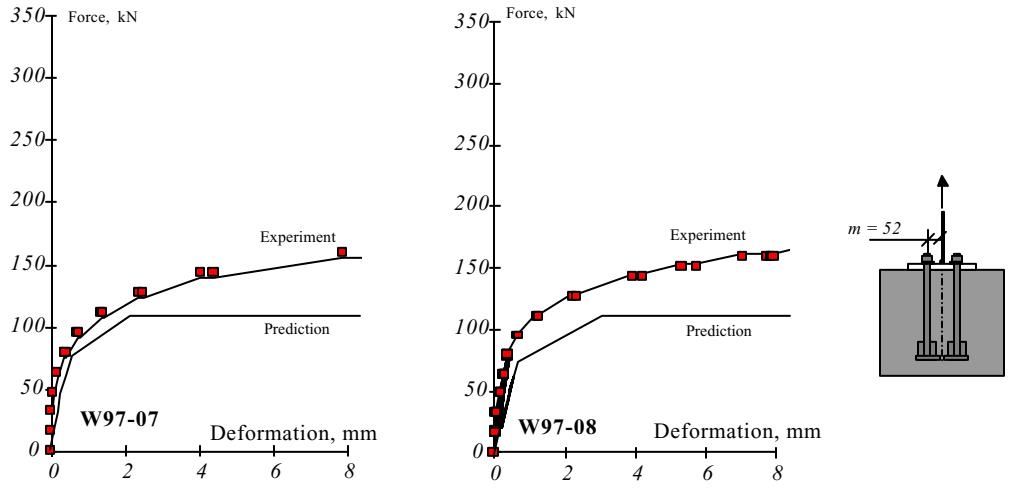

Figure 2.3.28 Load-deflection diagrams for experiments W 97-07 and W 97-08. (Sokol and Wald, 1997). Bolts M24, plate 12 mm, m = 52 mm, n = 40 mm, concrete block 550 x 550 x 500 mm. Mode 1 collapse and collaspe in concrete block (W 97–07) and no collapse reached because of very large deformations (W 97 – 08).

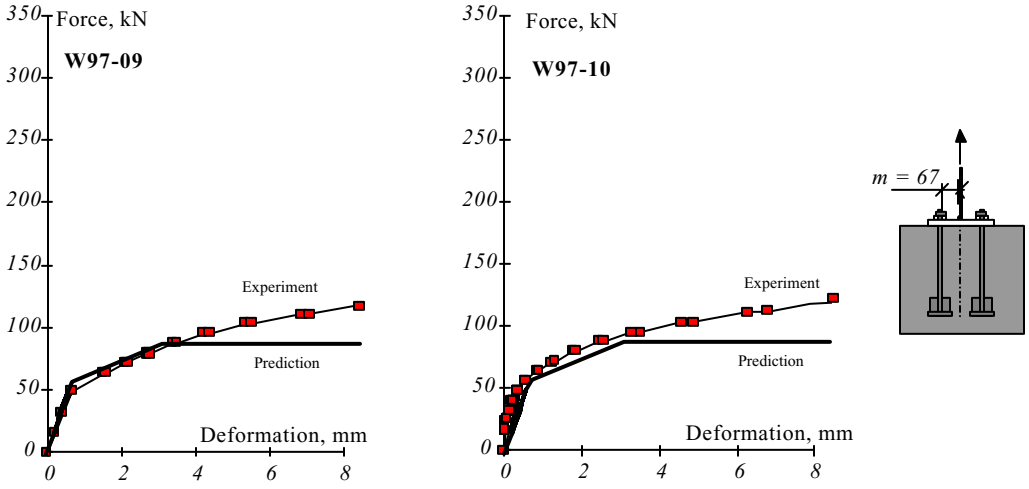

Figure 2.3.29 Load deflection diagram for experiment W 97-09 and W 97-10. (Sokol and Wald, 1997). Bolts M24, plate 12 mm, m = 65 mm, n = 40 mm, concrete block 550 x 550 x 500 mm. Collapse in the concrete block (W 97–09) and no collapse reached because of very large deformations (W 97–10).

2.4 Shear transfer

2.4.1 General introduction

Horizontal shear force may be resisted by (see Fig. 2.4.1):

a) Friction between the base plate, grout and concrete footing,
b) Shear and bending of the anchor bolts,
c) A special shear key, which is for example a block of I-stub or T-section or steel pad welded onto the underside of the base plate,
d) Direct contact, which can be achieved by recessing the base plate into the concrete footing.

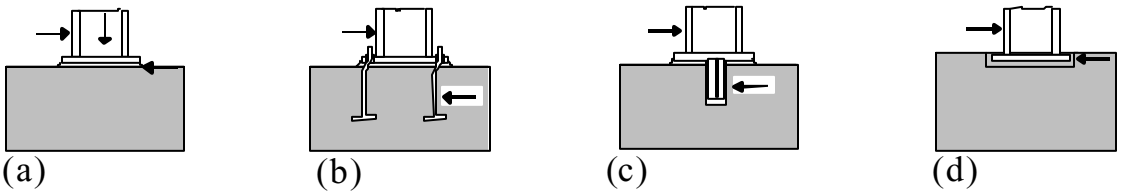

Figure 2.4.1 Column bases loaded by horizontal shear force.

In most cases, the shear force can be resisted through friction between the base plate and the grout. The friction depends on the minimum compressive load and on the coefficient of friction. Prestressing the anchor bolts will increase the resistance of the shear force transfer by friction.

Sometimes, for instance in slender buildings, it may happen that due to horizontal forces (wind loading) the normal compressive force is absent or is a tension force. In such cases, the horizontal shear force usually cannot be transmitted through friction between the base plate and the grout. If no other provisions are installed (e.g. shear studs), the anchor bolts will have to transmit these shear forces.

Because the grout does not have sufficient strength to resist the bearing stresses between the bolt and the grout, considerable bending of the anchor bolts may occur, as is indicated in Fig. 2.4.2. The main failure modes are rupture of the anchor bolts (local curvature of the bolt exceeds the ductility of the bolt material), crumbling of the grout, failure (splitting) of the concrete footing and pull out of the anchor bolt.

Due to the horizontal displacement, not only shear and bending in the bolts will occur, but also the tensile force in the bolts will be increased due to second order effects. The horizontal component of the increasing tensile force gives an extra contribution to the shear resistance.

The increasing vertical component gives an extra contribution to the transfer of load by friction. These factors explain the shape of the load deformation diagram in Fig. 2.4.2.

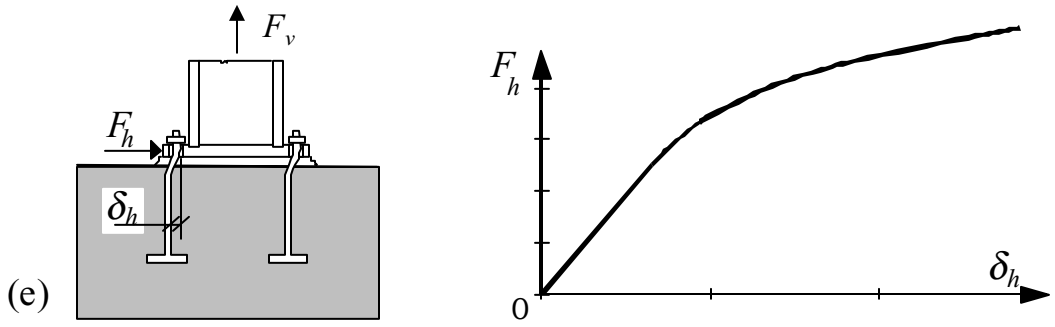

Figure 2.4.2 Column base loaded by shear and tension.

The thickness of the grout layer has an important influence on the horizontal deformations. In the tests reported by the Stevin Laboratory (Stevin, 1989), deformations at rupture of the anchor bolts were between about 15 and 30 mm, whilst grout layers had a thickness of 15, 30 and 60 mm. The deformations have to be taken into account in the check of the serviceability limit state. Because of the rather large deformations that may occur, this check may govern the design.

The size of the holes may have a considerable influence on the horizontal deformations, especially of course when oversized holes are applied. It may be useful in such cases to apply larger washers under the nuts, to be welded onto the base plate after erection, or to fill the hole by a two component resin. For the application of such resin, reference is made to (ECCS, 1994).

For the design of fasteners, the CEB has published a Design Guide (CEB, 1996). In section 2.4.2, the CEB design model for shear load transfer is summarised.

In the Stevin Laboratory (Stevin, 1989), a model for the load deformation behaviour of base plates loaded by combinations of tension or compression and shear has been developed. This model is described in section 2.4.3.

In section 2.4.4, the test results obtained in Delft (Stevin, 1989) are compared with the CEB model and the Stevin Laboratory model.

It is noted that in the models as explained here, only the behaviour of the base plate and the anchor bolts is considered. For other failure modes (for the concrete) reference is made to the CEB Design Guide.

2.4.2 CEB Design Guide model

2.4.2.1 Introduction

In the CEB Design Guide (CEB, 1996), the load transfer from a fixture (e.g. base plate) into the concrete is covered. The CEB Design Guide covers many types of anchors and the possible failure modes of the concrete. The design of the fixture (e.g. the base plate) must be performed according to the appropriate code of practice. In case of steel fixtures a steel construction code is used.

Much background information can be found in the CEB state of the art report: "Fastenings to concrete and masonry structures" (CEB, 1994). It reviews the behaviour of fastenings in concrete and masonry for the entire range of loading types (including monotonic, sustained, fatigue, seismic and impact loading), as well as the influence of environmental effects, based on experimental results. Existing theoretical approaches to prediction of the behaviour of anchors are described.

The CEB Design Guide consists of three parts:

Part I: General provisions.

1. Scope.
2. Terminology.
3. Safety concept.
4. Determination of action effects.
5. Non cracked concrete.
6. General requirements for a method to calculate the design resistance of a fastening.
7. Provisions for ensuring the characteristic resistance of the concrete member.

Part II: Characteristic resistance of fastenings with post installed expansion and undercut anchors.

8. General.
9. Ultimate limit state of resistance elastic design approach.
10. Ultimate limit state of resistance plastic design approach.
11. Ultimate limit state of fatigue.
12. Serviceability limit state.
13. Durability.

Part III: Characteristic resistance of fastenings with cast in place headed anchors.

14. General.
15. Ultimate limit state of resistance elastic design approach.
16. Ultimate limit state of resistance plastic design approach.

17. Ultimate limit state of fatigue.
18. Serviceability limit state.
19. Durability.

References.

The Design Guide makes a distinction between elastic analysis and plastic analysis. The use of elastic analysis is compulsory when the expected mode of failure is brittle. A brittle failure may be assumed in the case of concrete break-out, splitting failure or rupture of steel with insufficient ductility. The required ductility is determined by the degree of load redistribution assumed in the analysis. For example, in a plastic analysis, the ductility must be sufficient to accommodate yielding of all anchors on the tension side. It is stated that in the case of ductile behaviour of the anchorage, the elastic design approach is conservative.

For the transfer of shear forces, two methods are considered, namely:

- Friction between the fixture (e.g base plate) and the grout or concrete and
- Shear/bending of the anchors.

These two methods are described in chapter 4: "Determination of action effects".

2.4.2.2 Friction between base plate and grout/concrete

In section 4.1 of the CEB Guide it is stated that when a bending moment and/or a compression force is acting on a fixture, a friction force may develop, which for simplicity may conservatively be neglected in the design of the anchorage. If it is to be taken into account, then the design value of this friction force $V_{Rd,f}$ may be taken as:

$$V_{Rd,f} = V_{Rk,f} / \gamma_{Mf} = \mu \cdot C_{Sd} / \gamma_{Mf} \qquad (2.4.1)$$

with

μ	=	coefficient of friction
C_{Sd}	=	compression force under the fixture due to the design actions
γ_{Mf}	=	1.5 (ultimate limit state)
γ_{Mf}	=	1.3 (limit state of fatigue)
γ_{Mf}	=	1.0 (serviceability limit state)

In general, the coefficient of friction between a fixture and concrete may be taken as $\mu = 0.4$. The friction force $V_{Rd,f}$ should be neglected if the thickness of grout beneath the fixture is thicker than 3 mm (e.g. in case of levelling nuts), see Fig. 2.4.3(b) and for anchorages close to an edge, see Fig. 2.4.3(c).

In the elastic design approach, the friction force calculated by equation (2.4.1) is usually subtracted from the shear force acting on the fixture and in the plastic design approach it is added to the design shear resistance of the fastening.

For anchorages close to an edge it is generally assumed that the edge failure starts from the anchors closest to the edge. The resistance of the anchorage is increased if the friction force is acting on the side of the fixture farthest away from the edge (Fig. 2.4.3.(d)), but is not influenced by a friction force acting on the failed concrete (Fig. 2.4.3(c)).

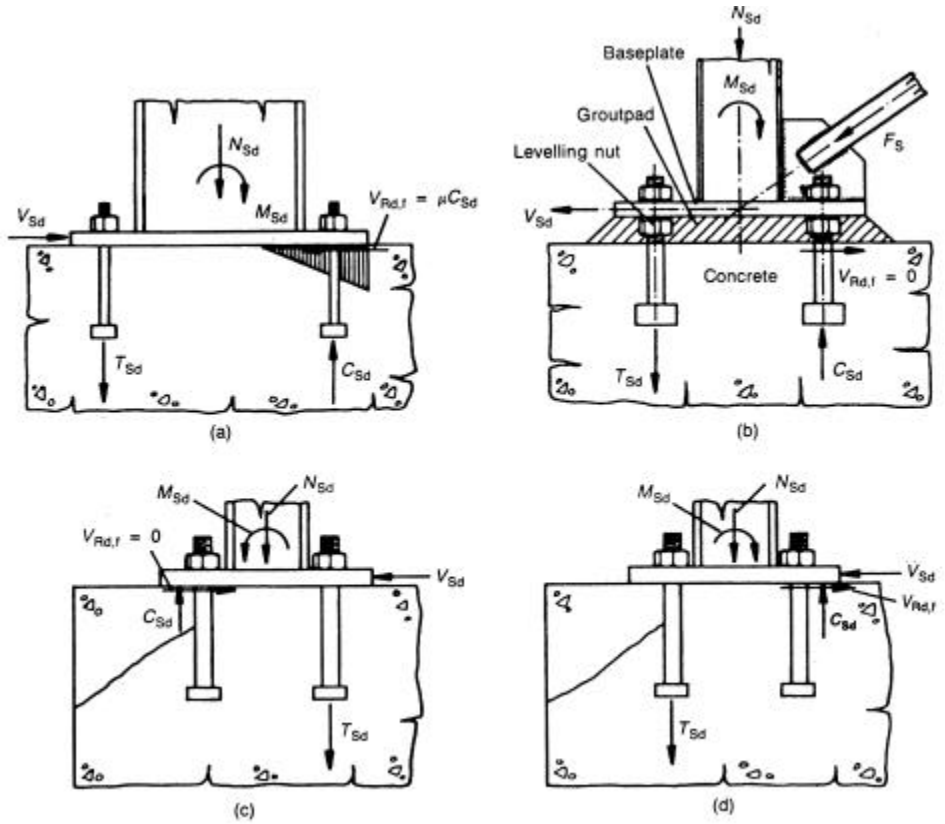

Figure 2.4.3 Friction force due to a resultin g compression reaction on the fixture. In cases (a) and (d), friction force may be considered in the design. In cases (b) and (c), friction force should not be considered in the design (Fig. 16 in the CEB Design Guide).

In conclusion, it can be stated that for "normal column bases", according to the CEB Guide, load transfer through friction should be neglected because of the fact that in normal steel constructions the thickness of the grout is always more than 3 mm.

2.4.2.3 Shear/bending of anchor bolts (elastic)

In section 4.2.1.3 of the CEB Guide, guidance is given for the design of anchors and concrete when anchors are loaded by shear, if elastic analysis is assumed. Much attention is paid to the distribution of the shear loads on the anchors.

(a) Distribution of shear loads

All anchors in a group are assumed to participate in carrying shear loads if the following two conditions are met:

(i) The edge distance is sufficiently large to ensure steel failure of the anchor; and

(ii) The anchors are welded to or threaded into the fixture, or in the case of anchorages with a clearance hole in the fixture, the diameter of the clearance hole is $d_c \leq 1.2d$. The bolt is then assumed to bear against the fixture, see Fig. 2.4.4(a).

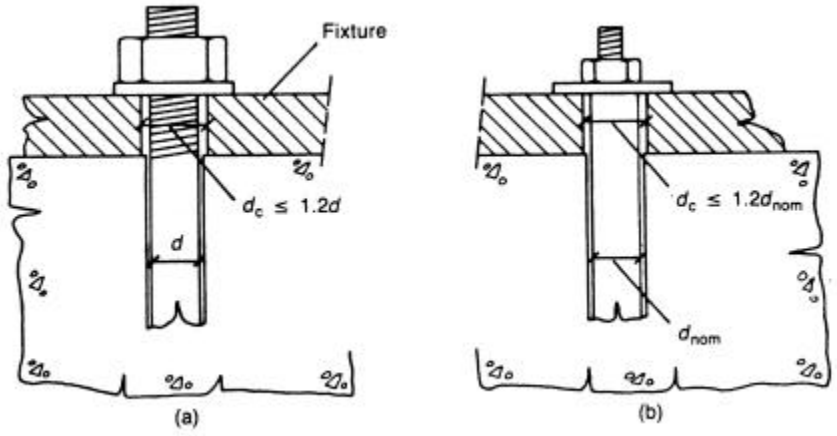

Figure 2.4.4 Examples of anchorages with a large edge distance with a clearance hole in the fixture where all anchors will contribute to the transmission of shear forces. In case (a) the bolt is assumed to bear against fixture. In case (b) the sleeve is assumed to bear against the fixture (Fig. 20 in the CEB Design Guide).

If the edge distance is small, so that concrete edge failure will occur and steel failure of the anchors will be precluded independent of the hole clearance, or if the hole clearance is larger than indicated in the previous paragraph, only those anchors having the lowest calculated resistance are assumed to carry loads. For example, see Figures 2.4.5 and 2.4.6. The positioning of slotted holes in the fixture parallel to the direction of the shear load can be used to prevent particular anchors in the group from carrying load. This method can be used to relieve anchors close to an edge, which would otherwise cause a premature edge failure (see Fig. 2.4.7).

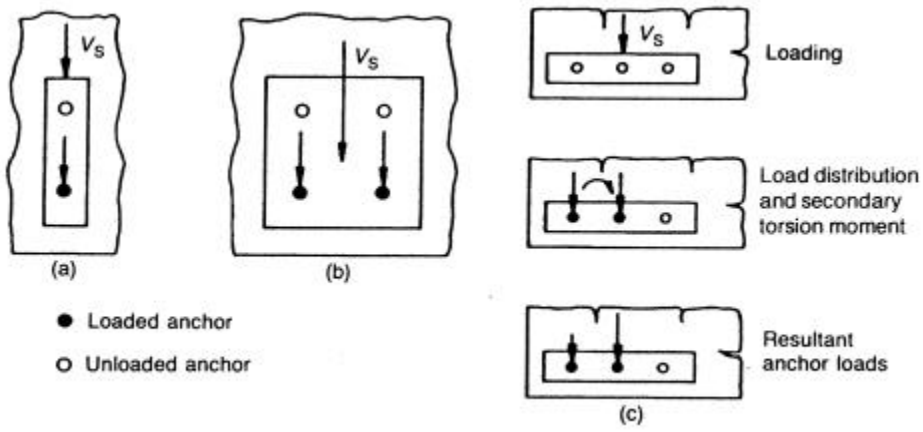

Figure 2.4.5 Examples of load distribution for anchorages close to an edge or corner of the concrete member (Fig. 22 in the CEB Design Guide).

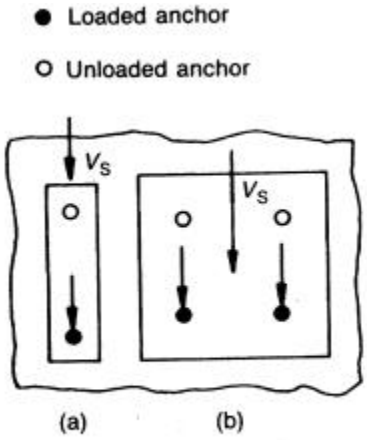

Figure 2.4.6 Examples of load distribution if the hole clearance is large (Fig. 23 in the CEB Design Guide).

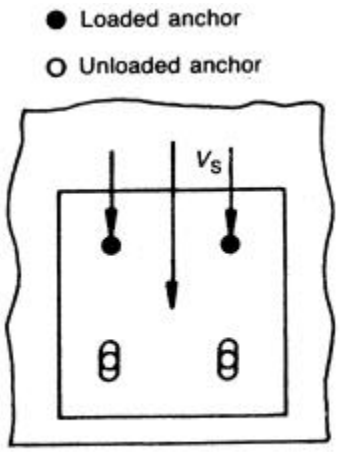

Figure 2.4.7 Example of load distribution for an anchorage with slotted holes (Fig. 24 in the CEB Design Guide).

For the resistance of anchor bolts, two cases are considered, namely *(b)* and *(c)*:

(b) Shear loads without lever arm

Shear loads acting on anchors may be assumed to act without a lever arm if both of the following conditions are fulfilled.

(1) The fixture must be made of metal and in the area of the anchorage be fixed directly to the concrete without an intermediate layer or with a levelling layer of mortar with a thickness ≤ 3 mm.

(2) The fixture must be adjacent to the anchor over its entire thickness.

(c) Shear loads with lever arm

If the conditions (1) and (2) of the preceding section (b) are not fulfilled, the length ℓ of the lever arm is calculated according to equation (2.4.2):

$$\ell = a_3 + e_1 \qquad (2.4.2)$$

with

e_1 = distance between shear load and concrete surface
a_3 = 0.5 d for post-installed and cast-in-place anchors (Fig. 2.4.8(a))
a_3 = 0 if a washer and a nut are directly clamped to the concrete surface (Fig. 2.4.8(b))
d = nominal diameter of the anchor bolt or thread diameter (Fig. 2.4.8(a))

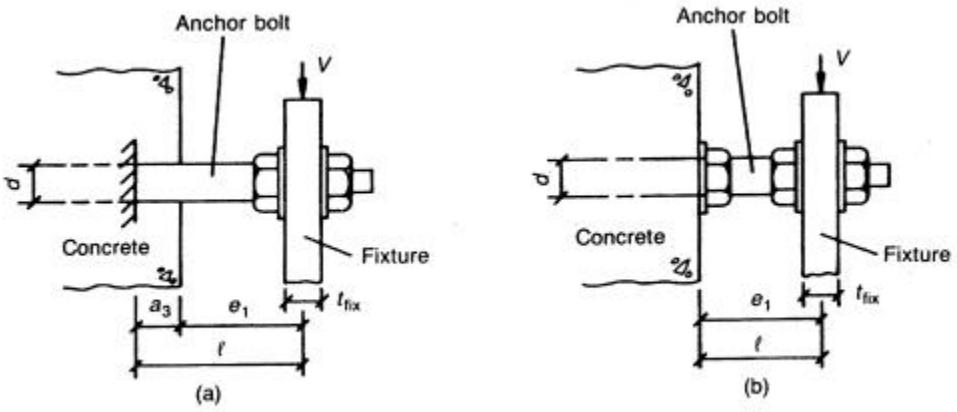

Figure 2.4.8 Lever arm (Fig. 26 in the CEB Design Guide).

The design moment acting on the anchor is calculated according to equation (2.4.3):

$$M_{Sd} = V_{Sd} \cdot \frac{\ell}{\alpha_M} \qquad (2.4.3)$$

The value of α_M depends on the degree of restraint of the anchor at the side of the fixture. No restraint (α_M = 1.0) should be assumed if the fixture can rotate freely (see Fig. 2.4.9(a)). Full restraint (α_M = 2.0) may be assumed only if the fixture cannot rotate (see Fig. 2.4.9(b)) and the hole in the fixture is smaller than 1.2d (the bolt is then assumed to bear against the fixture, see Fig. 2.4.4(a)) or if the fixture is clamped to the anchor by a nut and a washer (see Fig. 2.4.8). If restraint of the anchor is assumed, the fixture and/or the fastened element must be able to take up the restraint moment.

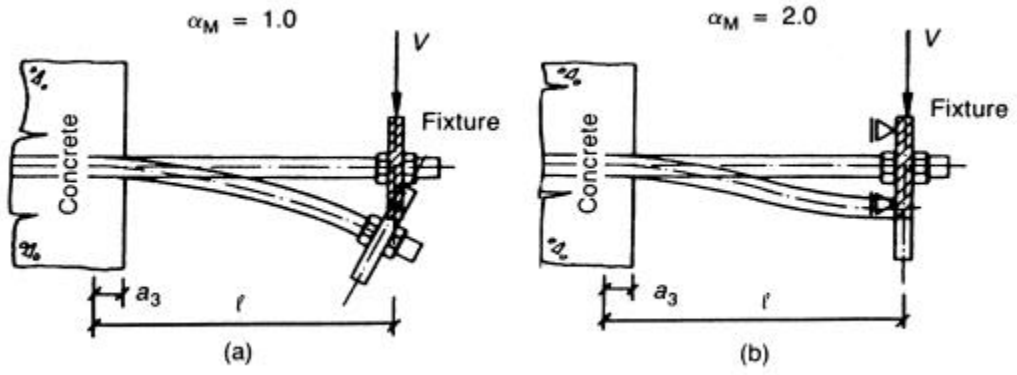

Figure 2.4.9 Examples of fastenings (a) without and (b) with full restrain of the anchor at the side of the fixture (Fig. 27 in the CEB Design Guide).

2.4.2.4 Plastic analysis

In section 4.2.2 of the CEB Guide, plastic analysis is dealt with. In section 4.2.2.1, the field of application is given. It is stated that in a plastic analysis it is assumed that significant redistribution of anchor tension and shear forces will occur in a group. Therefore, plastic analysis is acceptable only when the failure is governed by ductile steel failure of the anchor.

It is stated that pull-out or pull-through failure of the anchor may occur at large displacements allowing for some redistribution of tension forces. However, there may not be a significant redistribution of shear forces. In view of the lack of information on the required behaviour, a plastic analysis should not be used for this type of failure.

To ensure a ductile steel failure the CEB Guide gives several conditions that should be met. These conditions concern:

(1) The arrangement of the anchors. It may be assumed that base plates meet these conditions.

(2) The ultimate strength of a fastening as governed by concrete failure, should exceed its strength as governed by steel failure (equation (2.4.4)):

$$R_{d,c} \geq 1.25\, R_{d,s} \cdot f_{uk}/f_{yk} \qquad (2.4.4)$$

with

$R_{d,c}$ = design concrete capacity of the fastening (concrete cone, splitting or pull out failure (tension loading) or concrete pry-out or edge failure (shear loading))

$R_{d,s}$ = design steel capacity of the fastening

Equation (2.4.4) should be checked for tension, shear and combined tension and shear forces on the anchors.

(3) The nominal steel strength of the anchors should not exceed f_{uk} = 800 Mpa. The ratio of nominal steel yield strength to nominal ultimate strength should not exceed f_{yk} / f_{uk} = 0.8, while the rupture elongation (measured over a length equal to 5d) should be at least 12%.

(4) Anchors that incorporate a reduced section (e.g. a threaded part) should satisfy the following conditions:

(a) For anchors loaded in tension, the strength N_{uk} of the reduced section should either be greater than 1.1 times the yield strength N_{yk} of the unreduced section, or the stressed length of the reduced section should be ≥ 5d (d = anchor diameter outside reduced section).

(b) For anchors loaded in shear or which are to redistribute shear forces, the beginning of the reduced section should either be ≥ 5d below the concrete surface or in the case of threaded anchors the threaded part should extend ≥ 2d into the concrete.

(c) For anchors loaded in combined tension and shear, the conditions (a) and (b) above should be met.

(5) The steel fixture should be embedded in the concrete or fastened to the concrete without an intermediate layer or with a layer of mortar with a thickness ≤ 3 mm.

(6) The diameter of the clearance hole in the fixture should be ≤ 1.2d (the bolt is assumed to bear against fixture; see Fig. 2.4.4(a)).

2.4.2.5 Conclusions for the applicability of the CEB Design Guide for base plates

- From the above conditions, especially condition (5), it becomes clear that according to the CEB Design Guide plastic design is only allowed for base plates without grout layer or with a grout layer not thicker than 3 mm. For usual base plate construction this means that according to the CEB Design Guide, plastic design is not allowed.
- The above conclusion means that according to the CEB Design Guide, the only applicable method for base plates with grout layers thicker than 3 mm is elastic design with the model "Shear loads with lever arm", where the influence of the grout is disregarded. This seems logical since the grout does not have sufficient resistance to prevent high bending moments in the anchors.
- In condition (2) the relation between the required design concrete capacity of the fastening and the design steel capacity of the fastening is given. It appears that for e.g. 8.8 anchors it gives:

$$R_{d,c} \geq 1.56\, R_{d,s} \qquad (2.4.5)$$

In this COST publication it is assumed that failure of the concrete will not occur before failure of the base plate or anchor. The above requirement seems adequate to ensure this prerequisite.

2.4.2.6 Resistance functions for shear load

In section 9.3.1 of the Design Guide, the following required verifications in the case of shear loading are given (elastic design approach):

- Steel failure, shear load without lever arm ($V_{Rk,s}$)
- Steel failure, shear load with lever arm ($V_{Rk,sm}$)
- Concrete pry-out failure
- Concrete edge failure

For $V_{Rk,s}$ and $V_{Rk,sm}$ the following equations are given:

$$V_{Rk,s} = k_2 \cdot A_s \cdot f_{yk} \qquad (2.4.6)$$

$$V_{Rk,sm} = \frac{\alpha_M \cdot M_{Rk.s}}{\ell} \leq V_{Rk,s} \qquad (2.4.7)$$

with

k_2	=	0.6	(2.4.8)
A_s	=	stressed cross section in the shear plane	
$M_{Rk,s}$	=	$M^0_{Rk,s}$ (1- N_{Sd} /$N_{Rd,s}$)	(2.4.9)
$M^0_{Rk,s}$	=	characteristic bending resistance of an individual anchor	
$M^0_{Rk,s}$	=	1.5 $W_{e\ell}$· f_{yk}	(2.4.10)
$N_{Rd,s}$	=	$N_{Rk,s}$ / γ_{Ms}	(2.4.11)
$N_{Rk,s}$	=	A_s· f_{yk}	(2.4.12)
γ_{Ms}	=	1.20 if $f_{uk} \leq$ 800 Mpa and $f_{yk} / f_{uk} \leq$ 0.8	(2.4.13)
γ_{Ms}	=	1.50 if $f_{uk} \geq$ 800 Mpa or $f_{yk} / f_{uk} \geq$ 0.8	(2.4.14)
N_{Sd}	=	applied normal force	
α_M	=	factor depending on the support conditions, see Fig. 2.4.9	
ℓ	=	length of lever arm	

In section 2.4.4 of this COST publication, a comparison of the CEB model with test results obtained in the Stevin Laboratory will be presented, together with a comparison of the Stevin Laboratory model. The Stevin Laboratory model is presented in the next section.

2.4.3 Stevin Laboratory Model

2.4.3.1 Introduction

In normal steel construction a grout layer up to 60 mm thickness may be applied under the base plate. In most cases the shear force can be transmitted via friction between the base plate and the grout. Because the grout does not have sufficient strength to resist the bearing stresses between the bolt and the grout, considerable bending of the anchor bolts may occur, as is indicated in Fig. 2.4.2.

Fig. 4.2.10 gives one of the test specimens that were tested in the Stevin Laboratory (Stevin, 1989). It shows the bending deformation of the anchor bolts and also the crumbling of the grout and final cracking of the concrete.

In this section, the structural behaviour of anchor bolts loaded by combinations of shear and tensile force will be analysed.

Figure 2.4.10 One of the tested specimens loaded by a combination of shear force and tensile force.

2.4.3.2 The analytical model

In Fig. 2.4.11, the deformations and some important measures are indicated. Fig. 2.4.12 shows the schematisation of the deformations and the forces, which are taken into account in the analytical model. In the Figures, the following symbols are used:

A_s	=	tensile stress area of the anchor bolt
F_t	=	applied tensile force
F_h	=	applied shear force (horizontal force)
F_w	=	friction force between base plate and grout
N_b	=	normal force in the grout
F_a	=	normal force in the anchor bolt
δ_a	=	elongation of the anchor bolt
δ_b	=	compression of the grout layer
δ_h	=	horizontal displacement of the base plate
v	=	actual thickness of the grout layer
v_r	=	thickness of the grout layer in the analytical model: $v_r = v + 0.5\ d_b$ ($v_r = \ell$ as in CEB)
d_b	=	bolt diameter

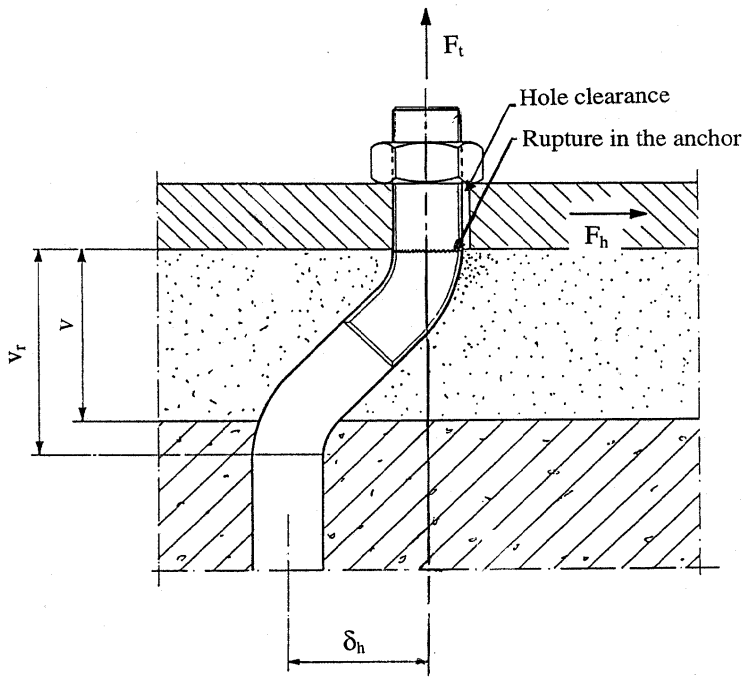

Figure 2.4.11 Deformation and some measurements of the tested anchor bolts.

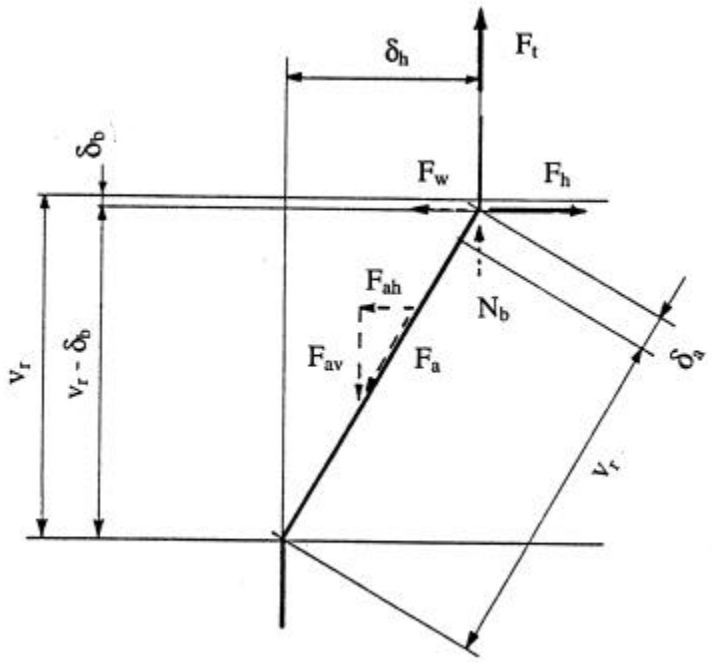

Figure 2.4.12 Schematisation of the deformations and forces in the analytical model.

Due to the horizontal displacement of the base plate, bending of the bolts will occur. Also, the tensile force in the bolt (F_a) will increase. Due to this, the shear force F_w between grout and base plate will increase too.

Already at rather small horizontal deformations (δ_h), the tensile force F_a in the bolt reaches the yield force $F_{yb} = A_s \cdot f_{yb}$. This means that the bending moments in the anchor bolts rapidly decrease and the horizontal component F_{ah} of F_a (Fig. 2.4.12) rapidly increases. Also the friction force F_w will increase.

Because of the high tensile force in the bolt, the bending moments in the bolt will be small. In the analytical model the bending moments in the bolts are not taken into account. The bearing stresses of the grout-bolt contact are not taken into account either, because they are small compared to other forces.

For the horizontal equilibrium it follows:

$$F_h = F_a \frac{\delta_h}{v_r + \delta_a} + F_w \tag{2.4.15}$$

$$F_w = f_w \left(F_a \frac{v_r - \delta_b}{v_r + \delta_a} - F_t \right) \tag{2.4.16}$$

with

f_w = coefficient of friction grout-base plate.

For the deformation it follows:

$$\delta_h^2 = (v_r + \delta_a)^2 - (v_r - \delta_b)^2 \tag{2.4.17}$$

Because δ_h^2 is small compared with δ_a, this can be simplified to:

$$\delta_h^2 = 2\, v_r (\delta_a + \delta_b) \tag{2.4.18}$$

For the "elastic" part of the behaviour, δ_a and δ_b can be written as:

$$\delta_a = \frac{F_a \cdot v_r}{E\, A_s} \tag{2.4.19}$$

$$\delta_b = \frac{(F_a - F_t)\, v_r}{E_{grout} A_{grout}} \tag{2.4.20}$$

Because $E_{grout}\ A_{grout}$ is much greater than EA_s, δ_b will be small compared with δ_a. Therefore δ_b is not taken into account further.

Because of the geometry it follows:

$$v_r + \delta_a = \sqrt{\delta_h^2 + v_r^2} \tag{2.4.21}$$

For (2.4.15), (2.4.16) and (2.4.18) can be written with (2.4.21):

$$F_h = F_a \frac{\delta_h}{\sqrt{\delta_h^2 + v_r^2}} + F_w \tag{2.4.22}$$

$$F_w = f_w \left(F_a \frac{v_r}{\sqrt{\delta_h^2 + v_r^2}} - F_t \right) \tag{2.4.23}$$

$$\delta_h = \sqrt{2\, v_r\, \delta_a} \tag{2.4.24}$$

For every δ_h the elongation δ_a can be calculated via (2.4.24), then with (2.4.19) the force F_a and with (2.4.22) and (2.4.23) the horizontal force F_h.

The above formulae are valid for $F_a \le F_{ay}$, where

$$F_{ay} = A_s \cdot f_{yb} \tag{2.4.25}$$

For $F_a = F_{ay}$ it follows with (2.4.22), (2.4.23) and (2.4.25):

$$F_h = \frac{f_y A_s}{\sqrt{\delta_h^2 + v_r^2}} (\delta_h + f_w\, v_r) - f_w F_t \tag{2.4.26}$$

with

$$\delta_h = v_r \sqrt{\frac{2 f_y}{E}} \tag{2.4.27}$$

For the coefficient of friction $f_{w,d}$ the following design values are proposed:

- sand-cement mortar $f_{w,d} = 0.20$
- special grout (e.g. Pagel IV) $f_{w,d} = 0.30$

2.4.3.3 Comparison with one of the tests

To demonstrate the analytical model, one of the test results is calculated, namely DT6 in (Stevin, 1989). In this test, a tensile force F_t = 141 kN was kept constant in the column, while the horizontal force F_h was increased.

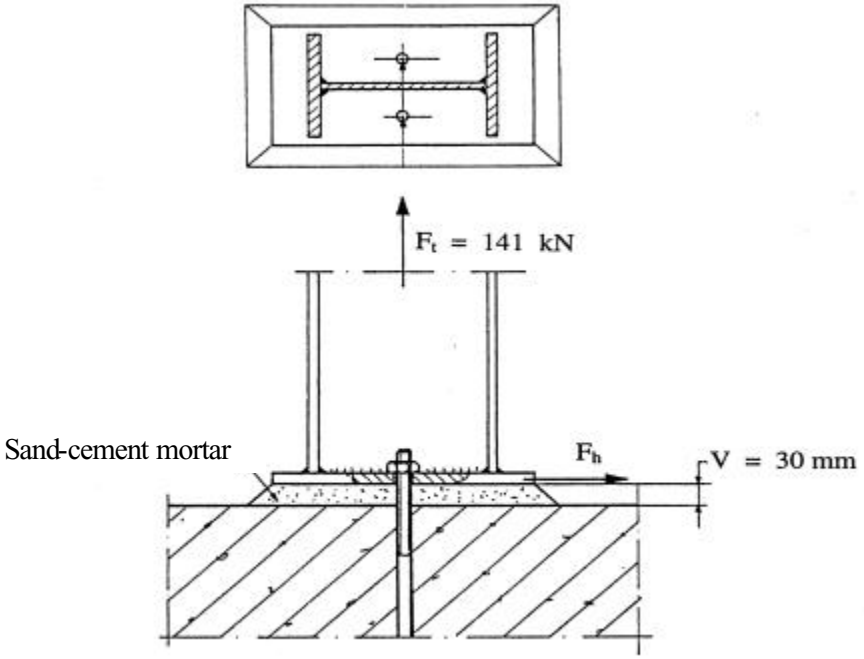

Figure 2.4.13 Test specimen DT6.

Data:

- 2 anchor bolts M20, grade 8.8
- f_{ub} = 1076 N/mm^2 (measured value)
- f_{yb} = 861 N/mm^2 (assumed as 0.8 f_{ub})
- ε_{ub} = 12% (measured value)
- A_s = 245 mm^2
- grout = sand-cement mortar
- v = 30 mm

Calculation:

$$v_r = v + 0.5\, d_b = 30 + 0.5 \cdot 20 = 40 \text{ mm}$$

For δ_h according to (2.4.27) it follows:

$$\delta_h = v_r \sqrt{\frac{2 f_{yb}}{E}} = 40 \sqrt{\frac{2 \cdot 861}{210\,000}} = 3.6 \text{ mm}$$

For F_h according to (2.4.26) it follows (2 bolts):

$$F_h = \frac{861 \cdot 245 \cdot 10^{-3}}{\sqrt{3.6^2 + 40^2}} (3.6 + 0.20 \cdot 40) \cdot 2 - 0.20 \cdot 141 = 122 - 28 = \underline{94 \text{ kN}}$$

E.g., for $\delta_h = 2 \cdot 3.6 = 7.2$ mm, it follows:

$$F_h = 158 - 28 = \underline{130 \text{ kN}}$$

Fig. 2.4.14 gives the test result together with the result of the analytical model. The value $F_{v.Rd}$ = 105 kN is explained in the next section.

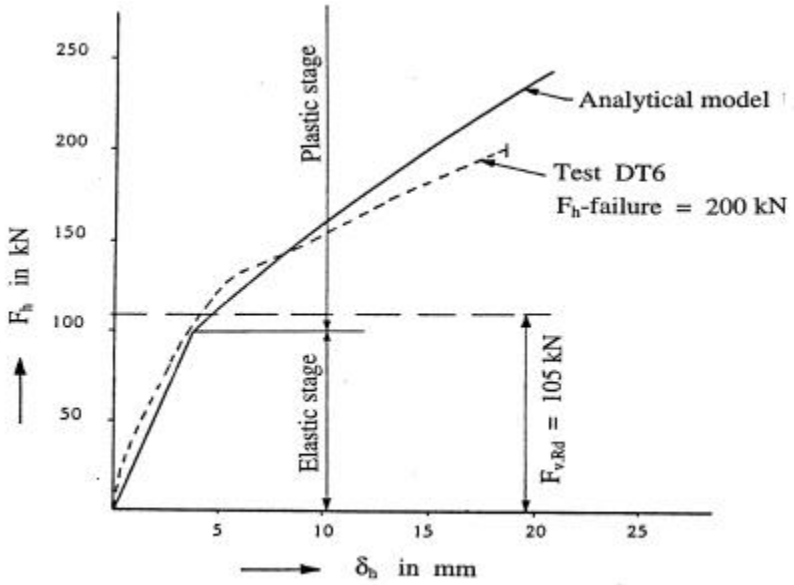

Figure 2.4.14 Comparison of the analytical model with the result of test DT6.

It is noted that in Fig. 2.4.14 a linear relationship is assumed till the value of δ_h equals δ_h according to (2.4.27) and F_a equals A_s f_{yb}. This part of the load deformation curve is called "elastic".

Failure occurred in the anchor bolts (rupture) at the edge of the base plate, due to local high bending strains.

2.4.3.4 Ultimate design strength

The ultimate strength is a function of the strength of the various parts in the column base and of the ductility of the anchor bolts. A greater ductility allows a greater horizontal displacement and thus a greater F_{ah} (Fig 2.4.12) and consequently a greater F_h.

It can also be noted that δ_h should be limited, both at serviceability and at ultimate limit state.

To predict the ultimate strength (if governed by the anchor bolt) a relation must be found between the local strain in the bolt and the horizontal deformation. Furthermore, the strain capacity (ductility) of the various anchor materials must be known.

In the tests it was clear that the applied 4.6 grade anchor bolts were much more ductile than the 8.8 grade bolts. A difference in ductility can also be found in the requirements in the relevant product standards.

It appeared not easy to establish a reliable model for the strains and to find reliable data for the bending strain capacity of various anchor bolt materials. Therefore, a simplified method is proposed for the strength of 4.6 and 8.8 grade anchor bolts. This simplified method is adopted in the Dutch Standard (NEN 6770, 1990).

- 4.6 anchors: $$F_{v.Rd} = \frac{0.375\, f_{ub} \cdot A_s}{\gamma_{Mb}} \qquad (2.4.28)$$

- 8.8 anchors: $$F_{v.Rd} = \frac{0.25\, f_{ub} \cdot A_s}{\gamma_{Mb}} \qquad (2.4.29)$$

with $\gamma_{Mb} = 1.25$. These resistance functions are similar to the "normal" Eurocode 3 functions for bolts loaded in shear:

- 4.6 and 8.8 bolts: $$F_{v.Rd} = \frac{0.60\, f_{ub} \cdot A_s}{\gamma_{Mb}} \qquad (2.4.30)$$

After checking the design resistance, the horizontal displacements should be checked for the serviceability limit state and for the ultimate limit state.

2.4.4 Comparison with test results

2.4.4.1 Test results and comparison with the Stevin Laboratory model

In the test programme (Stevin, 1989), 16 tests were carried out. In Fig. 2.4.15 the main dimensions of the test specimens are given. Table 2.4.1 gives a summary of the parameters in the test programme, while in table 2.4.2 a summary is given of the main test results and a

comparison with the proposed resistance functions, according to the Stevin Laboratory model (= NEN 6770).

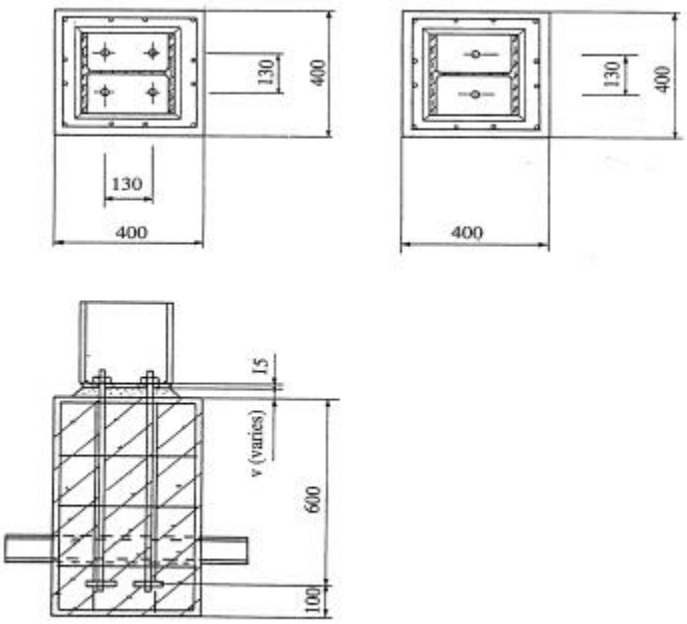

Figure 2.4.15 Test specimens; in the tests with 4.6 grade anchor bolts, four bolts were applied and in the tests with 8.8 grade anchors two bolts.

Table 2.4.1 Parameters in the tests.

Part of the base plate structure	Parameter	Variation
Grout	Type of grout	Special grout Pagel IV
		Sand - cement mortar 2:1
		No grout
	Thickness of grout	15 mm
		30 mm
		60 mm
Anchor bolt	Strength and dimension	4.6 M20
		8.8 M20
	Anchoring length	250 mm with a bend at the end of the bar
		600 mm with anchor plate
Concrete	Reinforcement	With reinforcement
		Without reinforcement

Table 2.4.2 Summary of test results and comparison with design values according to the proposed resistance functions (Stevin, 1989).

Test	Anchors				Thickness of grout (v)	Tensile force F_t	Measured ultimate shear force F_h	Failure mode *)	Design value $F_{v,Rd}$ **)	Test / design value
	number	Class	Yield stress f_{yb}	Ultimate stress f_{ub}						
			Mpa	MPa	Mm	kN	kN		kN	
DT1	4	4.6	290	423	30	182	170	Cracking	124	1.37
DT2	4	4.6	290	423	30	121	250	Cracking	124	2.06
DT3	4	4.6	290	423	30	121	240	Rupture	124	1.94
DT4	4	4.6	290	423	30	121	240	Rupture	124	1.94
DT5	2	8.8	-	1152	30	141	178	Rupture	113	1.57
DT6	2	8.8	-	1076	30	141	200	Rupture	105	1.90
DT7	2	8.8	-	1070	30	141	190	Rupture	105	1.81
DT8	2	8.8	-	1045	60	141	230	Rupture	102	2.25
DT9	4	4.6	290	423	60	121	180	Pull-out	124	1.45
DT10	2	8.8	-	1049	60	141	228	Rupture	102	2.23
DT11	4	4.6	290	423	15	121	270	Cracking	124	2.17
DT12	2	8.8	-	1176	15	141	255	Rupture	115	2.21
DT13	4	4.6	280	414	60	121	320	Rupture	122	2.62
DT14	4	4.6	283	411	60	121	305	Cracking	121	2.52
DT15	2	8.8	-	1089	30	200	200	Cracking	107	1.87
DT16	4	4.6	309	443	30	200	255	Cracking	130	1.96

*) Cracking = cracking of the concrete
Rupture = rupture of the anchor
Pull-out = pull-out of the anchor

**) These values were calculated with the measured material properties and dimensions.

2.4.4.2 Comparison with the CEB model

First the application of the CEB model is demonstrated for one of the tests. Test DT5 is taken as an example, see also table 2.4.2 and 2.4.3:

Bolts M20, grade 8.8
f_{ub}-measured = 1152 Mpa
take f_{yk} = $0.8 \cdot 1152 = 922$ MPa
take γ_{Ms} = 1.20 (for 8.8 bolts)

$A_s = \pi \cdot d_s^2 / 4 = 245\ mm^2 \rightarrow d_s = 17.66\ mm$

$N_{Rk,s} = A_s \cdot f_{yk} = 245 \cdot 922 \cdot 10^{-3} = 226\ kN$

$N_{Rd,s} = N_{Rk,s} / \gamma_{Ms} = 226 / 1.20 = 188\ kN$

$N_{Sd} = 141 / 2 = 70.5\ kN$

$$W_{e_\ell} = \frac{\pi \cdot d_s^3}{32} = \frac{\pi \cdot 17.66^3}{32} = 541\ mm^3$$

$M^0_{Rk,s} = 1.5\ W_{e_\ell} \cdot f_{yk} = 1.5 \cdot 541 \cdot 922 = 748 \cdot 10^3\ Nmm$

$M_{Rk,s} = M^0_{Rk,s} (1- N_{Sd} / N_{Rd,s}) = 748 \cdot 10^3 (1 - 70.5 / 188) = 468 \cdot 10^3\ Nmm$

$V_{Rk.s} = k_2 \cdot A_s \cdot f_{yk} = 0.6 \cdot 245 \cdot 922 \cdot 10^{-3} = 136\ kN$

$$V_{Rk,sm} = \frac{\alpha_M \cdot M_{Rk.s}}{\ell} = \frac{2 \cdot 468 \cdot 10^3}{30 + 20/2} 10^{-3} = 23.4\ kN \leq V_{Rk.s} = 136\ kN$$

For the test with 2 bolts it follows $2 \cdot 23.4 = 46.8\ kN \sim 47\ kN$, see table 2.4.3.

Table 2.4.3: Comparison of test results with design values according to the CEB model and Stevin Laboratory model.

Test	$N_{Rd,s}$ per bolt*)	N_{sd} per bolt	$N_{sd} / N_{Rd,s}$	$M^0_{Rk,s}$*)	$M_{Rk,s}$*)	Length ℓ	$V_{Rk,sm}$ group*)	Test / CEB	Test / Stevin**)
	kN	kN		Nm	Nm	mm	kN		
DT1	59	45.50	0.77	235	54	40	11	**15.6**	**1.4**
DT2	59	30.25	0.51	235	115	40	23	**10.9**	**2.0**
DT3	59	30.25	0.51	235	115	40	23	**10.4**	**1.9**
DT4	59	30.25	0.51	235	115	40	23	**10.4**	**1.9**
DT5	188	70.50	0.37	748	468	40	47	**3.8**	**1.6**
DT6	176	70.50	0.40	699	418	40	42	**4.8**	**1.9**
DT7	175	70.50	0.40	695	414	40	41	**4.6**	**1.8**
DT8	171	70.50	0.41	678	398	70	23	**10.1**	**2.3**
DT9	59	30.25	0.51	235	115	70	13	**13.7**	**1.5**
DT10	171	70.50	0.41	681	401	70	23	**10.0**	**2.2**
DT11	59	30.25	0.51	235	115	25	37	**7.3**	**2.2**
DT12	192	70.50	0.37	763	483	25	77	**3.3**	**2.2**
DT13	57	30.25	0.53	227	107	70	12	**26.2**	**2.6**
DT14	58	30.25	0.52	230	109	70	13	**24.4**	**2.5**
DT15	178	100.00	0.56	707	310	40	31	**6.5**	**1.9**
DT16	63	50.00	0.79	251	52	40	10	**24.5**	**2.0**

*) Calculated with the measured material properties and dimensions as given in table 2.4.2.

**) The Stevin values are taken from table 2.4.2.

2.4.5 Conclusions

2.4.5.1 Regarding the models

The CEB model gives very conservative results, especially when a large tensile force is present and / or the length ℓ (thickness of the grout layer) is large. The main reason is that the CEB model does not take account of the positive influence of the grout layer. The CEB model does not give rules to determine the deformation.

The Stevin Laboratory model gives much more consistent results. It gives also rules to determine the deformation.

2.4.5.2 Regarding the observed behaviour

- The strength in shear of anchor bolts is considerably lower than the shear strength of bolts in bolted connections between steel plates.
- The ductility of the anchor bolts is an important factor for the strength. The lower ductility of 8.8 grade bolts compared to 4.6 grade bolts is reflected in the lower coefficient of the resistance function.

$$\frac{F_{v.Rd}\text{-}8.8}{F_{v.Rd}\text{-}4.6} = \frac{0.25}{0.375} \cdot \frac{800}{400} = 0.67 \cdot 2 = 1.33\,1$$

- The influence of a tensile force F_t in the column can be neglected for the determination of the shear resistance.
- The shear resistance is almost independent of the thickness of the grout layer.
- The deformations are greatly dependent on the thickness of the grout layer.
- The type of grout has virtually no influence on the shear resistance.
- A "better" grout, e.g. "Pagel IV" gave less deformations in the tests. In general it can be stated that the quality of the grout layer has great influence on the strength and especially the deformations.
- In the design, not only the shear resistance should be checked, but also the deformations at serviceability and ultimate limit state.
- It is obvious that also other failure modes, like splitting of the concrete block, etc., should be checked. For this check the CEB Design Guide is probably a good guidance.

Chapter 3: Assembly procedure

3.1 Influence of load history

Once the resistance, stiffness and deformation capacity of the joint components have been calculated, the next step is to determine the resistance, stiffness and rotational capacity of the whole joint. The procedure to follow in this process is called the "assembly procedure".

In section 3.2 an overview of assembly procedures resulting from the COST C1 project is given, whereas in section 3.3 a simplified assembly procedure is described for practical design purposes.

Unlike beam-to-column joints, an important aspect of assembly procedures and their comparison with test results for column bases is the (monotonic) loading history applied to the joint. In case of beam-to-column joints without normal force in the beam, the rotation of the joints is only dependent on the applied moment. In the case of base plate joints, however, the moment-rotation characteristic is also dependent on the normal force in the column.

Consider the base plate joint of Figure 3.1.1.

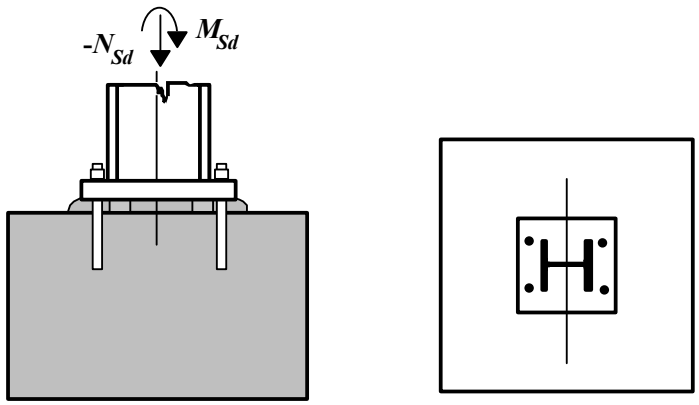

Figure 3.1.1 Base plate joint.

Assume that the base plate is loaded to its moment resistance M_{Rd} = 160 kNm in combination with a normal compressive force N_{Rd} = -660 kN.

With help of a design model, design moment-rotation diagrams are calculated as shown in Figure 3.1.2. In this figure two lines are indicated, the solid line labelled "proportional" and the dotted line labelled "non-proportional".

In the proportional case, the moment M_{Sd} is applied to the joint together with a normal force

N_{Sd} equal to $N_{Rd} \cdot M_{Sd} / M_{Rd}$. In other words, when the M_{Sd} is equal to zero, N_{Sd} is equal to zero and when M_{Sd} is equal to M_{Rd}, N_{Sd} is equal to N_{Rd}.

In the non-proportional case, it is assumed that the normal force N_{Rd} is applied first to the joint and that then the moment M_{Sd} is applied step by step until it reaches M_{Rd}.

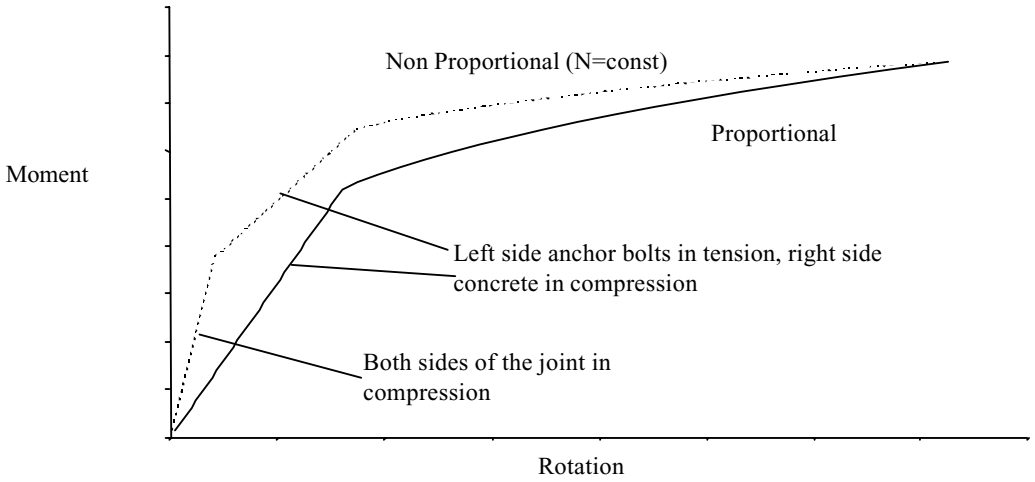

Figure 3.1.2 Design moment-rotation diagram for the joint of Figure 3.1.1.

From Figure 3.1.2 it can be seen that the initial stiffness under non-proportional loading is much higher then under proportional loading. This is because concrete in compression is much stiffer than anchor bolts in tension. In the case of non-proportional loading during the initial loading steps, both sides of the joint are firmly held in contact by the normal force N_{Rd}. That means that hardly no deformations occur, even if a small moment is applied to the joint. When the moment M_{Sd} exceeds a certain value, the left side of the joint is no longer in compression and the anchor bolts are activated. The joint looses then its high stiffness.

In case of proportional loading, the anchor bolts on the left hand side of the joint are activated immediately. The initial stiffness is therefore lower than in the case of non-proportional loading, where the anchor bolts are inactive.

In Figure 3.1.2 it can be seen that the design moment resistance of the joint is independent of the load history applied (proportional or non-proportional) to the joint. The normal force in the column has a critical effect on the design moment resistance.

When the normal force N_{Sd} acting at a joint is a tensile force, the initial stiffness in case of non-proportional loading will probably be lower than in case of proportional loading because due to the tensile normal force, all anchor bolts will be held in tension during the initial load

steps of non-proportional loading, which will result in a high flexibility.

Load history is important when reviewing the assembly procedures and also when comparing tests with design models. For instance, in many cases, tests are performed with non-proportional loading and design models assume proportional loading. The test results and the design models may in that case not be compared directly with each other and a correction needs to be made to take the load history into account.

In design pracitice, a proportional load history is normally considered.

3.2 Review of existing models

3.2.1 Overview

Chapter 2 describes how the load - deformation curve of each individual component of a column base joint may be determined. In order to end up with a moment-rotation curve, which represents the global behaviour of the joint, the component characteristics have to be assembled. For this purpose, appropriate analytical or mechanical models are used, for example spring models. The assembly of the components of a column base joint with an end plate is similar to that of beam-to-column joints. However, the assembly is significantly affected by the interaction of normal forces and bending moments.

Model	Mechanical	Analytical				
	Sophisticated Two dimensional	Complex Model	Simplified Stiffness	Simplified Strength	Simplified Strength	Simplified Strength and stiffness
M-ϕ curve	Non-linear	Non-linear	Stiffness	Strength	Strength	Non-linear
Components description	Non-linear	Bi-linear	Stiffness only	Strength only	Strength only	Bi-linear
Effective area of an equivalent rigid plate	Annex L [1] 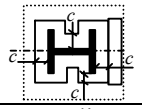	Rectangular for H section 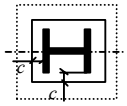	Rectangular for H section 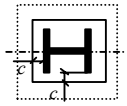	Annex L [1] 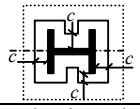	Rectangular 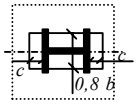	Web neglected 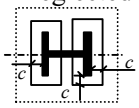
Stress to concrete	Non-linear springs	Elasto-plastic (12 stress patterns)	Three patterns only	Plastic only	Plastic only	Plastic only
Compatibility	Yes	Yes	Yes	Not for strain	Simplified	Simplified
Reference	Guisse et al, 1996	Wald, 1995	Wald et al., 1996	Wald et al., 1996	Guisse et al, 1996	Steenhuis, 1998

Figure 3.2.1 Comparison of different assembly procedures

Different prediction models are available for calculation, for list of models see Wald, 1993. Figure 3.2.1 gives a brief overview of the different assembly models based on component method, see Wald, 1995; Guisse at all., 1996; Wald, 1996; Steenhuis, 1998. It can be seen that some models consider the full non-linear behaviour, while others only deal with the resistance or with the stiffness of the joint. Most of the models fulfil the requirements for compatibility (i.e. equilibrium of internal forces, deformations, etc.), but some of them in a simplified way only.

The mechanical model presented in Guisse at all, 1996 is based on a 2D non-linear spring simulation, see Figure 3.2.2. It can take into account not only the non-linear behaviour of each component, but it can also simulate the influence of changes of the effective area under bending. This mechanical model is certainly useful for researchers performing scientific background studies and comparisons. Test results demonstrate a good accuracy of the model. However, the model is too complex for daily design practice. A more practical approach is the component method to predict the design resistance, stiffness and deformation capacity.

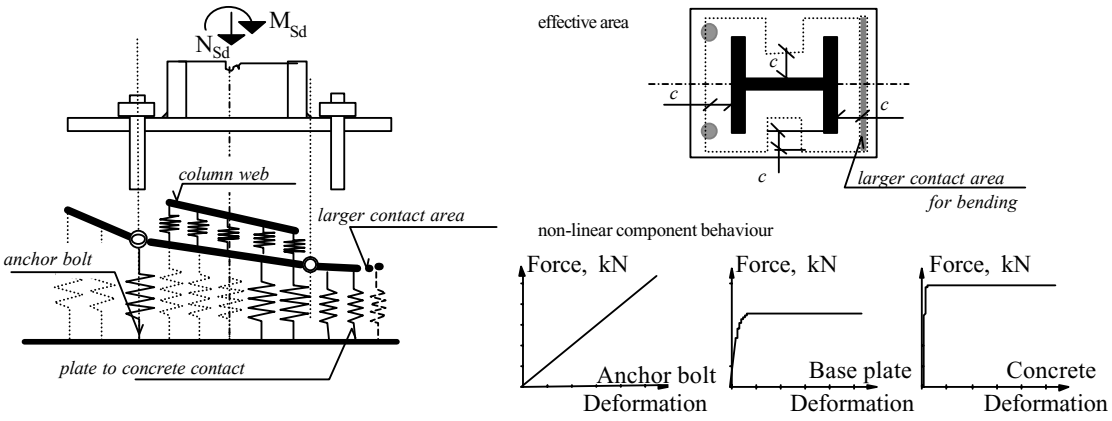

Figure 3.2.2 Mechanical model for the assembly procedure of components according to Guisse at all, 1996

As can be seen in Figure 3.2.1, the various models use different approaches to determine the effective area. In the models it is assumed that this effective area represents a rigid plate with a certain stress distribution in the compression zone. It can be understood that the shape of this effective area will strongly influence the complexity of the assembly models. This is because the assembly procedure should take the normal forces and the bending moments acting to the joint into account. Their actual values will influence the position of the neutral axis of stresses, which also depends on the shape of the effective area.

Most proposals for the effective area are based on the model given in Annex L of Eurocode 3 [1], which assumes plastic distribution of stresses in the concrete under the base

plate (bearing width 'c'). Furthermore, the models assume a certain pattern for the compressive stresses. The simplest approach is a full plastic stress distribution for the resistance calculation.

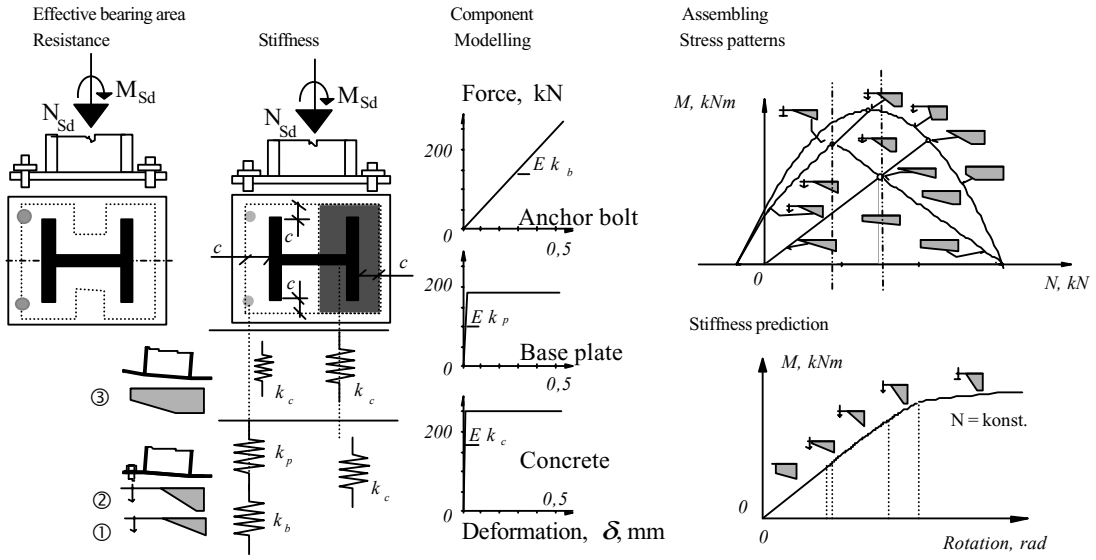

Figure 3.2.3 The Assembly based on rectangular shape of base plate Wald, 1995, the simplification to three patterns only for high bending moments and low bending moments respectively, the bi-linear load-deformation curves of the components and the moment-normal force diagram

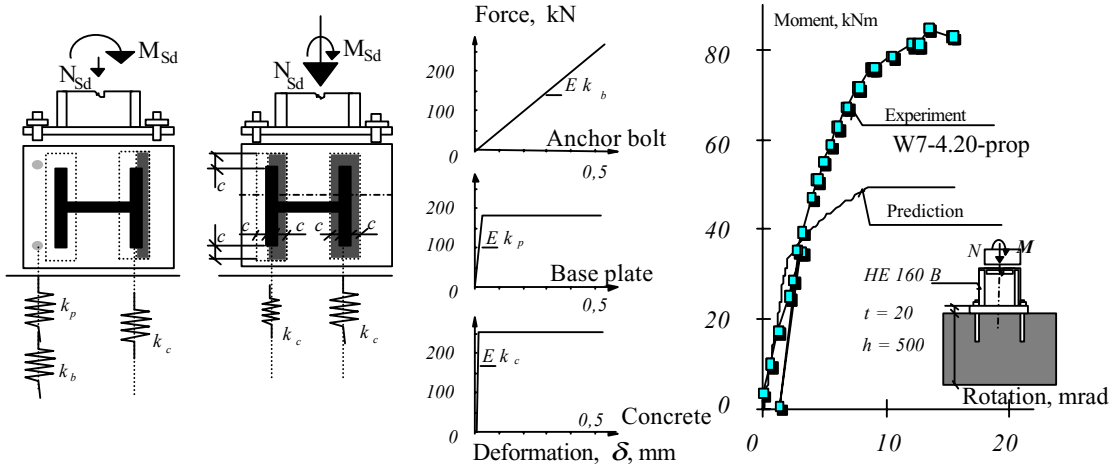

Figure 3.2.4 The assembling with an effective area around the column flanges only Steenhuis, 1998. For high bending moments and low bending moments respectively, the bi-linear load-deformation curves of the components and the moment-rotation diagram for the joint in comparison to test no W7-4.20-prop are shown, see Wald et al, 1995

The prediction of the rotational stiffness has to be based on simplifications of the effective

area in order to allow for the development of a procedure with a limited degree of complexity. The simplified area using a rectangular shape enables taking all stress distributions (12 patterns) into account. A simpler solution, for example with only three categories of high, medium and low normal force is also an option, see Figure 3.2.3 from Wald, 1993, where f_y represents yielding in the tension part and f_j represents the concrete bearing resistance. The simplest modelling takes the areas under the flanges only into account, see Figure 3.2.4 based on Steenhuis, 1998. This has the advantage of simple modelling without losing accuracy under pure bending, when the contact is correctly predicted, but it has the disadvantage of losing the accuracy under high normal force and a very small bending moment, especially for cross sections with a significant effective area under the column web.

3.2.2 Simplified 'Prague' model for resistance and stiffness

3.2.2.1 Strength Design

The effective bearing area A_{eff} and bearing strength f_j is calculated according to Eurocode 3 Annex L, 1992. This area is used for strength calculation Wald (1995). The resistance of the tension part of column bases loaded by an axial force and a bending moment $F_{t.Rd}$, is calculated according to Eurocode 3 Annex J, 1998. The equilibrium of internal forces could be calculated in elastic or plastic stages. The active part of the effective area A_{eff} can be calculated from the equilibrium equation, see Figure 3.2.5.

$$N_{Rd} = A_{eff}\ f_j - \sum F_{t.Rd} \tag{3.2.1}$$

$$M_{Rd} = \sum F_{t.Rd}\ r_b + A_{eff}\ f_j\ r_c \tag{3.2.2}$$

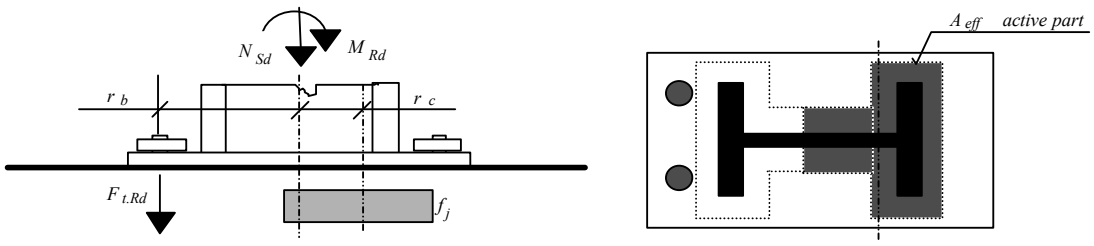

Figure 3.2.5 Equilibrium of internal forces

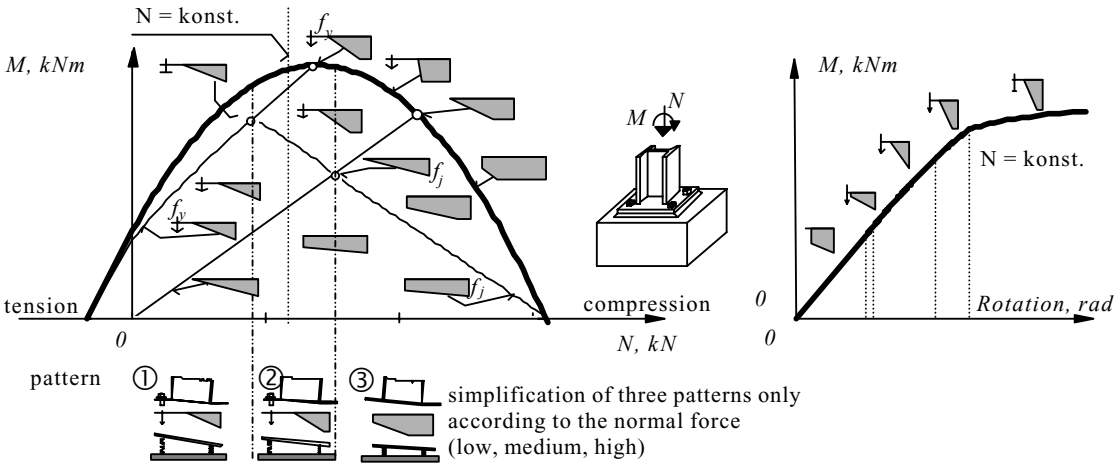

Figure 3.2.6 Moment - normal force resistance diagram for column base introducing the internal force distribution in elastic and inelastic region, f_y is representing yielding of the tension part, f_j is bearing resistance of the concrete, see Wald, 1995

3.2.2.2 Rotational Stiffness

The rotational stiffness is determined according to stiffness model published in Eurocode 3 Annex J, 1998.

$$S_j = \frac{E \; z^2}{\mu \sum_i \frac{1}{k_i}} \tag{3.2.3}$$

where E is the modulus of elasticity of the steel and z is the lever arm. The ratio between the rotational stiffness μ with respect to the bending moment can be calculated as

$$\mu = \frac{S_{j,ini}}{S_j} = \left(\kappa \frac{M_{Sd}}{M_{Rd}} \right)^{\xi} \quad \geq 1 \tag{3.2.4}$$

In the formula above, ξ is shape parameter of the curve, κ is coefficient introducing the beginning of non-linear part of the curve and M_{sd} is acting bending moment, see WALD, 1995.

The extension of the model compared to Eurocode approach is the introduction of the normal force. It is distinguished between three basic collapse modes of the base plate joint, see Wald and Sokol, 1995 and Wald and Sokol, 1997. They differ by the bearing stress distribution

under the base plate with respect to the tension part, see Figure 3.2.7.

The concrete bearing stress f_j is never reached, when the column base joint is loaded by low axial force (compared to the ultimate bearing capacity). The collapse occurs either by yielding of the bolts or by development a plastic mechanism in the base plate (pattern 1). When medium axial force is applied, the concrete bearing stress f_j and the strength of the tension part $F_{t.Rd}$ are reached at the collapse (pattern 2). For a high axial force, collapse of the concrete occurs while stress in the tension part is not developed (pattern 3).

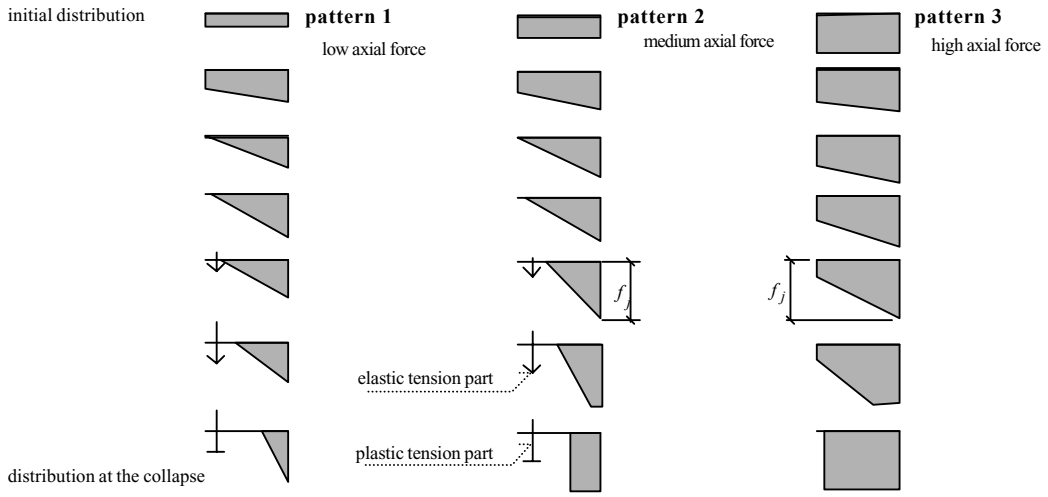

Figure 3.2.7 The stress distribution for three patterns of the base plate joint in initial and collapse stages

The axial force $N_{1.2}$ representing the boundary between low and medium forces is calculated for two anchor bolts, see Wald et al, 1996 and Wald, 1995.

$$N_{1.2} = \frac{a_p\, b_p^2\, f_j^2 \left(2\, z + a_p\right) \frac{1}{k_c}}{4\left(a_p\, b_p\, f_j\, \frac{1}{k_c} + 4\, A_s\, f_t \left(\frac{1}{k_b} + \frac{1}{k_p}\right)\right)} - 2\, A_s\, f_t \qquad (3.2.5)$$

where $f_t = F_{t.Rd} / A_s$ is equivalent stress in the tension part, a_p, b_p are dimensions of the effective area of the plate, see Figure 3.2.8, and z is the lever arm of anchor bolts.

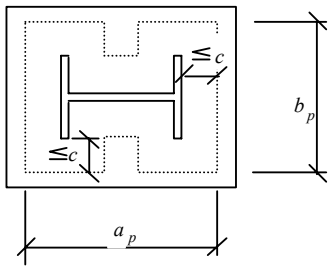

Figure 3.2.8 Simplification of the effective area for the stiffness calculations

The boundary between medium and high forces $N_{2.3}$ is given by

$$N_{2.3} = \frac{\left(2\ z + a_p\right)\ b_p\ f_j - 2\ A_s\ f_t}{2} \quad \leq \quad a_p\ b_p\ f_j \tag{3.2.6}$$

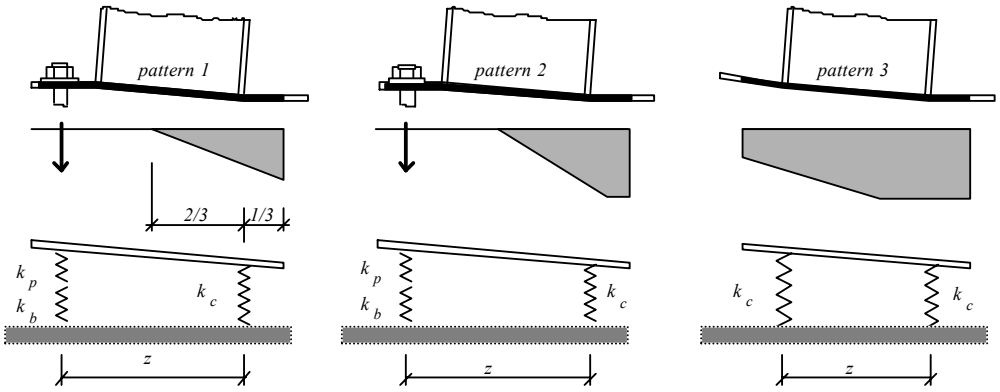

Figure 3.2.9 The spring simulation of deformation of the base plate joint

Table 3.2.1 Values to be considered in stiffness calculation for different patterns Wald and Sokol, 1995

Pattern	Relevant Stiffness coefficients k_i	κ	ξ	Lever arm	
1 Low axial force $N_{Sd} \le N_{1.2}$	k_p, k_b, k_c	1,1	6	$z_1 = \frac{1}{3}(2r_b + a_p)$	
2 Medium axial force $N_{1.2} < N_{Sd} < N_{2.3}$	k_p, k_b, k_c	linear transition		linear transition between z_1 and z_3	$\sqrt{\frac{\sum \frac{1}{k}(for\ pattern1)}{\sum \frac{1}{k}(for\ pattern3)}}$
3 High axial force $N_{2.3} \le N_{Sd}$	k_c, k_c	1,5	8	$z_3 = \frac{a_p}{\sqrt{3}}$	

3.2.3 Simplified 'Liège' model for resistance

3.2.3.1 Introduction

Experimental tests have been carried out at the University of Liège (Guisse et al, 1996) on column bases with two or four anchor bolts. They have shown that the column bases have a very high semi-rigid behaviour, even for so-called nominally pinned connections; this is known to be potentially beneficial when designing building frames.

On the basis of the knowledge got from these tests and fom the available literature, a simple analytical model aimed at predicting the ultimate and design resistances has been developed and validated through comparisons with the experiments.

The model, which is briefly described in this section appears as an application of the principles of the component method, with some references to annexes L and J of Eurocode 3 for what regards the characterization of the individual basic components.

But nowadays a complete model requires also the prediction of the rotational stiffness of the column bases.

However, the complexity of the problem is such that the development of a simple and reliable stiffness model appeared as quite contingent. Guisse et al therefore decided to focus on the

development of a scientific tool, i.e. a mechanical model, allowing, through rather long and iterative calculation procedures, to simulate accurately the non-linear response of the column bases from the first loading steps to failure.

The interested reader will find details about the simple analytical model and the more sophisticated one in (Guisse et al, 1996). In the next paragraphs, guidelines on how to use the simple analytical model for the evaluation of the resistance of column bases are given.

3.2.3.2 Scope of the presented model

All the figures given here below relate to a "4 anchor bolts" configuration but the procedure applies both to "2 and 4 anchor bolts" configurations. The equations presented cover cases where a part of the concrete block is subjected to compressive forces (contact zone with the base plate). The model may easily be extended to cases where no contact forces develop between the block and the foundation (forces carried out by the anchor bolts in tension only).

3.2.3.3 Description of the model

PRELIMINARY CALCULATIONS

Evaluation of the resistance properties of the components

- concrete in compression
- anchor bolts in tension
- base plate in bending

Definition of the rigid equivalent plate

- Calculation according Annex L Eurocode 3 (or improved procedure if available) $\rightarrow$ A_{eff}
- Definition of a fictitious rigid equivalent plate b_{eff} x h_{eff} with an area equal to A_{eff} (Figure 3..2.10)

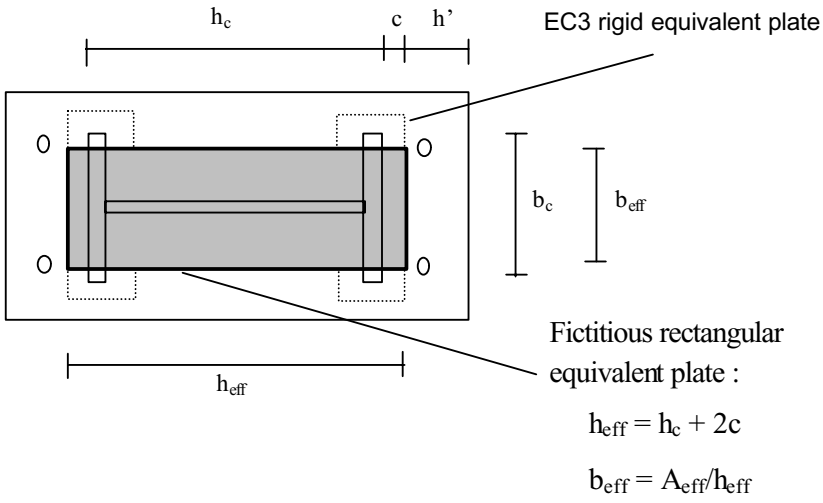

Figure 3.2.10 Equivalent rectangular rigid plate

- As an approximation, b_{eff} may be chosen as equal to 0,8 b_c.

CALCULATION PROCEDURE

At ultimate limit state (column based subjected to M^*_{Rd} and N^*_{Rd}), two different situations may occur :

- bolts are activated in tension;
- bolts are not activated in tension.
- Two sets of formulae are available to cover both situations.

The user first makes an assumption and decides whether, at first sight, anchor bolts are likely or not to be activated in tension. According to his decision, he follows hereafter one of the two procedures respectively named :

- assembly procedure with no anchor bolts in tension;
- assembly procedure with anchor bolts in tension.

Inside the procedures, a criterion is given to check the validity of the assumption. If it is not fulfilled, the user selects then the procedure he had first disregarded.

The proposed formulae simply results from the expression of the equilibrium between the applied bending moment and axial force and the resultant forces in the anchor bolts and/or the

contact forces between the base plate and the concrete foundation (a rectangular distribution of contact stresses is assumed).

Assembly procedure with no anchor bolts in tension

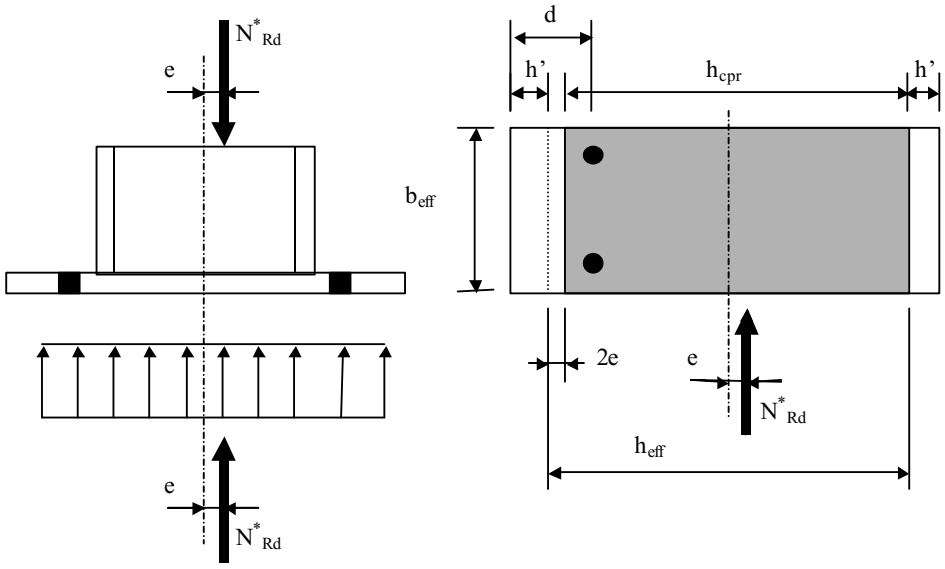

Figure 3.2.11 Internal and external forces if no anchor bolts in tension

h_{cpr}, which is defined as h_{eff}-2e, is derived from both following equilibrium equations (Figure 3.2.11) :

$$\frac{M^*_{Rd}}{N^*_{Rd}} = e \tag{3.2.7}$$

$$e = \frac{1}{2}\left[h_{eff} - \frac{N^*_{Rd}}{b_{eff} f_j}\right] \tag{3.2.8}$$

At the same time, the values of M^*_{Rd} and N^*_{Rd} are extracted.

The solution is valid as long as :

$$h_{cpr} \geq h_{eff} + h' - d \tag{3.2.9}$$

Assembly procedure with anchor bolts in tension

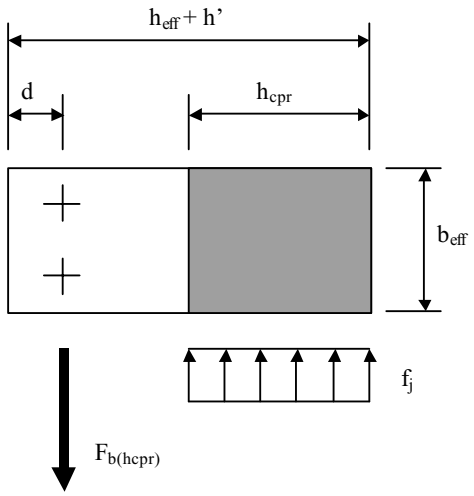

Figure 3.2.12 Internal forces if one anchor bolt row in tension

h_{cpr} is derived from the three following equations (Figure 3.2.12)

$$h_{cpr} = \frac{N^*_{Rd} + 2F_{t.Rd}}{b_{eff} f_j + 2F_{t.Rd} \dfrac{1}{h_{eff} + h' - d}} \tag{3.2.10}$$

$$\frac{M^*_{Rd}}{N^*_{Rd}} = e \tag{3.2.11}$$

$$\begin{aligned} M^*_{Rd} = {} & b_{eff} h_{cpr} f_j \frac{h_{eff} - h_{cpr}}{2} \\ & + F_{t.Rd} \frac{(h_{eff} + h' - d) - h_{cpr}}{0{,}5(h_{eff} + h' - d)} \left(\frac{h_{eff}}{2} + h' - d\right) \end{aligned} \tag{3.2.12}$$

The values of M^*_{Rd} and M^*_{Rd} are extracted at the same time.

The solution is valid as long as :

$$0{,}5(h_{eff} + h' - d) < h_{cpr} < (h_{eff} + h' - d) \tag{3.2.13}$$

If $0{,}5(h_{eff} + h' - d) > h_{cpr}$, then the anchor bolts are subjected to forces equal to their design resistances in tension and equations (3.2.10) to (3.2.12) have to be replaced by the following ones:

$$h_{cpr} = \frac{N^*_{Rd} + F_{t.Rd}}{b_{eff} f_j} \tag{3.2.14}$$

$$\frac{M^*_{Rd}}{N^*_{Rd}} = e \tag{3.2.15}$$

$$M^*_{Rd} = b_{eff} h_{cpr} f_j \frac{h_{eff} - h_{cpr}}{2} + F_{t.Rd}\left(\frac{h_{eff}}{2} + h' - d\right) \tag{3.2.16}$$

3.2.4 Simplified 'Delft' model for resistance and stiffness

This paragraph presents an assembly procedure for determination of strength properties M_{Rd} under normal force N_{Sd} and rotational stiffness S_j for column base steel joints neglecting the contribution of the column web. The assembly procedure based on Eurocode 3 Annex L, but the contribution of the column web is neglected, see Figure 3.2.13.

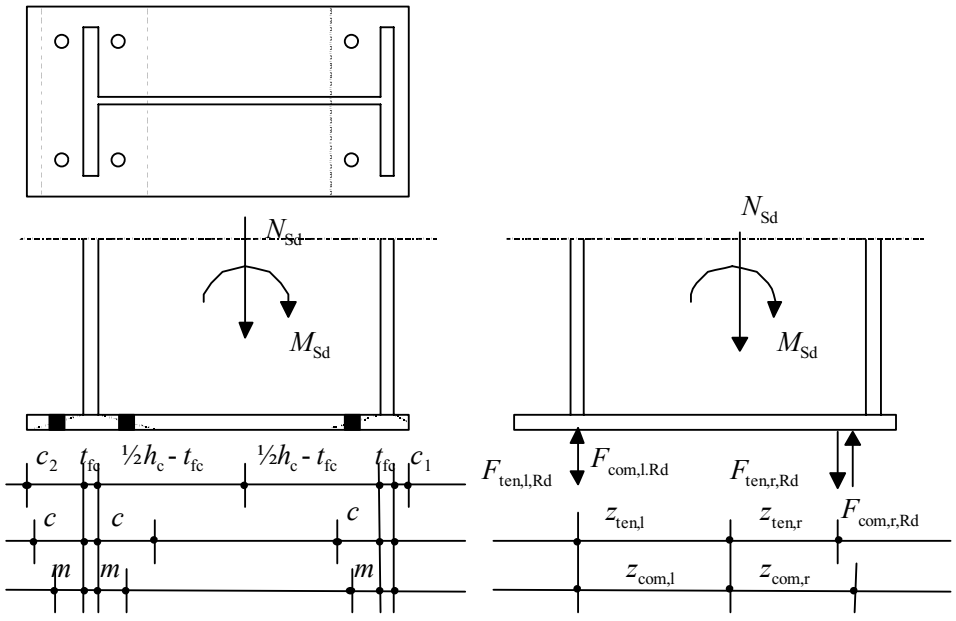

Figure 3.2.13 Base plate joint used as example in assembly procedure

In Figure 3.2.13 the complicated behaviour of the base plate is simplified to a system with four springs: two springs acting in compression more or less under the flanges of the column and two springs acting in tension representing the anchor bolts.

A designer needs to decide which springs will be activated to resist the loading on the joint (normal force N_{Sd} and moment M_{Sd}). This decision can be made as follows. Since the joint is loaded with a normal compressive force and it is loaded with a moment in clockwise direction, the right side of the joint will be activated in compression and not in tension. In the course of this paragraph it is assumed that $M_{sd} / N_{Sd} > z_{com,r}$, so the left anchor bolts will be activated. The assembly procedure is of course not restricted to this loading case: N_{Sd} may be a tensile force and M_{sd} may be opposite to clockwise.

In Table 3.2.2 the assembly procedure is summarized for N_{Sd} as compressive force, M_{sd} clockwise and $M_{sd} / N_{Sd} > z_{com,r}$.

Table 3.2.2: Summary sheet Assembly procedure neglecting the contribution of the column web, part curve "left bolts in tension, right concrete in compression".

Presentation for constant normal force N_{Sd} *Range of validity:* $N_{Sd}\, z_{com,r} < M_{Rd}$	**Presentation for proportional loading** *Range of validity:* $z_{com,r} < e_S < \infty$ $e_S = M_{Sd} / N_{Sd}$
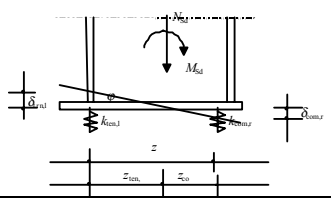	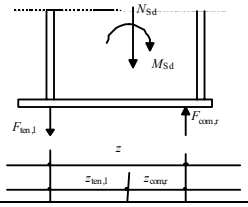
Strength M_{Rd} = the smallest of: $F_{ten,l,Rd}\, z + z_{com,r}\, N_{Sd}$ $F_{com,l,Rd}\, z - z_{ten,l}\, N_{Sd}$ z = $z_{com,r} + z_{ten,l}$	**Strength** M_{Rd} = the smallest of: $\dfrac{F_{ten,l,Rd}\, z}{1 - \dfrac{z_{com,r}}{e_S}}$ $\dfrac{F_{com,r,Rd}\, z}{1 + \dfrac{z_{ten,l}}{e_S}}$ z = $z_{com,r} + z_{ten,l}$
Stiffness $S_j = \dfrac{E\, z^2}{\mu \Sigma\, 1/k_i}$ $\varphi = \dfrac{M_{Sd} - e_k\, N_{Sd}}{S_j}$ $e_k = \dfrac{z_{com,r}\, k_{com,r} - z_{ten,l}\, k_{ten,l}}{k_{com,r} + k_{ten,l}}$ $\mu = (1{,}5\, y)^{2,7}$ but $\mu \geq 1$ $y = \dfrac{M_{Sd} + \frac{1}{2} z\, N_{Sd}}{M_{Rd} + \frac{1}{2} z\, N_{Sd}}$	**Stiffness** $S_j = \dfrac{e_S}{e_S - e_k} \dfrac{E\, z^2}{\mu \Sigma\, 1/k_i}$ $\varphi = \dfrac{M_{Sd}}{S_j}$ $e_k = \dfrac{z_{com,r}\, k_{com,r} - z_{ten,l}\, k_{ten,l}}{k_{com,r} + k_{ten,l}}$ $\mu = (1{,}5\, y)^{2,7}$ but $\mu \geq 1$ $y = \dfrac{1 + \frac{\frac{1}{2} z}{e_S}}{\frac{M_{Rd}}{M_{Sd}} + \frac{\frac{1}{2} z}{e_S}}$
Modelling 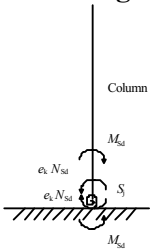	**Modelling** 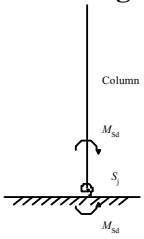

The procedure is given in two presentations: a presentation for constant normal force and a presentation for proportional loading. The difference between both is the loading history. In the presentation for constant normal force, in a first step the normal force N_{Sd} is applied. Then, in a second step, the moment M_{Sd} is built up, till the moment resistance M_{Rd} has been reached. In the presentation for proportional loading, during the load history the ratio $e_S = M_{Sd} / N_{Sd}$ remains constant. The means, in the beginning of the loading history, both M_{Sd} and N_{Sd} are small. The moment M_{Sd} and N_{Sd} are built up simultaneously until M_{Sd} reaches M_{Rd}. The first presentation is useful for the calibration of the assembly procedure with tests, where it is common first to apply a normal force and in a second step the bending moment. The second presentation has more practical benefit, because unlike in the case of a constant normal force, with proportional loading it is during the whole loading history clear which components act in tension or compression. This results finally in advantages for modelling, see Table 3.2.2.

The assembly procedure for strength is rather straightforward and can be derived from simple equilibrium as can be seen from Table 3.2.2.

The assembly procedure for stiffness is similar to the stiffness model of Eurocode 3 Annex J. However, there are some differences. When focusing on the presentation for proportional loading the differences are as follows:

In Eurcode 3 Annex J the stiffness formula is $S_j = \dfrac{E z^2}{\mu \Sigma \dfrac{1}{k_i}}$ when a joint is loaded with pure bending moment. For base plates, an additional factor $\dfrac{e_S}{e_S - e_k}$ should be taken into account. This factor reflects the fact that due to normal force, the stiffness of a joint is will be higher or lower. The factor e_k is dependent on the stiffness of the components in the joints. When $N_{Sd} = 0$, $\dfrac{e_S}{e_S - e_k}$ is equal to 1, so the expression becomes equal to the one in Annex J.

In Annex J the ratio between the initial stiffness and the secant stiffness μ is equal to $(1{,}5\, y)^{2{,}7}$ but $\mu \geq 1$ with $y = M_{Sd} / M_{Rd}$. However, due to the normal force acting at the joint, certain component may be brought in an earlier stage to collapse, which has an effect on the ratio μ. This effect is taken into account be adopting $y = \dfrac{1 + \dfrac{½ z}{e_S}}{\dfrac{M_{Rd}}{M_{Sd}} + \dfrac{½ z}{e_S}}$. The implication is that even if M_{Sd} is small, the ratio μ may be larger than 1 due to the normal force.

The assembly procedure is very simple and straightforward to apply by practitioners. The procedure has no iterative character, which makes it suitable for code implementation.

3.3 Tentative assembly model

3.3.1 Simplified model

In section 3.2 a description is given of assembly models that describe the moment-rotation characteristics of base plate joints. For practical use, these models may be improved by further simplification. First simplifications are described in (Steenhuis, 1998). In this COST report, a simplified assembly model is given covering all load cases and all situations.

Due to its simplicity, this model will differ from test results in some respects. However, a designer can apply this simplified assembly procedure in a straightforward manner, without iterative procedures.

In section 3.3.2 the assembly procedure with respect to strength is described. Section 3.3.3 describes the assembly procedure with respect to stiffness. In section 3.3.4 a summary table is given for the whole assembly procedure. A comparison with tests is presented in section 3.3.5.

3.3.2 Strength

The assembly procedure for strength is described based on an example as shown in Figure 3.3.1 In Figure 3.3.1 the drawing convention is that the arrow representing the normal force indicates compression ($N_{Sd} \leq 0$). A positive applied moment is represented by a clockwise arrow as shown ($M_{Sd} > 0$). The complicated behaviour of the base plate is simplified to a system with four springs: two springs acting in compression under the flanges of the column and two springs acting in tension representing the anchor bolts. The loading is assumed to act proportionally. This accords with the behaviour of structural systems, where an increase of normal force in the column is coupled with an increase of the bending moment to be transferred.

In this model, the contribution of the resistance of the concrete under the column web is neglected. This may lead to some conservatism in case of slender column sections, especially with respect to strength properties. However, taking into account the contribution of the concrete portion under the column web will lead to onerous iterative procedures. In this simplified assembly procedure it is proposed to neglect this influence. For the simple case of a compressive normal force without bending moment it is of course possible to include this contribution as done in (Eurocode 3 Annex L, 1992).

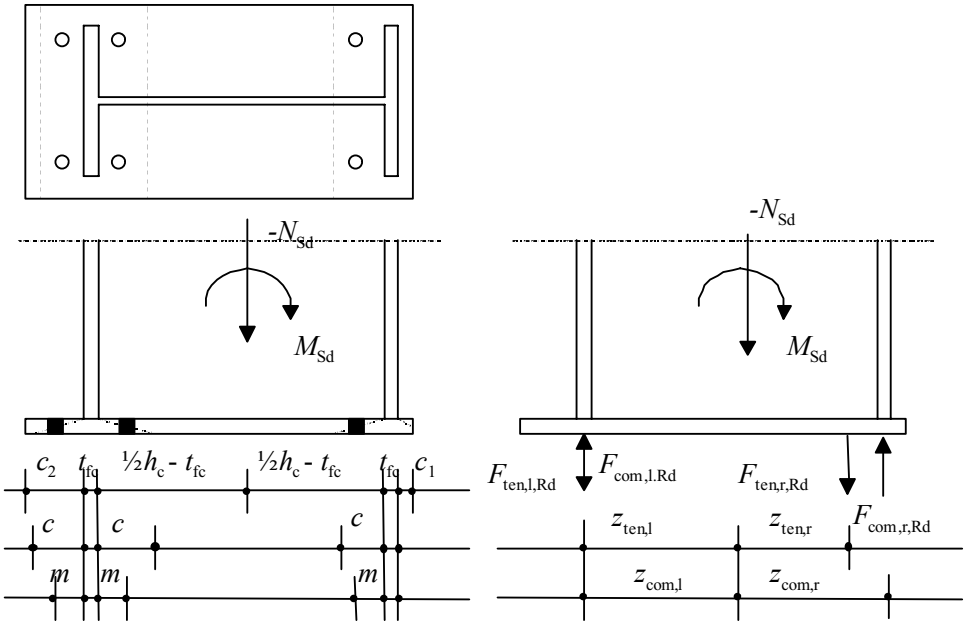

Figure 3.3.1 Base plate joint used as example in assembly procedure

The symbols in Figure 3.3.1 are as follows:

$F_{ten,l,Rd}$ = the capacity of the left side of the joint in tension determined by the components "base plate in bending" and "anchor bolts in tension" see chapter 2;

$F_{ten,r,Rd}$ = the capacity of the right side of the joint in tension determined by the components "base plate in bending" and "anchor bolts in tension" see chapter 2;

$F_{com,l,Rd}$ = the capacity of the left side of the joint in compression determined by the components "base plate in bending", "concrete in compression" and "column web and flange in compression", see chapter 2;

$F_{com,r,Rd}$ = the capacity of the right side of the joint in compression determined by the components "base plate in bending", "concrete in compression" and "column web and flange in compression", see chapter 2;

$z_{ten,l}$ = the distance between the center of the column and the tensile reaction force on the left side of the joint, $z_{ten,l} = ½(h_c - t_{f,c})$

$z_{ten,r}$ = the distance between the center of the column and the tensile reaction force on the right side of the joint, $z_{ten,r} = ½h_c - t_{f,c} - m$

$z_{com,l}$ = the distance between the center of the column and the compressive reaction force on the left side of the joint, $z_{com,l} = ½(h_c - t_{f,c})$.

$z_{com,r}$ = the distance between the center of the column and the compressive reaction force on the right side of the joint, $z_{com,r} = ½(h_c - t_{f,c})$.

As a simplification, the compressive reaction forces are, in accordance with Revised Annex J, assumed to act at the center of the column flanges. For the case of non-extending base plates, this simplification is not fully in line with the real behaviour of the components "concrete in compression" and "base plate in bending", but this simplification is felt to be accurate enough

for practical situations.

A designer needs to decide which springs will be activated to resist the loading on the joint (normal force N_{Sd} and moment M_{Sd}). This decision can be made as follows. Since the joint is loaded with a normal compressive force and it is loaded with a moment in clockwise direction, the right side of the joint will be activated in compression and not in tension. Whether the left side of the joint is activated in tension or compression can be determined with the following procedure:

> Define $e_S = M_{sd} / N_{Sd}$ as the eccentricity of actions
>
> If $e_S < -z_{com,r}$ then the anchor bolts on the left hand side of the joint will be activated. In the other case, the concrete will be activated.

For this example it is assumed that $e_S < -z_{com,r}$, so the left anchor bolts will be activated. The resistance for bending moment M_{Rd} under a constant normal force N_{Sd} can now be determined based on simple equilibrium as follows:

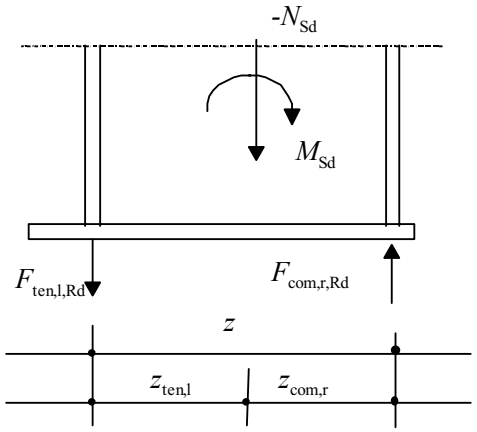

Figure 3.3.2 Resulting system of forces

Consider Figure 3.3.2:

$$\frac{M_{Sd}}{z_{com,r} + z_{ten,l}} + \frac{N_{Sd} z_{com,r}}{z_{com,r} + z_{ten,l}} < F_{ten,l,Rd} \tag{3.3.1}$$

$$\frac{M_{Sd}}{z_{com,r} + z_{ten,l}} - \frac{N_{Sd} z_{ten,l}}{z_{com,r} + z_{ten,l}} < F_{com,r,Rd} \tag{3.3.2}$$

If during the loading history of a column base joint the ratio e_S remains constant (proportional loading), the equilibrium equations can be presented as follows:

$$M_{Sd} < \frac{F_{ten,l,Rd}\, z}{1 + \frac{z_{com,r}}{e_S}} \tag{3.3.3}$$

$$M_{Sd} < \frac{F_{com,r,Rd}\, z}{1 - \frac{z_{ten,l}}{e_S}} \tag{3.3.4}$$

The maximum value for M_{sd} under a normal force N_{Sd} is defined as M_{Rd}, hence:

$$M_{Rd} = \text{the minimum of: } \frac{F_{ten,l,Rd}\, z}{\frac{z_{com,r}}{e_S} + 1} \text{ and } \frac{-F_{com,r,Rd}\, z}{\frac{z_{ten,l}}{e_S} - 1} \tag{3.3.5}$$

$$N_{Rd} = M_{Rd} / e_S \tag{3.3.6}$$

where:

$$z = z_{com,r} + z_{ten,l} \tag{3.3.7}$$

A similar procedure can be used to derive formulae for all other load cases (tensile normal force and anti-clockwise moments). The resulting formulae are given in section 3.3.4.

3.3.3 Stiffness

The stiffness model is described based on the example of Figure 3.3.1. For the components "anchor bolts in tension" and "base plate in bending" and "concrete in compression" and "base plate in bending", elastic stiffness factors are defined in accordance with chapter 2 of this report. The component "column web and flange in compression" is not considered to contribute to the flexibility of the joint. The elastic stiffness factor for the left bolt group is equal to $k_{ten,l}$. and the elastic stiffness factor for the right concrete portion is equal to $k_{com,r}$. The model of the equivalent springs is shown in Figure 3.3.3.

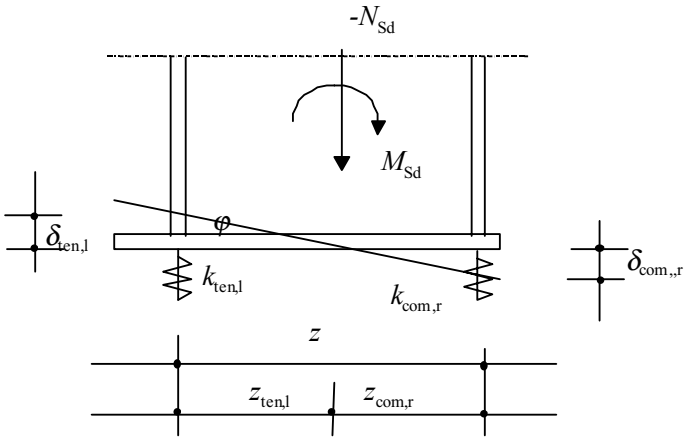

Figure 3.3.3 Spring model

It is assumed that the springs act at locations as described in section 3.3.2.

The elastic deformation of the joint can be calculated as follows:

$$\delta_{en,l} = \frac{\frac{M_{Sd}}{z_{com,r} + z_{ten,l}} + \frac{N_{Sd} z_{com,r}}{z_{com,r} + z_{ten,l}}}{E\, k_{ten,l}} = \frac{M_{Sd} + N_{Sd} z_{com,r}}{z\, E\, k_{ten,l}} \qquad (3.3.8)$$

$$\delta_{om,r} = \frac{\frac{M_{Sd}}{z_{com,r} + z_{ten,l}} - \frac{N_{Sd} z_{ten,l}}{z_{com,r} + z_{ten,l}}}{E\, k_{com,r}} = \frac{M_{Sd} - N_{Sd} z_{ten,l}}{z\, E\, k_{com,r}} \qquad (3.3.9)$$

The rotation of the joints is as defined as follows:

$$\varphi = \mu(\delta_{en,l} + \delta_{om,r}) / z \qquad (3.3.10)$$

Where:

μ *is* a factor equal to 1 or more. In Revised Annex J (Eurocode 3 , 1998) the factor μ varies between 1 and 3 for end plated joints. For instance, μ = 1 when M_{Sd} is smaller than 2/3 M_{Rd} and μ = 3 when M_{Sd} is M_{Rd}. The value of μ for M_{Sd} is between 2/3 M_{Rd} and M_{Rd} is equal to:

$$\mu = (1{,}5\,\frac{M_{Sd}}{M_{Rd}})^{2,7}$$

It is proposed to adopt a similar model for base plate joints.

Hence:

$$\varphi = \mu(\delta_{\text{en,l}} + \delta_{\text{com,r}}) / z = \mu(\frac{M_{\text{Sd}} + N_{\text{Sd}} z_{\text{com,r}}}{z\, E\, k_{\text{ten,l}}} + \frac{M_{\text{Sd}} - N_{\text{Sd}} z_{\text{ten,l}}}{z\, E\, k_{\text{com,r}}}) / z \tag{3.3.11}$$

$$\varphi = \frac{\mu}{z^2 E}(\frac{M_{\text{Sd}} + N_{\text{Sd}} z_{\text{com,r}}}{k_{\text{ten,l}}} + \frac{M_{\text{Sd}} - N_{\text{Sd}} z_{\text{ten,l}}}{k_{\text{com,r}}}) \tag{3.3.12}$$

If the moment $N_{\text{Sd}}\, e_{\text{k}}$ is defined as the moment M_{Sd} required if $\varphi = 0$ under a constant normal force N_{Sd}, see Figure 3.3.4, then:

$$\varphi = \frac{\mu}{z^2 E}(\frac{N_{\text{Sd}}\, e_{\text{k}} + N_{\text{Sd}} z_{\text{com,r}}}{k_{\text{ten,l}}} + \frac{N_{\text{Sd}}\, e_{\text{k}} - N_{\text{Sd}} z_{\text{ten,l}}}{k_{\text{com,r}}}) = 0 \tag{3.3.13}$$

Hence:

$$\frac{e_{\text{k}} + z_{\text{com,r}}}{k_{\text{ten,l}}} + \frac{e_{\text{k}} - z_{\text{ten,l}}}{k_{\text{com,r}}} = 0 \tag{3.3.14}$$

$$k_{\text{com,r}}\,(e_{\text{k}} + z_{\text{com,r}}) + k_{\text{ten,l}}\,(e_{\text{k}} - z_{\text{ten,l}}) = 0 \tag{3.3.15}$$

$$e_{\text{k}} = \frac{z_{\text{ten,l}}\, k_{\text{ten,l}}\; z_{\text{com,r}}\, k_{\text{com,r}}}{k_{\text{com,r}} + k_{\text{ten,l}}} \tag{3.3.16}$$

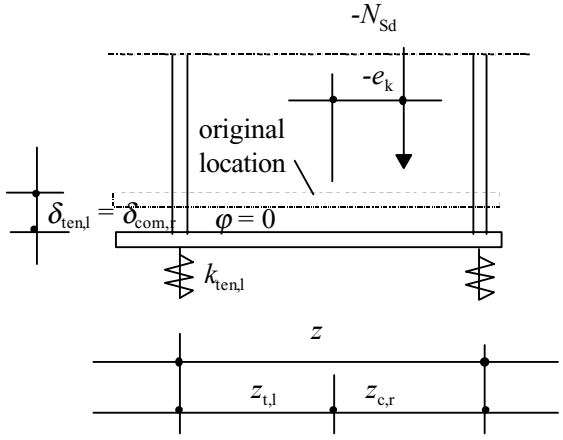

Figure 3.3.4 Definition of e_{k} under zero rotation

Hence, e_{k} is defined as the centroid of the springs with stiffness coefficients $k_{\text{ten;l}}$ and $k_{\text{com;r}}$ It has to be noted that e_{k} is a purely theoretical definition. This can be seen in Figure 3.3.4 where the left tensile spring (anchor bolts), acts in compression.

By defining $S_{\text{j}} = M_{\text{Sd}} / \varphi$, S_{j} can be written:

$$S_j = \frac{M_{Sd}}{M_{Sd} + e_k N_{Sd}} \frac{E z^2}{\mu \Sigma \frac{1}{k_i}} \tag{3.3.17}$$

hence:

$$S_j = \frac{e_S}{e_S + e_k} \frac{E z^2}{\mu \Sigma \frac{1}{k_i}} \tag{3.3.18}$$

where:

$$\Sigma \frac{1}{k_i} = \frac{1}{k_{ten,l}} + \frac{1}{k_{com,r}} \tag{3.3.19}$$

Thus, when calculating the stiffness of a base plate joint, a modification factor equal to $\frac{e_S}{e_S + e_k}$ is used, which reflects the contribution of the normal force in the proportional loading.

3.3.4 Overview of resistance and stiffness formula for all loadcases

In section 3.3.2 and 3.3.3 a description of the moment rotation relationship was given for the case when the left side of the joint was in tension and the right side in compression. In Table 3.3.1 an overview is given for all situations. For all loadcases, i.e. normal force $N_{Sd} > 0$ or $N_{Sd} \leq 0$ and moment $M_{Sd} > 0$ or $M_{Sd} \leq 0$, formula are given.

Table 3.3.1: Moment resistance M_{Rd} ($M_{Sd} > 0$ is clockwise, $M_{Sd} \le 0$ is anti-clockwise) and rotational stiffness $S_{j.}$ dependent on the direction of normal force N_{Sd} ($N_{Sd} > 0$ is tension, $N_{Sd} \le 0$ is compression) and $e_S = \frac{M_{Sd}}{N_{Sd}} = \frac{M_{Rd}}{N_{Rd}}$

$N_{Sd} > 0$ $e_S > z_{ten.l}$	$N_{Sd} \le 0$ $e_S \le - z_{com.r}$	$N_{Sd} > 0$ $0 < e_S \le z_{ten.l}$	$N_{Sd} > 0$ $- z_{ten.r} < e_S \le 0$	$N_{Sd} > 0$ $e_S \le - z_{ten.r}$	$N_{Sd} \le 0$ $e_S > z_{com.l}$	$N_{Sd} \le 0$ $0 < e_S \le z_{com.l}$	$N_{Sd} \le 0$ $- z_{com.r} < e_S \le 0$
$M_{Rd} = \min\left(\frac{F_{ten,l,Rd}\, z}{\frac{z_{com,r}}{e_S} + 1}; \frac{-F_{com,r,Rd}\, z}{\frac{z_{ten,l}}{e_S} - 1}\right)$		$M_{Rd} = \min\left(\frac{F_{ten,l,Rd}\, z}{\frac{z_{ten,r}}{e_S} + 1}; \frac{F_{ten,r,Rd}\, z}{\frac{z_{ten,l}}{e_S} - 1}\right)$	$M_{Rd} = \max\left(\frac{F_{ten,l,Rd}\, z}{\frac{z_{ten,r}}{e_S} + 1}; \frac{F_{ten,r,Rd}\, z}{\frac{z_{ten,l}}{e_S} - 1}\right)$	$M_{Rd} = \max\left(\frac{-F_{com,l,Rd}\, z}{\frac{z_{ten,r}}{e_S} + 1}; \frac{F_{ten,r,Rd}\, z}{\frac{z_{com,l}}{e_S} - 1}\right)$		$M_{Rd} = \max\left(\frac{-F_{com,l,Rd}\, z}{\frac{z_{com,r}}{e_S} + 1}; \frac{-F_{com,r,Rd}\, z}{\frac{z_{com,l}}{e_S} - 1}\right)$	$M_{Rd} = \min\left(\frac{-F_{com,l,Rd}\, z}{\frac{z_{com,r}}{e_S} + 1}; \frac{-F_{com,r,Rd}\, z}{\frac{z_{com,l}}{e_S} - 1}\right)$
$S_j = \frac{e_S}{e_S + e_k} \frac{E\, z^2}{\mu\, (\frac{1}{k_{ten,l}} + \frac{1}{k_{com,r}})}$ $e_k = \frac{z_{com,r}\, k_{com,r} - z_{ten,l}\, k_{ten,l}}{k_{com,r} + k_{ten,l}}$ $z = z_{com,.r} + z_{ten,l}$		$S_j = \frac{e_S}{e_S + e_k} \frac{E\, z^2}{\mu\, (\frac{1}{k_{ten,l}} + \frac{1}{k_{ten,r}})}$ $e_k = \frac{z_{ten,r}\, k_{ten,r} - z_{ten,l}\, k_{ten,l}}{k_{ten,r} + k_{ten,l}}$ $z = z_{ten,.r} + z_{ten,l}$		$S_j = \frac{e_S}{e_S + e_k} \frac{E\, z^2}{\mu\, (\frac{1}{k_{com,l}} + \frac{1}{k_{ten,r}})}$ $e_k = \frac{z_{ten,r}\, k_{ten,r} - z_{com,l}\, k_{com,l}}{k_{ten,r} + k_{com,l}}$ $z = z_{ten,.r} + z_{com,l}$		$S_j = \frac{e_S}{e_S + e_k} \frac{E\, z^2}{\mu\, (\frac{1}{k_{com,l}} + \frac{1}{k_{com,r}})}$ $e_k = \frac{z_{com,r}\, k_{com,r} - z_{com,l}\, k_{com,l}}{k_{com,r} + k_{com,}}$ $z = z_{com,.r} + z_{com,l}$	
$\mu = (1{,}5\, \frac{M_{Sd}}{M_{Rd}})^{2,7}$ but $\mu \ge 1$							
Left side in tension Right side in compression		left side in tension right side in tension		left side in compression right side in tension		left side in compression right side in compression	
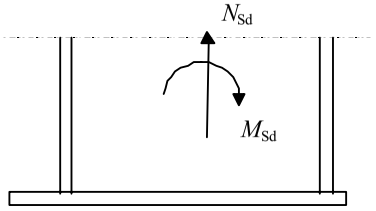							

3.3.5 Comparison with test data

The assembly procedure described in this chapter together with the models the strength and stiffness of the components as given in chapter 2 have been implemented in a spreadsheet. Using the model of this report, predictions have been made of moment rotation curves of three series of tests carried out by Wald et al, 1995 and Vandegans, 1997. The predicted moment rotation curves have been compared with the test curves. In the prediction, the real measured properties of the materials have been adopted with partial safety factors equal to 1,0.

Also work has been done to compare the model test carried out by others. This work has not been concluded yet. Since in this report comparison are only made for two series of tests, without further confirmation, the model cannot be recommended for use in practice.

The tests show that the behaviour of a base plate joint is very sensitive to the quality of the concrete or grout immediately under the base plate. In the model presented in this document it is assumed that the concrete and the grout are of good quality.

The results of the comparison of the model with the other test series by Wald et al, 1995 and Vandegans, 1997 are reported in Figure 3.3.5 to Figure 3.3.20. In the case of non-proportional loading, first the design moment M_{Rd} and the design normal force N_{Rd} have been calculated based on the methods given in this chapter. Then, the non-proportional loading in the model is simulated by first applying the design normal force N_{Rd} to the model. Then the moment M_{Sd} is applied in steps from 0 to M_{Rd}. The value of N_{Rd} is in general somewhat lower then the normal force actually applied in the test.

In general, despite all simplifications, the model design model shows good agreement with the test data. Only in case of very high normal force, e.g. test S220-190, see Figure 3.3.15, the model is conservative. This could be expected because the contribution of the web to the load carrying capacity of the base plate is neglected in the assembly model.

Also, it should be noted that the model works equally well in cases where only one bolt row is located in between the column flanges and in cases where two bolt rows are applied outside the column flanges.

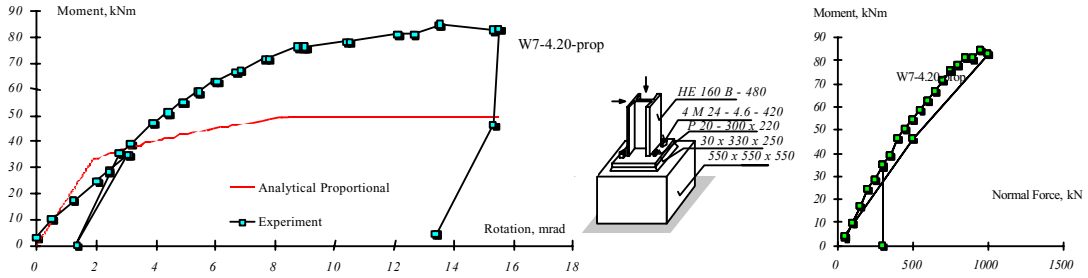

Figure 3.2.14 Experimental and predicted moment - rotational diagrams for shown normal force history, experiment W7-4.20-prop, (Wald et al, 1995)

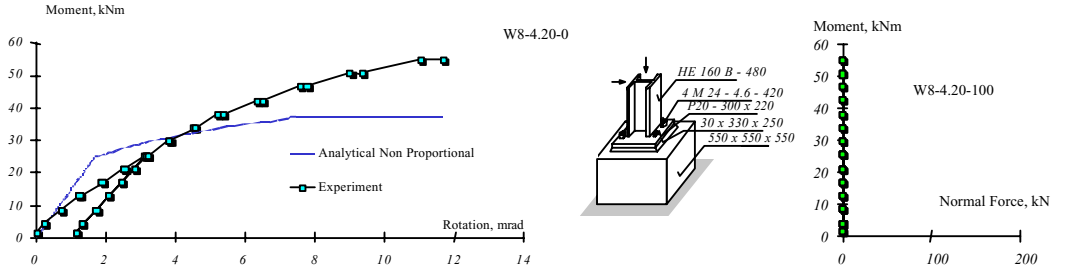

Figure 3.2.15 Experimental and predicted moment - rotational diagrams for shown normal force history, experiment W8-4.20-const0, (Wald et al, 1995)

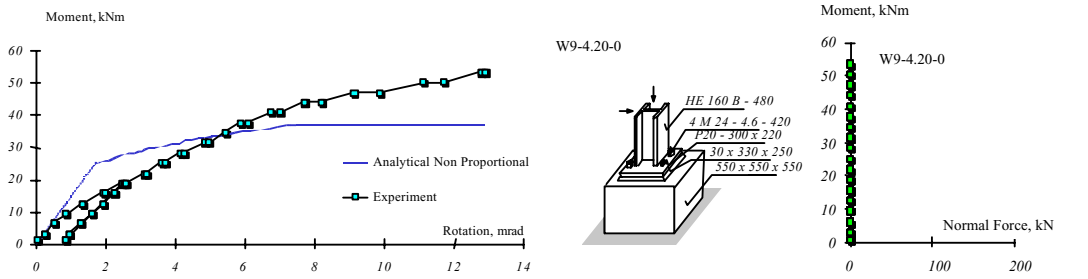

Figure 3.2.16 Experimental and predicted moment - rotational diagrams for shown normal force history, experiment W9-4.20-0, (Wald et al, 1995)

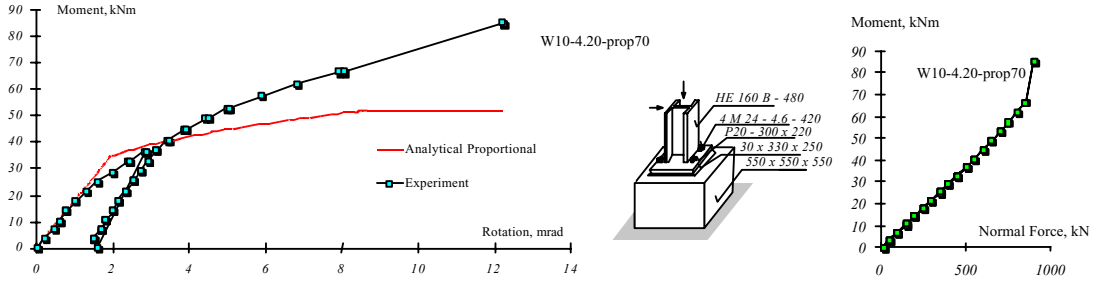

Figure 3.2.17 Experimental and predicted moment - rotational diagrams for shown normal force history, experiment W10-4.20-prop70, (Wald et al, 1995)

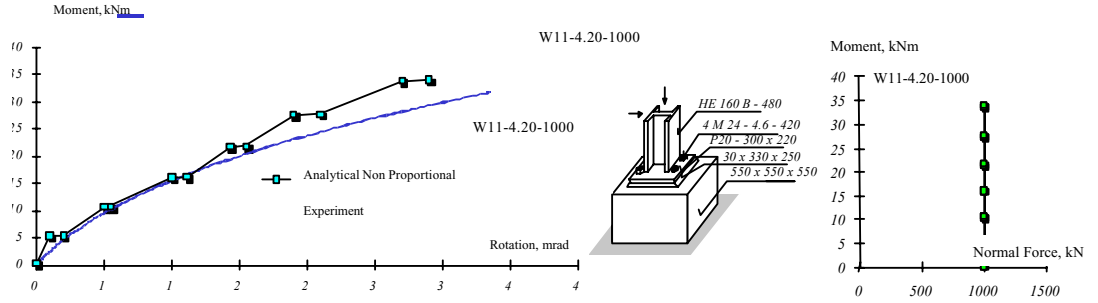

Figure 3.2.18 Experimental and predicted moment - rotational diagrams for shown normal force history, experiment W11-4.20-1000, (Wald et al, 1995)

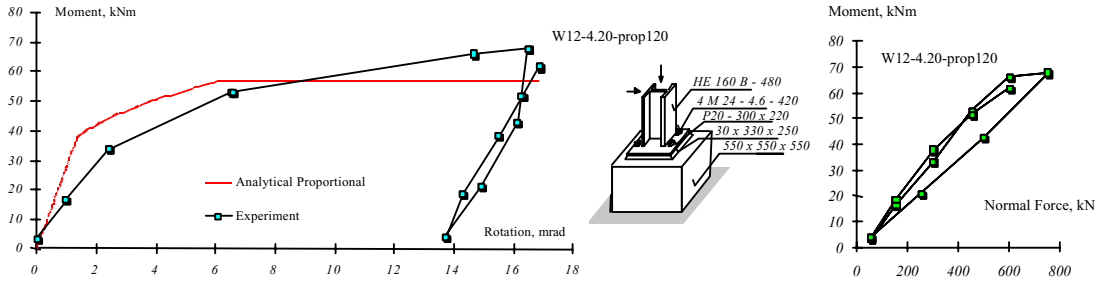

Figure 3.2.19 Experimental and predicted moment - rotational diagrams for shown normal force history, experiment W12-4.20-prop120, (Wald et al, 1995)

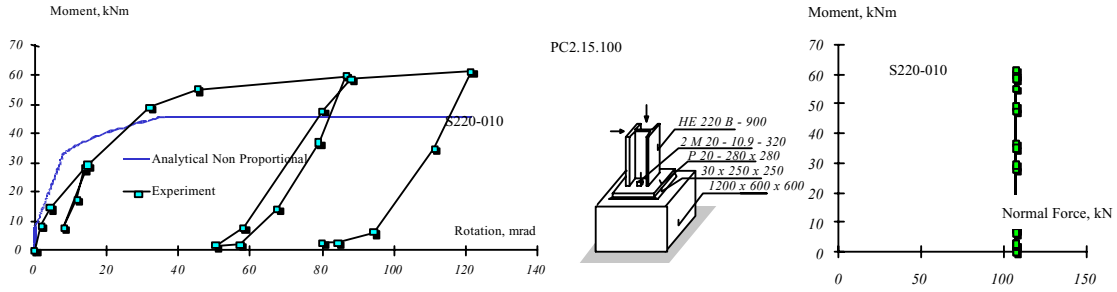

Figure 3.2.20 Experimental and predicted moment - rotational diagrams for shown normal force history, experiment S220-010, (Vandegans, 1997)

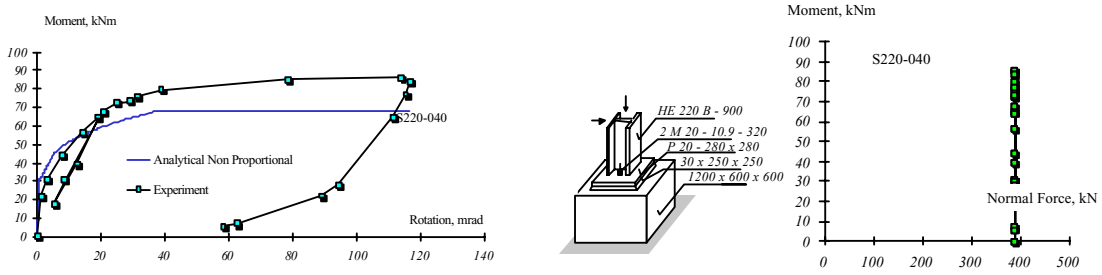

Figure 3.2.21 Experimental and predicted moment - rotational diagrams for shown normal force history, experiment S220-040, (Vandegans, 1997)

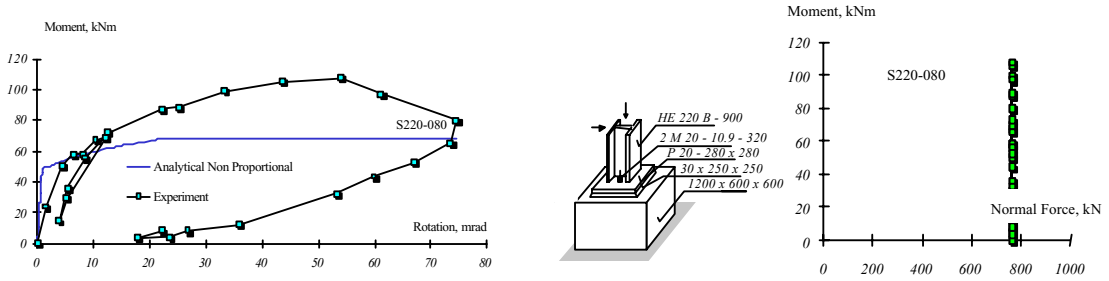

Figure 3.2.22 Experimental and predicted moment - rotational diagrams for shown normal force history, experiment S220-080, (Vandegans, 1997)

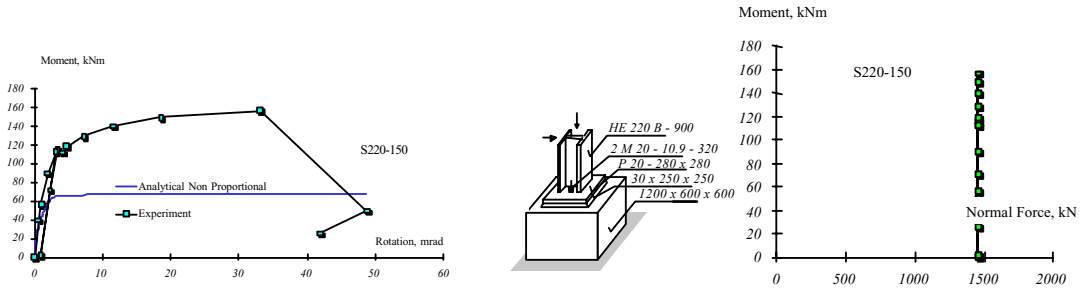

Figure 3.2.23 Experimental and predicted moment - rotational diagrams for shown normal force history, experiment S220-150, (Vandegans, 1997)

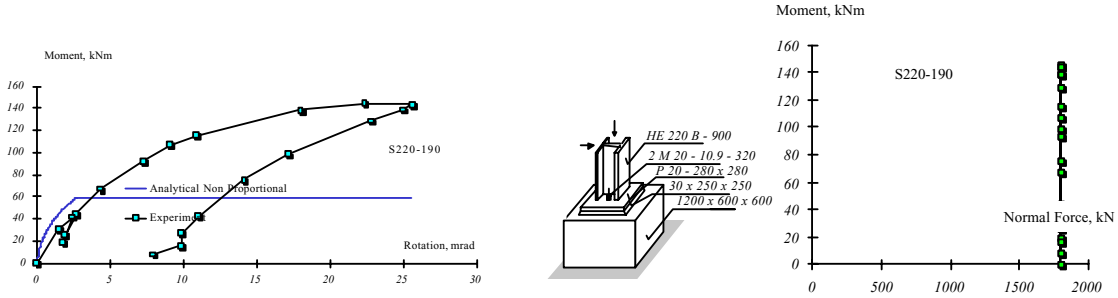

Figure 3.2.24 Experimental and predicted moment - rotational diagrams for shown normal force history, experiment S220-190, (Vandegans, 1997)

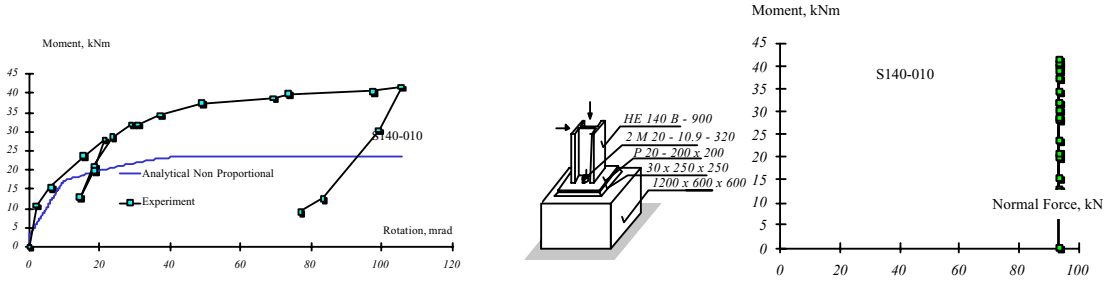

Figure 3.2.25 Experimental and predicted moment - rotational diagrams for shown normal force history, experiment S140-010, (Vandegans, 1997)

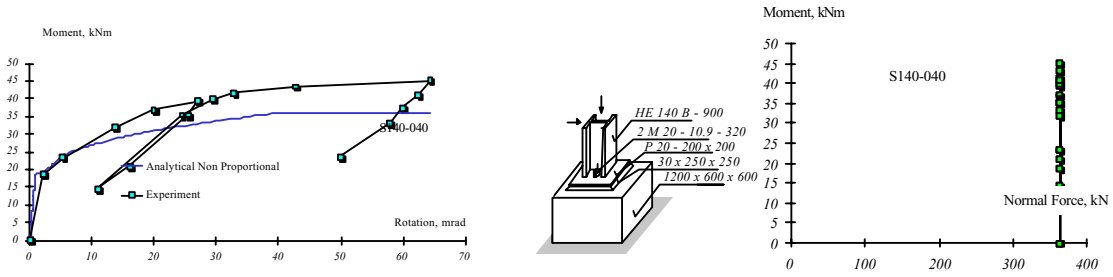

Figure 3.2.26 Experimental and predicted moment - rotational diagrams for shown normal force history, experiment S140-040, (Vandegans, 1997)

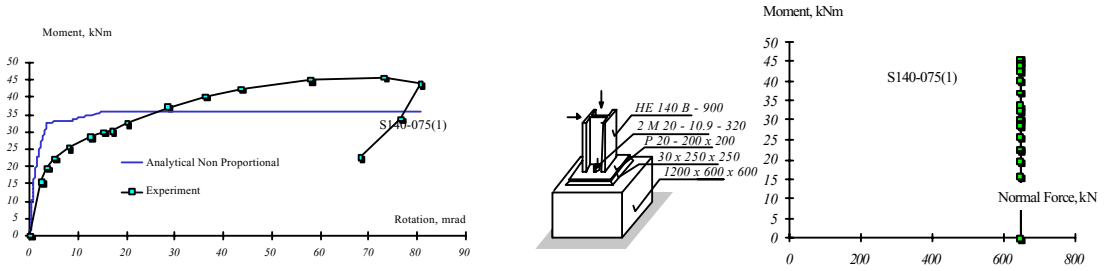

Figure 3.2.27 Experimental and predicted moment - rotational diagrams for shown normal force history, experiment S140-075(1) , (Vandegans, 1997)

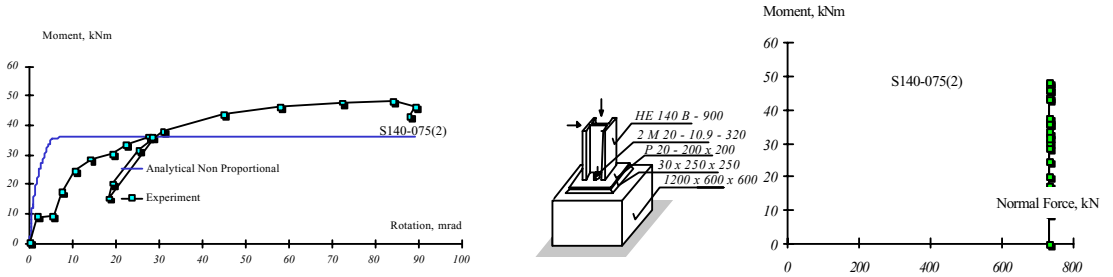

Figure 3.2.28 Experimental and predicted moment - rotational diagrams for shown normal force history, experiment S140-075(2) , (Vandegans, 1997)

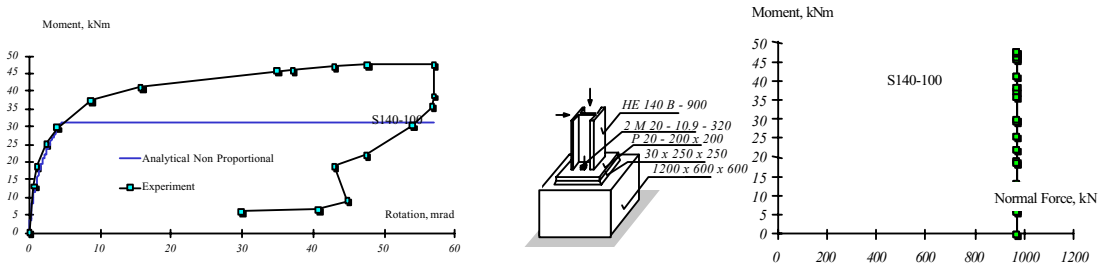

Figure 3.2.29 Experimental and predicted moment - rotational diagrams for shown normal force history, experiment S140-100, (Vandegans, 1997)

Chapter 4: Modelling and idealisation for frame analysis

4.1 Introduction

Analysis of steel frames is commonly carried out assuming the column bases to be either rigid or entirely free to rotate (pinned). However, introducing a rotational stiffness in the analysis model at the column bases produces a more realistic prediction of the frame behaviour. Compared to analysis with pinned bases, lateral (sway) deflections are reduced. Compared to analysis with fixed bases, lateral (sway) deflections are increased, which is particularly important in the design of unbraced frames.

Some national design standards give recommendations for the modelling of column bases which attempt to reflect the real column base behaviour rather that the extremes of fixed or pinned bases. For example, these recommendation relate the column base stiffness to the stiffness of the supported column, and do not necessarily reflect the actual column base details.

The proposal contained in this publication allow to calculate the rotational stiffness and the moment resistance of column bases. This chapter briefly describes the procedure for incorporating these calculated characteristics in the frame analysis.

4.2 Modelling

Careful examination of both the test results and the proposed models demonstrates that the stiffness and the resistance of column bases are influenced by the relationship between the applied moment and the applied normal force, see Figure 4.1.

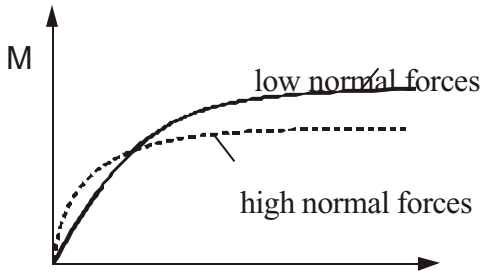

Figure 4.1 Influence of the normal force on the moment-rotation behaviour

Hence, the determination of the joint properties needs some consideration of the global frame response. On the other side the frame response depends on the joint behaviour if the joint may not be assumed be rigid. This leads to an iterative procedure. This section is aimed in providing some guidance how to model a column base joint in the frame in order to take into account this interaction in a practical way.

In general, the joint behaviour needs to be considered in the frame analysis. However, in certain cases, it is

possible to neglect the joint behaviour by making simplified assumption, i.e. to assume that the joints may be modelled either as continuous or as pinned. This approach is used in daily design in most cases. The tool to justify this approach is the classification system which is discussed more in detail in chapter 5. With the help of the classification system, it is possible to classify a joint as rigid (in this case, the deformation of the joint are small compared to the deformation of the frame and hence, the rotation of the joint may be neglected) or as nominally pinned (in this case, the joint will not transmit significant moments and it is able to rotate like an ideal hinge). Dependent on the classification the column bases may be modelled as shown in Figure 4.2.

Method of global analysis	**Classification of the column base**		
elastic	nominally pinned	rigid	semi-rigid
rigid-plastic	nominally pinned	full-strength	partial-strength
elastic-plastic	nominally pinned	rigid and full-strength	semi-rigid partial strength semi-rigid full-strength rigid partial strength
Type of joint model	simple 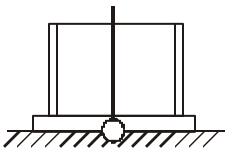	continuous 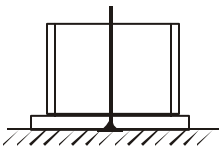	semi-continuous 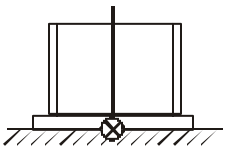

Figure 4.2 Joint modelling dependent on the classification and on the method of global analysis

As above-mentioned actual behaviour of a column base joint depends on its actual loading. This may be expressed by means of the actual M_{Sd}/N_{Sd} ratio, where M_{Sd} is the applied moment and N_{Sd} is the applied normal force. This aspect is discussed more in detail in chapter 3.1.

In order to determine the column base properties, a 'good guess' of the acting forces (i.e. the ratio M_{Sd}/N_{Sd}) is required. The following iterative procedure is recommended to take the interaction between frame behaviour on one side and the column base behaviour on the other side into account. This general procedure is illustrated in Figure 4.3

If a joint is modelled either as continuous, it is obvious that there is no interaction between the joint behaviour and the frame response. Therefore it is recommended to start the procedure with the assumption of rigid and full-strength joints which are modelled in the frame as continuous, see Figure 4.2, as a first guess. (Note that the design model presented in the previous chapters assumes that the column bases may transfer typically some moments, this is for example due the presence of normal forces. Therefore the 'simple' modelling is of minor interest in this case and it is recommended to use the 'continuous' modelling as a starting point.)

With the assumption of rigid column bases, the frame analysis can be performed without any knowledge of the column base properties. In practice, this step is made anyway in the pre-design stage in order to get an idea about

the section sizes. As a result, the forces acting on the column bases are known. Based in the M/N ratio obtained in this analysis the resistance and the stiffness of the joints may be determined according to the models described in chapters 2 and 3.

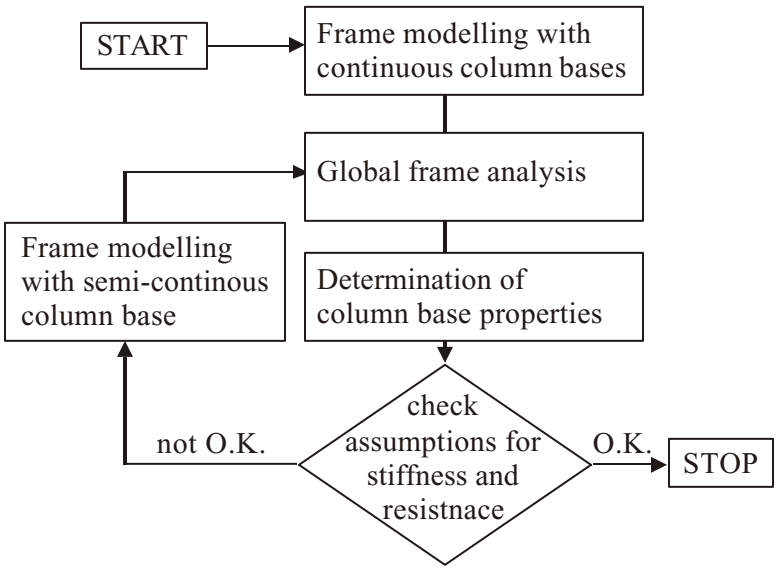

Figure 4.3 Iterative procedure

Of course one have to check now if the assumptions made in the beginning are valid. This is easy because a classification of the joint will give the answer: If the actual stiffness is higher than a certain classification boundary, the assumption of rigid column was valid. If this is not the case, a further frame analysis is necessary. However, the actual joint stiffness should now be taken into account and the column bases are modelled as semi-continuous. Because the joint behaviour influences the frame response, the resulting data for M and N acting on the joints will differ from the previous calculation and new values for the stiffness and resistance should be derived. The iteration can be continued by repeating the two previous steps. The procedure can be escaped if the difference between the column base stiffness of the last step and the previous step is less than an An approach to find such an "acceptable value" is proposed by Steenhuis et al (1994).

4.3 Idealisation

Generally the column base behaviour may be represented in the frame by using a non-linear rotational spring. However, the spring should be linear for a simple elastic global analysis. As the general behaviour of a column base joint is non-linear a so-called 'idealisation' of the moment-rotation curve is necessary to derive a linearised curve as shown in figure 4.4. Here, a linear stiffness Ş (secant stiffness) at the level of the applied moment is taken as a lower bound value. If the applied moment is not know, the secant stiffness should be determines at the rotation when the moment -rotation curve reaches the plastic moment resistance (dashed line).

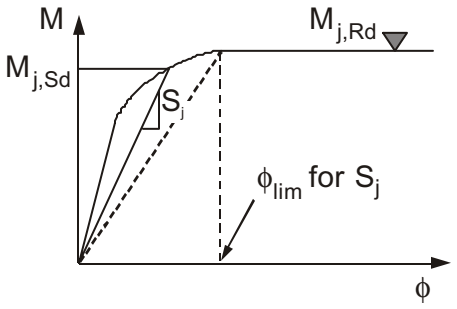

Figure 4.4 Linearised moment-rotation curve

Based on the requirement, that a simplified curve should lead to safe results on one side but should give on the other side most economic solutions, the revised Annex J of Eurocode 3 uses an empirical approach to determine a more economical value model for an idealised stiffness of beam-to-column joints. Parameter studies were carried out in order to compare the frame behaviour when on one side the more accurate model (i.e. the non-linear moment rotation curve) is used as a reference and one the other side the proposed simplified curve is used to represent the joint behaviour. However such studies are not yet available for column bases and the only safe approach is to take a secant stiffness to the non-linear curve

Chapter 5: Classification of column base joints

5.1 Scope

In Eurocode 3 Chapter 6 and revised Annex J, the stiffness classification of beam-to-column joints into rigid, semi-rigid and pinned joints is seen to be dependent on the structural system, according its "braced" or "unbraced" character. In fact, this criterion should not be the single one to determine the class of the joints; it is obvious that the "sway" or "non sway" character of the structure is a significant parameter as well. So in order to clarify the point, without entering in long explanations, it can be stated that the recommendations provided in Eurocode 3 for the stiffness classification of beam-to-column joints are limited to joints belonging to "braced - non sway" and "unbraced - sway" structures; the other cases, respectively "braced - sway" and "unbraced - non sway" being not presently covered.

Similar conclusions apply to the proposals made in the present chapter for the stiffness classification of column bases.

For what regards the strength classification, the same boundaries than those proposed in Eurocode 3 revised Annex J for beam-to-column joints may be referred to for column bases so as to distinguish between full-strength, partial strength and pinned joints.

5.2 Column bases in "braced - non-sway" frames

A modification of the actual moment-rotation characteristic of column bases is likely to affect the whole response of "braced - non-sway" frames, and in particular the lateral displacements of the beams and the buckling resistance of the column. This second aspect - the buckling resistance of the columns - is the one for which the influence is rather important, as seen in Figure 5.1 (Wald and Seifert, 1991) , which shows how the buckling length coefficient of a column pinned at the upper extremity is affected by the variation of the column base rotational stiffness. The buckling length coefficient K is reported on the vertical axis and is expressed as the ratio between the elastic critical load ($F_{cr,pin}$) of the column pinned at both extremities and that of the same column but restrained by the column base at the lower extremity ($F_{cr,res}$); it is shown to vary from *1,0* (pinned - pinned support conditions) to *0,7* (pinned - fixed support conditions).

$$K = \sqrt{\frac{F_{cr,pin}}{F_{cr,res}}} \tag{5.1}$$

$$F_{cr,pin} = \frac{\pi^2 E I_c}{L_c^2} \tag{5.2a}$$

$$F_{cr,res} = \frac{\pi^2 E I_c}{\left(K L_c\right)^2} \tag{5.2b}$$

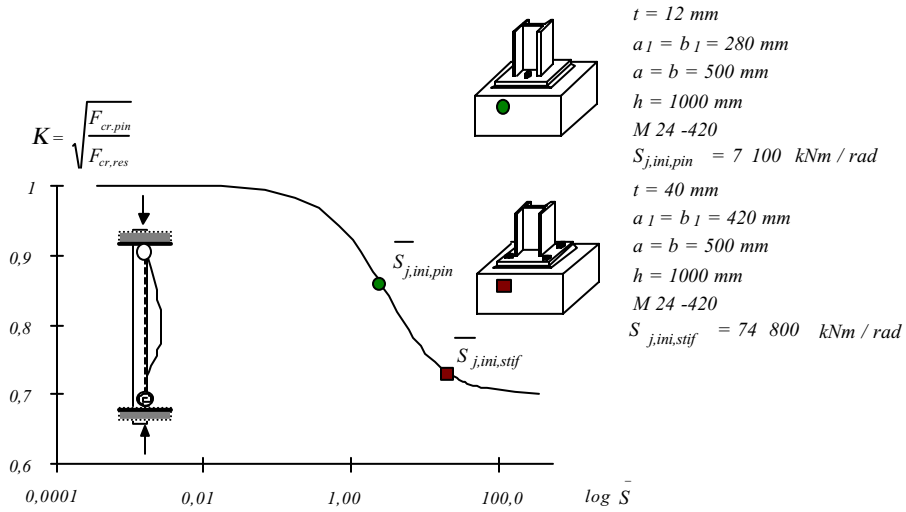

Figure 5.1 Elastic critical buckling load versus column base initial stiffness

where E is the modulus of elasticity of steel; L_c and I_c are respectively the system length and the moment of inertia of the column. In Figure 5.1, the non-dimensional stiffness $\overline{S}$ of the column base is reported in a logarithmic scale on the horizontal axis.

$$\overline{S} = \frac{S_{j,ini} L_c}{E I_c} \tag{5.3}$$

$S_{j,ini}$ is the initial elastic stiffness in rotation of the column base. The numerical values indicated in Figure 5.1 have been obtained by considering the particular case of a $4\ m$ length column with a *HE 200 B* cross-section.

The actual initial stiffness of two typical column bases is reported in Figure 5.1:

- column base with a base plate and two anchor bolts inside the H cross-section; this configuration is traditionally considered as pinned, but possesses an initial stiffness $S_{j,ini,pin}$ equal to $7\ 100\ kNm/rad$;
- column base with a base plate and four bolts outside the column cross-section; such a column base is usually considered as rigid even if its initial stiffness $S_{j,ini,stif} = 74\ 800\ kNm/rad$ is not infinite.

As for beam-to-column joints, it may be concluded that stiff column bases always deforms slightly in rotation while presumably pinned ones exhibit a non-zero rotational stiffness. Some column bases are however so flexible or so rigid that the structural frame response obtained by considering the actual column base characteristics in rotation is not significantly different from that obtained by modelling respectively the column bases as perfectly pinned or rigid. For beam-to-column joints, this has led to the concept of stiffness classification into pinned, semi-rigid and rigid joints, see Eurocode 3.

The stiffness classification in Eurocode 3 revised Annex J is achieved by comparing the initial stiffness of the beam-to-column joints to boundary values. For instance, rigid beam-to-column joints are characterised by a stiffness higher than $8 E I_b / L_b$ where I_b and L_b are respectively the moment of inertia and the length of the beam. This rigidity check is based on a so-called "5% criterion" which says that a joint may be considered as rigid if the ultimate resistance of the frame in which it is incorporated is not affected by more than 5% in comparison with the situation where fully rigid joints are considered.

A rigid classification boundary for column bases may be derived by adopting the same basic principle. To achieve it, the single storey - single bay “braced - non-sway” frame shown in Figure 5.2.a is considered. The study of the sensitivity of the frame to a variation of the column base stiffness properties is influenced by the beam and column characteristics in bending, $E I_b / L_b$ and $E I_c / L_c$ respectively. Two limit cases are however obtained when:

- the beam is rather stiff as shown in Figure 5.2.b ($E I_b / L_b = \infty$);
- the beam is rather flexible (or when a pinned joint connect the beam to the column); this situation is illustrated in Figure 5.2.c ($E I_b / L_b = 0$).

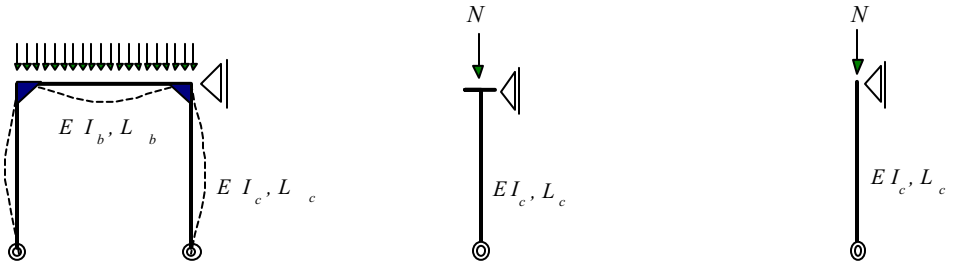

a) Portal frame (non-sway) b) Isolated column (top-fixed) c) Isolated column (top-pinned)

Figure 5.2 Portal frame and isolated columns for classification study

The application of the "5% criterion" to the first limit case (column fixed at top extremity) writes as follows:

$$\frac{\frac{\pi^2 E I_c}{(K L_c)^2}}{\frac{\pi^2 E I_c}{(0,5 L_c)^2}} \geq 0,95 \qquad (5.4)$$

For sake of simplicity, it is first applied to the critical elastic buckling loads and not to the ultimate ones (integrating the effects of plasticity, imperfections, ...); it may be demonstrated that by doing so a safe value of the rigid stiffness boundary is obtained.

From Equation (5.4), the minimum value of the buckling length coefficient may be derived:

$$K \leq 0,513 \qquad (5.5)$$

According to Eurocode 3 Annex E on the «effective buckling length of members in compression», the K coefficient is expressed as a function of restraint coefficients (k_l, k_u) at both column ends and writes in this specific case:

$$K = \frac{1+0,145\,(k_l + k_u) - 0,265\,k_l\,k_u}{2 - 0,364\,(k_l + k_u) - 0,247\,k_l\,k_u} \qquad (5.6)$$

with:

$$k_l = \frac{4EI_c / L_c}{4EI_c / L_c + S_{j,ini}} \qquad \text{at lower extremity} \qquad (5.7.a)$$

$$k_u = 0 \qquad \text{at upper extremity} \qquad (5.7.b)$$

From Equations (5.5) to (5.7), the minimum value of the elastic initial stiffness $S_{j,ini}$ that presumably rigid column bases have to exhibit may be derived as follows (rounded value) :

$$S_{j,ini} \geq 48EI_c / L_c \qquad (5.8)$$

A similar approach may be followed for the second limit case (Figure 5.2.c) and the following boundary is extracted:

$$S_{j,ini} \geq 40EI_c / L_c \qquad (5.9)$$

This limit is less restrictive than the first one; this shows that:

- the stiffness requirement is system dependent;
- the stronger requirement on joint stiffness is obtained in structure where the flexibility at the extremities of the column is strictly resulting from that of the column base.

This is physically understandable and, as a consequence, the following simple stiffness classification boundary to distinguish between rigid and semi-rigid column bases is suggested:

Rigid column bases: $S_{j,ini} \geq 48EI_c / L_c$ (5.10.a)

Semi-rigid column bases: $S_{j,ini} < 48EI_c / L_c$ (5.10.b)

As a further step, a less conservative boundary may be derived by applying the "5 % criterion" to the ultimate resistance F_u of the column. This one may be approximately expressed as (Massonnet and Save, 1976) :

$$\frac{1}{N_u} = \frac{1}{N_p} + \frac{1}{N_{cr}} \tag{5.11}$$

where N_p and N_{cr} designate respectively the squash load and the critical elastic buckling load of the column.

As $N_{cr} = N_p / \overline{\lambda}^2$, $\overline{\lambda}$ being the reduced slenderness of the column, Equation (5.11) writes also:

$$N_u = N_p \frac{1}{1 + \overline{\lambda}^2} \tag{5.12}$$

With reference to Figure 5.2.b, the reduced slenderness of the column with a fully stiff column base at lower end equals :

$$\overline{\lambda}_{\text{rigid column base}} = 0{,}5\overline{\lambda}_o \tag{5.13.a}$$

while that of the column with a semi-rigid column base writes :

$$\overline{\lambda}_{\text{semi-rigid column base}} = K\overline{\lambda}_o \tag{5.13.b}$$

where $\overline{\lambda}_o$ is the reduced slenderness of the column assumed as pinned at both extremities (K = 1).

The application of the "5 % criterion" to the ultimate column resistance therefore gives, N_p being considered as constant :

$$\frac{1 + (0{,}5)^2 \overline{\lambda}_o^2}{1 + K^2 \overline{\lambda}_o^2} \geq 0{,}95 \tag{5.14.a}$$

or :

$$K \le 0{,}513\sqrt{1+\frac{1}{5\bar{\lambda}_o^2}} \qquad (5.14.b)$$

Expression (5.14.b) may be compared to the (5.5) one. For high $\bar{\lambda}_o$ values, both expressions are similar. In such cases, the ultimate resistance N_u equals N_{cr} and a high boundary value of $S_{j,ini}$ (see Formula 5.8) is required.

For low values of $\bar{\lambda}_o$, the condition (5.14.b) relaxes and, as a consequence, less severe boundary values of $S_{j,ini}$ are required, the influence of the cross-section yielding becoming then more predominant than the instability.

For $\bar{\lambda}_o$ = 0,48, Equation (5.14.b) writes K ≤ 0,7, what means that any column base, even a perfectly pinned none, will be considered as rigid.

By integrating Formulae (5.14.b) in Formulae (5.6) to (5.7.b), the following stiffness boundaries are obtained :

$$\text{If } \bar{\lambda}_o \le 0{,}48 \qquad S_{j,ini} \ge 0 \qquad (5.15.a)$$

$$\text{If } \bar{\lambda}_o > 0{,}48 \qquad S_{j,ini} \ge \frac{1{,}145 - 0{,}838\,\mu}{1{,}026\,\mu - 1}\frac{4EI_c}{L_c} \qquad (5.15.b)$$

with :

$$\mu = \sqrt{1+\frac{1}{5\bar{\lambda}_o^2}} \qquad (5.16)$$

For practical applications, simpler expressions are proposed which fit rather well, as seen in Figure 5.3, with the exact ones (Formulae 5.15) in the usual range of application ($\bar{\lambda}_o$ ≤ 2 to 3). These are:

$$\text{If } \bar{\lambda}_o \le 0{,}5 \qquad S_{j,ini} \ge 0 \qquad (5.17.a)$$

$$\text{If } 0{,}5 < \bar{\lambda}_o < 3{,}93 \qquad S_{j,ini} \ge 7\,(2\,\bar{\lambda}_o - 1)EI_c/L_c \qquad (5.17.b)$$

$$\text{If } \bar{\lambda}_o \ge 3{,}93 \qquad S_{j,ini} \ge 48\,EI_c/L_c \qquad (5.17.c)$$

As a safe approximation, Formula (5.8) may obviously be applied for any column slenderness.

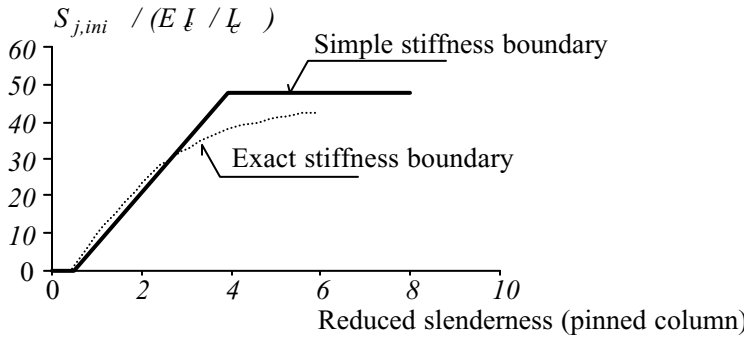

Figure 5.3 Exact and simple stiffness boundaries

Such an approach allows to classify the column bases according to the column properties only. A more precise boundary dependent on the k_u coefficient (Formulae 5.6) could obviously be derived but its application would be far more complicated, and this seems not to be in line with the expected simplicity.

A similar stiffness boundary could be defined, on the same basis, for pinned joints. The value obtained is however so low that few actual column bases are likely to exhibit such a lower initial stiffness. On the other hand, in the present case, the boundary is an upper value, and even if the actual joint stiffness is higher, nothing may prevent the designer to consider still the joint as pinned, as it is presently done in design. As a consequence, no pinned classification boundary is derived and proposed here.

5.3 Column bases in "unbraced – sway" frames

The "unbraced – sway" frames are more sensitive than "braced – non-sway" ones to the variation of the rotational properties of column bases, mainly because of their high sensitivity to lateral deflections as well as to changes of the overall stability conditions when the lateral flexibility increases.

To illustrate this statement, a single-bay single-storey "unbraced – sway" frame is considered in Figure 5.4. The diagram indicates the evolution with increasing values of $\overline{S}$ of the ratio $\beta_s = y_S / y_P$ between the lateral deflection y_S of the frame with actual column base stiffness and the deflection y_P of the frame with assumed ideally pinned column bases. The non-dimensional stiffness $\overline{S}$ defined by Equation (5.3) is again reported in a logarithmic scale. First order elastic theory is used to compute the y values.

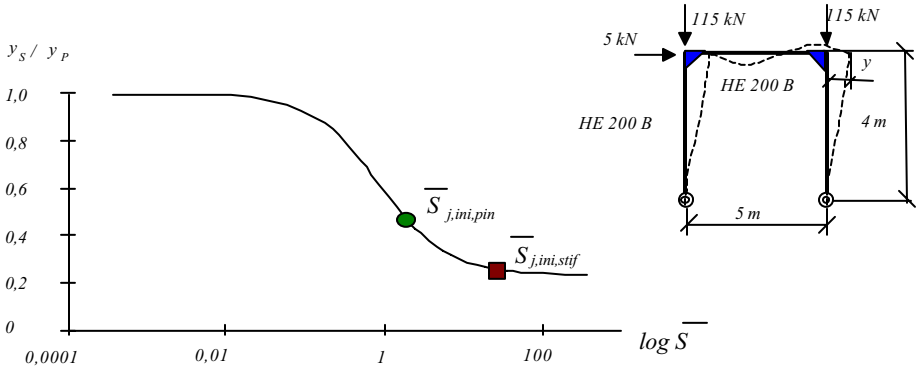

Figure 5.4 Sensitivity of the sway deflection to a variation of the column base stiffness in a portal frame

A stiffness classification boundary similar to that expressed in the case of "braced – non-sway" frames may again be derived here on the basis of a "5% resistance criterion". For "unbraced – sway" frames also it may be demonstrated that the more restrictive situation corresponds to the limit case where the beam flexural stiffness is rather high in comparison with that of the columns. The derivation of the classification boundary is therefore carried out by referring to the isolated column represented in Figure 5.5.b.

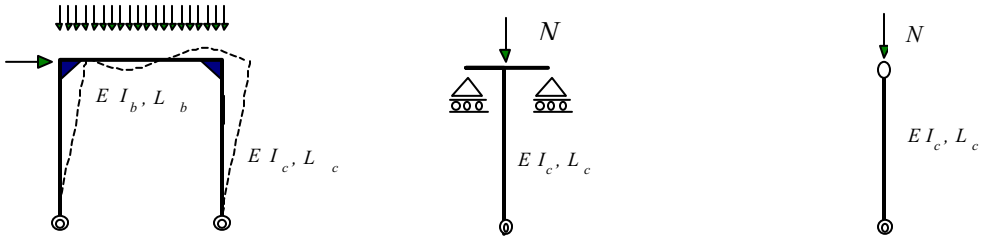

a) Portal frame (non-sway) b) Isolated column (top-fixed) c) Isolated column (top-pinned)

Figure 5.5 "Unbraced – sway" portal frame and isolated columns for classification study

According to the well-known Merchant-Rankine formula, the elasto-plastic second order resistance load factor λ_u of the whole frame may be expressed as:

$$\frac{1}{\lambda_u} = \frac{1}{\lambda_{cr}} + \frac{0.9}{\lambda_p} \tag{5.18}$$

where λ_{cr} and λ_p designate respectively the elastic critical load factor (resulting from an elastic linear instability analysis) and the plastic load factor (resulting from a rigid plastic first order analysis).

The range of application of the formula is defined as follows:

$$4 \le \frac{\lambda_{cr}}{\lambda_p} \le 10 \tag{5.19}$$

From Equations (5.18) and (5.19), it may be easily demonstrated – by keeping λ_p constant – that the application of the "5% resistance criterion" to the load-factor λ_u results in a possible variation of 20% of the value of λ_{cr}. As a consequence, the following criteria may be written:

$$\frac{\frac{\pi^2 EI_c}{(KL_c)^2}}{\frac{\pi^2 EI_c}{(L_c)^2}} \ge 0{,}80 \tag{5.20}$$

As a result:

$$K \le 1{,}118 \tag{5.21}$$

For "unbraced – sway" frames, the K - k relationship given by Equation (5.6) has to be replaced by the following one:

$$K = \sqrt{\frac{1 - 0{,}2\,(k_l + k_u) - 0{,}24\,k_l\,k_u}{1 - 0{,}8\,(k_l + k_u) + 0{,}6\,k_l\,k_u}} \tag{5.22}$$

while Equations (5.7.a) and (5.7.b) remain unchanged. The combination of these equations leads to the following expression of the stiffness classification boundary:

$$S_{j,ini} \ge 9EI_c / L_c \tag{5.23}$$

However the "5% resistance criterion" fully disregards the aspects of lateral frame deflections which have been pointed out as important. It may be shown (Wald and Sokol, 1997) that the lateral deflection y_S of the portal frame illustrated in Figure 5.5.a writes:

$$y_S = \frac{F\,L_c^3}{2\,E\,I_c}\,\frac{1}{12}\,\frac{4\,(3 + \overline{S}) + 6\,(4 + \overline{S})\,\zeta}{\overline{S} + 6\,(1 + \overline{S})\,\zeta} \tag{5.24}$$

where

$$\overline{S} = \frac{S_{j,ini}}{E\,I_c / L_c} \tag{5.25}$$

$$\varsigma = \frac{E\ I_b / L_b}{E\ I_c / L_c} \tag{5.26}$$

For $\bar{S} \Rightarrow \infty$, the deflection for the frame with rigid column bases may be derived from (5.24):

$$y_R = \frac{F\ L_c^{\ 3}}{2E\ I_c} \frac{1}{12} \frac{4+6\ \varsigma}{1+6\ \varsigma}, \tag{5.27}$$

In comparison with the case where rigid column bases are used (Formula 5.27), the actual frame - where the column bases possesses some degree of flexibility - will experience a larger deflection (Formula 5.24); this increase of the lateral displacement may be expressed in terms of percentage *w* as follows:

$$\frac{y_S}{y_R} = 1 + \omega \tag{5.28}$$

As far as classification is concerned, an "ω % resistance criterion" may be suggested with the objective to limit the increase of the lateral displacement of the actual frame to ω % of the deflection evaluated in the case of rigid column bases. In Formula (5.28), this means that the sign "=" should be replaced by "≤". By combining expressions (5.24), (5.27) and (5.28), the value of the minimum rotational stiffness that the column bases should exhibit to be considered as rigid from a displacement point of view is derived:

$$\bar{S} \geq \frac{12 + 24\ \varsigma - 6\varsigma\ (1+\omega)\ \frac{4+6\ \varsigma}{1+6\ \varsigma}}{(4+6\ \varsigma)\ \omega} \tag{5.29}$$

This condition is illustrated in Figure 5.6 (Wald and Sokol, 1997). The required stiffness is seen to be rather insensitive to the values of ς for significant values of *w*. Conservatively the values obtained for $\varsigma = 0$ may be selected, i.e.:

- for $\omega = 20\%$, the following stiffness boundary is obtained $\bar{S} \geq 20$
- for $\omega = 10\%$ $\bar{S} \geq 30$
- for $\omega = 5\%$ $\bar{S} \geq 60$.

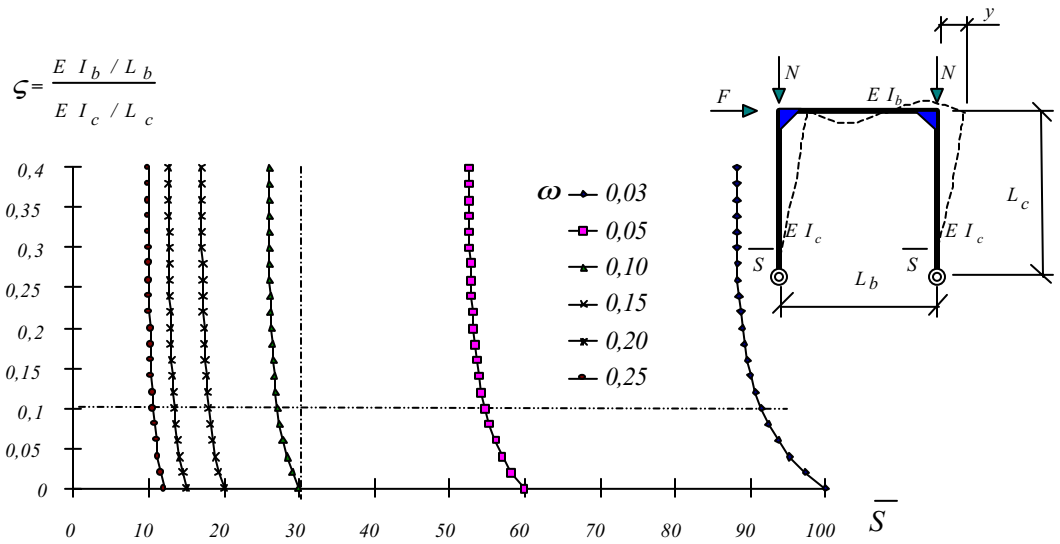

Figure 5.6 Displacement classification criteria for column bases

As a consequence, the displacement classification criterion is seen to be much more restrictive than the resistance one given by Equation (5.23). The selection of the value for the boundary is obviously strongly related to the level of accuracy which is thought to be necessary for the evaluation of the lateral frame deflection. A value of 10% appears to be quite realistic and the following stiffness classification boundary for presumably rigid column bases may be therefore proposed:

Rigid column bases: $$S_{j,ini} \geq 30\ E\ I_c / L_c \qquad (5.30.a)$$

Semi-rigid column bases: $$S_{j,ini} < 30\ E\ I_c / L_c \qquad (5.30.b)$$

For similar reasons than those given for "braced – non-sway" frames no classification boundary for presumably pinned column bases is suggested.

5.4 Proposed classification

The proposed stiffness classification for column bases is based on the sensitivity of the frame response to the flexural characteristic of the column. The classification boundaries may be easily evaluated for two structural systems, respectively the "braced – non-sway" and "unbraced – sway" ones. No recommendation is available for the other cases.

The stiffness boundaries are shown in Figure 5.7. They are as follows:

- ***"braced – non-sway" frames***

  Rigid column bases:

  If $\overline{\lambda}_o \le 0,5$ $\quad S_{j,ini} \ge 0$ (5.31.a)

  If $0,5 < \overline{\lambda}_o < 3,93$ $\quad S_{j,ini} \ge 7\,(2\,\overline{\lambda}_o - 1) EI_c/L_c$ (5.31.b)

  If $\overline{\lambda}_o \ge 3,93$ $\quad S_{j,ini} \ge 48\,EI_c/L_c$ (5.31.c)

  Semi-rigid column bases:

  If $\overline{\lambda}_o \le 0,5$ $\quad$ *all joints rigid* (5.31.d)

  If $0,5 < \overline{\lambda}_o < 3,93$ $\quad S_{j,ini} < 7\,(2\,\overline{\lambda}_o - 1) EI_c/L_c$ (5.31.e)

  If $\overline{\lambda}_o \ge 3,93$ $\quad S_{j,ini} < 48\,EI_c/L_c$ (5.31.f)

- ***"unbraced – sway" frames***

  Rigid column bases: $S_{j,ini} \ge 30\,E\,I_c / L_c$ (5.32.a)

  Semi-rigid column bases: $S_{j,ini} < 30\,E\,I_c / L_c$ (5.32.b)

In Figure 5.7, the value of the stiffness boundary for the "braced - non sway" frames is shown in a particular case where the reduced slenderness of the columns is equal to $\overline{\lambda}_o = 1.36$, what leads to a stiffness boundary value of $12\,EI_c/L_c$.

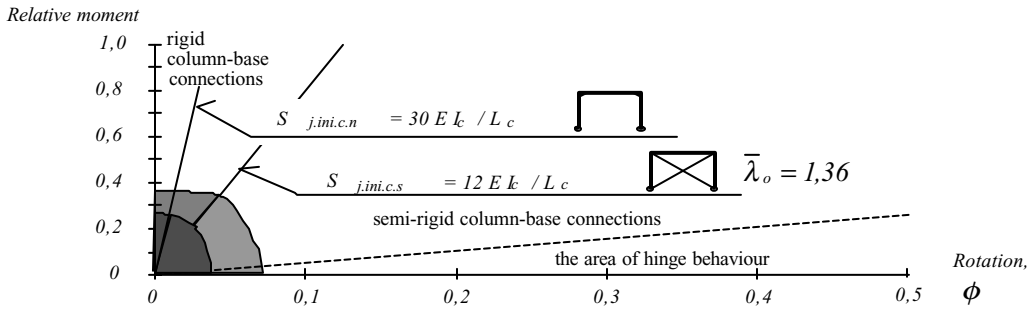

Figure 5.7 Proposed classification system according to the initial stiffness

Chapter 6: References

Alma J.G.J., Bijlaard, F.S.K. (1980): Berekening van kolomvoetplaten, Rapport No. BI-80-46/63.4.3410, IBBC-TNO, Delft.

Bouwman, L.P., Gresnigt A.M., Romeijn, A. (1989): Onderzoek naar de bevestiging van stalen voetplaten aan funderingen van beton. (Research into the connection of steel base plates to concrete foundations), Stevin Laboratory report 25.6.89.05/c6, Delft.

Bijlaard F.S.K. (1982): Rekenregels voor het ontwerpen van kolomvoetplaten en experimentele verificatie, Rapport No. BI-81-51/63.4.3410, IBBC-TNO, Delft.

CEB (1994): Fastenings to concrete and masonry structures, State of the art report. Comité Euro-International du Béton. Thomas Telford Publishing, London, ISBN 07277 19378.

CEB (1996): Design of fastenings in concrete, Design Guide. Comité Euro-International du Béton. Thomas Telford Publishing, London, ISBN: 0 7277 2558 0.

DeWolf J.T. (1978): Axially Loaded Column Base Plates, Journal of the Structural Division ASCE, Vol. 104, No. ST4, pp. 781-794.

DeWolf J.T., Sarisley E. F. (1980): Column Base Plates with Axial Loads and Moments, Journal of the Structural Division ASCE, Vol. 106, No. ST11, pp. 2167-2185.

ECCS (1994): European recommendations for bolted connections with injection bolts. ECCS publication No. 79, Brussels.

Eligehausen R. (1990): Design of fastenings in concrete using partial safety factors, in German, Bauingenieur, No. 65, pp. 295-305.

Eligehausen R. (1991): Fastenings to Reinforced Concrete and Masonry Structures, State-of-art Report, Part I, Part II, CEB bulletin N° 206, EPF Lausanne.

Eurocode 3 (1992): ENV 1993-1-1, Part 1.1, Design of Steel Structures, European Prenorm, CEN, Brussels.

Eurocode 3, Revised Annex J (1998): Joints in Building frames, CEN, Document ENV 1993-1-1:1992/A2, Brussels.

Guisse S., Vandegans D., Jaspart J.P. (1996): Application of the component method to column bases - Experimentation and development of a mechanical model for characterization. Report n° MT195, Research Centre of the Belgian Metalworking Industry, Liège, Belgium.

Hawkins N.M. (1968): The bearing strength of concrete loaded through rigid plates, Magazine of Concrete Research, Vol. 20, No. 63, March, pp. 31-40.

Hawkins N.M. (1968): The bearing strength of concrete loaded through flexible plates, Magazine of Concrete Research, Vol. 20, No. 63, June, pp. 95-102.

Jaspart J.P. (1991): Etude de la semi-rigidité des noeuds poutre-colonne et son influence sur la résistance et la stabilité des ossatures en acier, Ph.D. Thesis, Department MSM, University of Liège.

Lambe T.W., Whitman R.V. (1969): Soil Mechanics, MIT, John Wiley & Sons, Inc., New York.

Massonnet Ch., Save M. , (1976), Calcul plastique des constructions, Volume 1: Structures dépendant d'un paramètre, Third edition, Nelissen, Liège, Belgium.

Murray T.M. (1983): Design of Lightly Loaded Steel Column Base Plates, Engineering Journal AISC, Vol. 20, pp. 143-152.

NEN 6770 (1990): Staalconstructies TGB 1990, Basiseisen en basisrekenregels voor overwegend statisch belaste constructies (TGB 1990 Steel Structures, Basis requirements and basic rules for calculation of predominantly statically loaded structures), Delft.

Niyogi S.K. (1973): Effect of Side Slopes on Concrete Bearing Strength, Journal of the Structural Division, ASCE, Vol. 104, No. ST3, pp. 599-604.

Salmon C.G., Schenker L., Johnston G. J. (1957): Moment-Rotation Characteristics of Column Anchorages, Transaction ASCE, Vol. 122, No. 5, pp. 132-154.

SBR (1973): Mortelvoegen in montagebouw, Rapport no. 34, Stichting Bouwreseach, Samson Alphen aan de Rijn.

Shelson W. (1957): Bearing Capacity of Concrete, Journal of the American Concrete Institute, Vol. 29, No. 5, Nov., pp. 405-414.

Sokol Z., Wald F. (1997): Experiments with T-stubs in Tension and Compression, Research Report G1496, CVUT, Praha.

Steenhuis C.M. (1998): Assembly procedure for base plates, report 98-CON-R0447, TNO Building and Construction Research, Delft, the Netherlands.

Steenhuis C.M., Gresnigt A.M., Weynand K. (1994): Pre-Design of semi-rifig joint in steel frames, in COST C1, Proceeding of the 2nd state of the art workshop, Prague, pp. 131-140.

Stockwell F.W. Jr. (1975): Preliminary Base Plate Selection, Engineering Journal AISC, Vol. 21, No. 3, pp. 92-99.

Vandegans D. (1997): Column Bases: Experimentation and Application of Analytical Models, Research Centre of the Belgian Metalworking Industry, MT 196, p.80, Brussels, Belgium.

Wald F. (1993): Column-Base Connections, A Comprehensive State of the Art Review, CVUT, Praha.

Wald F. (1995): Patky Sloupù - Column Bases, CVUT Praha, 1995, p. 137, ISBN 80-01-01337-5.

Wald F. (1999): Anchor bolts design, Aktion 6p12, CVUT, Praha.

Wald F., Obata M., Matsuura S., Goto Y. (1993): Prying of Anchor Bolts, Nagoya University Report, pp. 241-249.

Wald F., Obata M., Matsuura S., Goto Y. (1993): Flexible Baseplates Behaviour using FE Strip Analysis, Acta Polytechnica, CVUT Vol. 33, No. 1, Prague, pp. 83-98.

Wald F., Seifert J. (1991): The Column-Base Stiffness Classification, Proceedings of the Nordic Steel Colloquium, 9-13 September, Odense, pp. 413-421.

Wald F., Sokol Z. (1995): The Simple column - base stiffness modelling, in Steel Structures - Eurosteel 95, ed. Kounadis, Balkema, Rotterdam, pp. 277-286.

Wald F., Sokol Z. (1997): Column Base Stiffness Classification, Proccedings of SDSS 97, Colloquium on Stability and Ductility of Steel Structures, Nagoya, Japan, pp. 675 - 682.

Wald F., Sokol Z. (1997): Model of Column Base Stiffness, in STESSA 97, in International Conference Behaviour of Steel Structures in Seismic Areas, Kyoto, Japan, pp. 672 - 679, ISSN 88-85651-76-3.

Wald F., Sokol Z., Šimek I., Barantova Z. (1995): Column Base Semi-Rigid Behaviour, Poddajnost patek ocelových skelet, in Czech, Report G 8118, CVUT, Praha.

Wald F., Sokol Z., Steenhuis M. (1996): Proposal of the Stiffness Design Model of the Column Bases, in Connection in Steel Structures III, Behaviour, Strength, and Design, Proceedings of the Third International Workshop, May 29-31, 1995, Trento, Italy, Pergamon Press, London, 1996, p. 237 - 249, ISBN 0-08-042821-5.

Yee Y.L., Melchers R.E. (1986): Moment rotation curves for bolted connections, Journal of the Structural Division, ASCE, Vol. 112, ST3, pp. 615-635.

Zoetemeijer P. (1974): A design method for the tension side of statically loaded bolted beam-to-column connections, Heron, Delft University, Vol. 20, n° 1.

Zoetemeijer P. (1985): Summary of the researches on bolted beam-to-column connections, Report 6-85-7, University of Technology, Delft, The Netherlands.